19
Drug Product Design

Prodrugs and Drug Carriers

Routes of Administration

The principles of thermodynamics, chemical equilibria, surface and colloidal phenomena, kinetics of decomposition, diffusion of drugs through membranes, and solubility and complexation constitute the subject of previous chapters. This chapter introduces the subject of dosage form design and controlled drug delivery systems. It applies the principles of chemistry, biology, and physical pharmacy to the formulation of drug delivery systems.

Of the systems discussed some are presently approved by the U.S. FDA and are accepted in medical practice; others are in various stages of research and clinical trial. The field of new drug design and controlled delivery is developing rapidly, and limitations of space militates against the inclusion here of all new systems and devices. For example, no mention is made of new dosage forms for vaginal and intrauterine routes, delivery to the brain, erythrocyte carriers, and drugs targeted to lymph cells of the immune system.

Although the present rapid introduction into commerce of new drugs and devices makes the study of drug design and delivery somewhat difficult and confusing, the subject is simpler that it appears from a perusal of current pharmaceutical literature.

The chapter begins with a discussion of prodrugs and drug carriers. It is then organized according to routes of administration and the controlled delivery devices and absorption enhancers that have recently been developed.

The rationale for the controlled delivery of drugs is to promote therapeutic benefits while at the same time minimizing toxic effects. New drug delivery approaches to medication technology are finding use in long-term fertility control; genetically related enzyme replacement therapy; transdermal, nasal, and pulmonary administration; and treatment of glaucoma and ocular infections. Normal drug dosing may follow a "sawtooth" kinetic profile (Fig. 19–1), in which the dose first

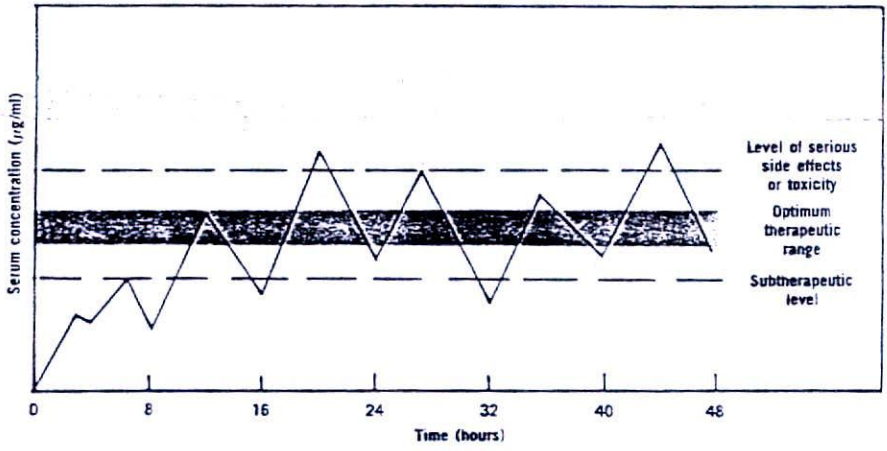


Fig. 19–1. Undesirable sawtooth kinetic profile under conditions of normal dosing, and optimum therapeutic profile obtainable with some newer delivery devices.

greatly exceeds the desired therapeutic level, then falls to a subclinical level, and on subsequent dosing rises to dangerously high values, falling again to ineffective concentrations, in continuous cycles of excessive–ineffective levels. Controlled, sustained drug delivery can reduce the undesirable fluctuation of drug levels, enhancing therapeutic action and eliminating dangerous side effects. Furthermore, the localization through preprogrammed drug delivery methods of a drug in the vicinity of its target cells can prevent systemic or side effects involving other tissues.

The most popular sustained drug delivery forms and devices used today make use of inert polymers, such as the silastics, or biodegradable polylactic acids. By the use of these materials suitable drug levels can be sustained in certain regions of the body such as the eye, vagina, the surface of the skin, or in a subcutaneous depot. Polymeric forms and recently introduced therapeutic systems will be considered in some detail following a brief discussion of chemical and biologic approaches to prolonged and intensified action of drugs in the body. The physical and chemical properties of polymers used in many of the new dosage forms are discussed in Chapter 20.

PRODRUGS AND DRUG CARRIERS

Prodrugs. According to the prodrug approach to drug delivery, a medicinal agent is chemically modified, for example, by the addition of an ester group to improve the absorption and concentration of the parent compound at the target site in the body.[1] In a prodrug, the ester group or similar carrier moiety is chemically removed in the gut or at the tissue site, usually by enzymatic action, and the parent drug is freed to produce its pharmacologic action. Prodrug formation and other chemical modifications may also facilitate pharmaceutical processing and improve the stability of the parent drug. Sparingly soluble salts of the penicillins are examples of chemical analogs that have been used for some time to promote higher blood levels and bring about better distribution in the tissues. Pivampicillin is quite lipophilic and produces high blood levels of the parent drug, ampicillin, through a prodrug mechanism. Erythromycin prodrugs are available that are tasteless and stable in aqueous suspension, the parent molecules being protected with chemical groupings that are eventually lost in the tissue.

The prodrug principle has significantly advanced the delivery of targeted drugs to selected sites in the body. Seki et al.[2] studied the effect of various esterases on the enzymatic hydrolysis of esters of *p*-acetylaminobenzoic acid and acetylated acetaminophen. The results showed that ester prodrugs could be formulated to hydrolyze at specific sites in the body.

Mercaptopurine together with methotrexate is used in the chemotherapy of lymphocytic leukemia. When taken orally, mercaptopurine is only about 50% absorbed. Waranis and Sloan[3] investigated the possibility of delivering mercaptopurine through hairless skin in the form of a prodrug, acyloxymethyl mercaptopurine, administered in the solvents, isopropyl myristate and propylene glycol. The solubility parameters (see pp. 224–227) of the several prodrug derivatives were found to correlate well with their permeability through the skin preparation.

Bundgaard and his associates[4,5] have studied the preparation and properties of prodrugs over the past decade. Proteins and small peptides constitute new and important classes of drugs, yet they do not pass readily through biomembranes and are easily metabolized by peptidases when given by various routes of administration. Bundgaard and Móss[5] are preparing derivatives of small peptides to yield prodrugs that show enhanced delivery and chemical stability but that break down rapidly in the body to release the biologically active parent compound. To date, prodrugs have been made from various proteins and peptides: thyrotropin-releasing hormone (TRH), luteinizing hormone–releasing hormone (LH–RH), fibrinopeptides, and collagen. Takakura et al.[6] have prepared a prodrug of mitomycin C and dextran as a delivery system in cancer chemotherapy and are studying the properties of a soybean trypsin inhibitor conjugated to dextran as a model to optimize the delivery of protein drugs. Mitomycin C is a useful antibiotic against neoplastic disease but, like other anticancer agents, it does not differentiate in its action against tumor and normal cells. Sato et al.[7] developed a polymeric prodrug—mitomycin C–dextran. They found that the prodrug liberated the parent, mitomycin C, with a greater activity against various tumors than uncomplexed mitomycin C. See Figure 11–5 for complexation of mitomycin with cyclodextrin.

Liposomes. Biologic entities, including red blood cells and liposomes, have been used as drug carriers to promote controlled release in the body. *Liposomes* are uni- or multilayered vesicles of phospholipids, first described in 1965 by Bangham et al. at Cambridge.[8] They fall in the size range of 250 Å (25 nm) to 10 μm in diameter, and may be prepared, according to one procedure, by combining a phospholipid such as phosphatidylserine, cholesterol, and cholesterol oleate in chloroform and allowing the solution to evaporate. The mixture of lipids is then dissolved in ethanol and the solution is added to isotonic saline solution containing ethylenediaminetetraacetic acid (EDTA) with stirring at pH 7.4 and 37° C. The procedure is conducted under aseptic conditions and only sterile preparations are used. In experimental work the liposome vesicles are prepared freshly each day. The finished liposomes are nearly spherical and consist of unilamellar or multilamellar lipid bilayers alternating with aqueous regions. Figure 19–2*a* depicts a unilamellar liposome. The lipid

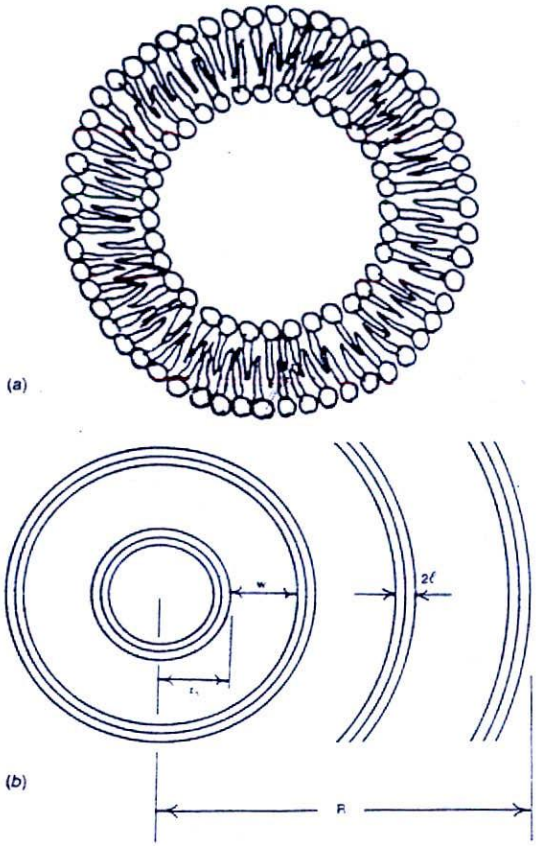


Fig. 19–2. (a) A liposome showing a single phospholipid bilayer (unilamellar liposome). (b) Drawing of a multilamellar liposome with $n = 4$ lamellae. Each lamella consists of a lipid bilayer of thickness 2ℓ and alternates with water layers of thickness w. The core is a unilamellar liposome of radius r. (From C. Pidgeon and C. A. Hunt, J. Pharm. Sci. 70, 78, 1981, reproduced with permission of the copyright owner.)

bilayers can entrap lipid-soluble drugs and the water layers can dissolve water-soluble compounds. Drugs are introduced into liposomes by simply mixing the phospholipid and other lipid components with an aqueous solution of the drug.

Martin[9] has discussed the many factors that must be taken into consideration in the manufacture of liposomal preparations, including the choice of solvents, sterility requirements, pyrogen control, and stability of the ingredients and of the final product. One industrial-scale production method is discussed[9] with particular attention to obtaining liposomes that are of uniform size and are capable of encapsulating a maximum amount of the aqueous drug solution.

Pidgeon and Hunt[10] provide formulas to calculate the total surface area, TSA, of N liposomes; the volume of water VW_1 encapsulated in a single-layer liposome or the total volume of water, TVW, in a population of N single-layer liposomes; and the encapsulation ratio, E, or ratio of entrapped water volume to total volume of lipid. Needed for these calculations are the number N of liposome particles,* the radius R of a liposome, and the volume of lipid in the single-layer liposome. These are important quantities to know, for the distribution of liposomes in the body when injected intravenously is a function of the dose (number N of liposome particles), the size, and the surface area of the liposomes. We assume a *homogeneous population* of liposomes, in that the radius, surface area, and n, number of layers or lamellae, are the same for all particles. Shown in Figure 19–2b is a liposome of $n = 4$ lamellae. The heterogeneous case in which the radius, surface area, and number of layers differ among the vesicles in a population is discussed by the authors[10] and will not be treated here.

Example 19–1. Calculate the volume VW_1 of water entrapped in a spherical single-layer† liposome using equation (1) of Pidgeon and Hunt[10]:

$$VW_1 = \frac{4}{3}\pi R^3 - VL_1 \qquad (19-1)$$

in which $VL_1 = 1.99 \times 10^{-5}\ \mu m^3$ is the volume of phospholipid constituting the single lipid layer of the liposome and $R = 0.0225\ \mu m$ is the outside radius of the liposome.

$$VW_1 = \frac{4}{3}\pi(0.0225)^3 - 1.99 \times 10^{-5} = 2.78 \times 10^{-5}\ \mu m^3$$

This is the volume of water in the *core* of a single liposome (see Fig. 19–2a).

If the single-layer homogeneous liposome preparation is found to contain $N = 4.04 \times 10^{16}$ liposome particles, the total volume of phospholipid TVL_1 present is

$$TVL_1 = N \times VL_1 = (4.04 \times 10^{16})(1.99 \times 10^{-5}) = 8.04 \times 10^{11}\ \mu m^3$$

The total volume of entrapped water, TVW_1, in the $N = 4.04 \times 10^{16}$ liposomes is $TVW_1 = N \times VW_1 = (4.04 \times 10^{16})(2.78 \times 10^{-5}) = 1.123 \times 10^{12}\ \mu m^3$. The ratio of the total volume of enclosed water, $TVW = N_1 VW_1 = \frac{4}{3}\pi NR^3 - NVL_1 = \frac{4}{3}\pi N_1 R_1^3 - TVL$ to the total volume of phospholipid, TVL yields the *encapsulation ratio*, $E = TVW/TVL_1$,

$$E = \frac{\frac{4}{3}\pi N_1 R_1^3}{TVL_1} - \frac{TVL_1}{TVL_1} = \frac{\frac{4}{3}\pi N_1 R_1^3}{TVL_1} - 1 \qquad (19-2)$$

For a preparation of $N_1 = 4.04 \times 10^{16}$ liposomal particles each of radius $R_1 = 0.0225\ \mu m$, and a total phospholipid volume in the preparation of $TVL_1 = 8.04 \times 10^{11}\ \mu m^3$, the encapsulation ratio E is found to be

$$E = \frac{\frac{4}{3}\pi(4.04 \times 10^{16})(0.0225)^3}{8.04 \times 10^{11}\ \mu m^3} - 1 = 1.40$$

Thus the ratio of water to phospholipid in this preparation is 1.40 to 1.

*The authors describe a procedure to calculate N, the number of particles. It is assumed for our purposes that N has been obtained by an appropriate method, and in the example to follow its value is given.

†The subscript 1 on terms such as VW_1 and VL_1 indicates that we are dealing with a single-layer (unilamellar) liposome.

The total surface area TSA_p, that is, the area for the entire population of liposomes, is given by the equation

$$TSA_p = \sum_{i=1}^{k} 4\pi N_i R_i^2 \qquad (19-3)$$

where the summation is over the n phospholipid layers from $i = 1$ to k. Since we are dealing with a single-layer liposome, $k = 1$; therefore $N_i = N_1 = 4.04 \times 10^{16}$ and $R_i^2 = R_1^2 = (0.0225\ \mu m)^2 = 5.06 \times 10^{-4}$. And we have for the total surface area of liposomes: $TSA = 4\pi(4.04 \times 10^{16})(5.06 \times 10^{-4}) = 2.57 \times 10^{14}\ \mu m^2$

Lichtenberg and Markello[11] calculated the surface area and entrapped aqueous volume of spherical multilamellar liposomes from a knowledge of the liposome's outer radius, thickness of the interlamellar aqueous layers, and number of bilayers. From their calculations, based on an approach taken earlier by Schwartz and McConnell[12], the authors concluded that most vesicles have a definite distance between the lamellae in a given population of liposomes, with most of the aqueous medium enclosed in the internal core of the liposome. Hydrophilic drugs are encapsulated predominantly in this central aqueous cavity. *Problem 19–2*, page 551, illustrates the calculations of Lichtenberg and Markello.[11] From their results and those of Schwartz and McConnell[12], the authors concluded that liposomes consist of up to 10 lamellae, each lamella or lipid layer being about 50 Å thick: Large liposomes, fully swollen, have diameters approximately 1.5 μm with interlamellar distances of about 60 Å and a large aqueous core with a diameter somewhat greater than 1.0 μm.

Hydrophilic drugs and amphiphilic compounds such as mitomycin are not well entrapped in lipid carriers, whereas lipophilic compounds are well retained in the biologic drug carriers. When mitomycin is chemically modified to form a lipophilic prodrug it may be entrapped in liposomes and in oil-in-water emulsions.[13] Negatively and positively charged lipids can be used to produce charged liposomes. Abra et al.[14] investigated the delivery of negatively charged liposomes and the effect of vesicle size on the deposition in the lungs. Liposome preparations also have been used to administer drugs topically.[15]

Wiessner et al.,[16] studied the binding of the peptide insulin by the liposome dipalmitoyl phosphatidyl choline. Insulin, an amphiphilic molecule, may cause fusion (melting) of liposomes resulting in their aggregation; and care must be used to avoid such deleterious effects of insulin in single-layer liposomes. Guzman et al.[17] studied the entrapment of the cardiac glycosides digitoxin, digoxin, and ouabain in liposomes prepared from egg yolk phosphatidylcholine. The authors reported that drugs with high or low octanol–aqueous buffer partition coefficients are better incorporated in the vesicles than those with intermediate partition coefficients. Digoxin, with an intermediate partition coefficient, is poorly entrapped in the liposomes. Cholesterol is known to promote a close packing of the phosphatidylcholine bilayer molecules and its addition to the liposomal preparation greatly reduced the capacity of the vesicles to entrap digoxin. When charged lipids are included in the formation of liposomes, the electrostatic repulsion between adjacent bilayers resulted in an increase in the aqueous space between the bilayer molecules. Thus the addition of diacetylphosphate, a negatively charged species, increases the incorporation of ouabain, a water-soluble cardiac glycoside.

Payne et al.[18] reviewed the limitations of liposomes as biologic carriers, including chemical and physical instability, problems of sterility, drug incompatibility, and immunologic and toxicologic difficulties. These adverse effects greatly limit aqueous suspensions of liposomes as drug carriers, and suggest the possible advantages of formulations that may be stored dry and hydrated before use to yield an aqueous suspension of liposomes. The authors refer to these formulations as *proliposomes*. They are free-flowing granular products which, when water is added, disperse to yield isotonic suspensions of liposomes for intravenous use or administration by other routes. The authors discussed the nature of the lipid drug, the suitability of carriers such as sodium chloride and sorbitol, and the amount of lipid drug deposited onto the carrier. These factors markedly influence the preparation of proliposomes and formation of an aqueous suspension of the liposomes. A stability study showed that the size distribution of the hydrated proliposomes did not change significantly over a 9-month period at 20° C. When amphotericin B was incorporated in the liposomes, its potency did not decrease over a 6-month period.

Gregoriadis[19] has prepared a comprehensive three-volume treatise on liposome technology. Other works on dosage form design and controlled delivery devices are listed on page 550.

Monolithic and Reservoir Devices.[20] The word *monolithic* refers to a single mass or block of material. In the field of controlled drug delivery, the term *monolithic device* refers to a rate-controlling polymer matrix throughout which the drug is dissolved or dispersed. In contrast to a matrix or monolithic system, a reservoir device consists of a shell-like dosage form with the drug or agent contained within a rate-controlling membrane. Systems of reservoir and matrix form are shown in Figure 19–3. The device may be spherical or cylindrical, or it may consist of layers of the drug or other agent sandwiched between layers of rate-controlling and other membranes. This third form, known as a *laminated reservoir system* (see p. 543, Fig. 19–22), is designed mainly for attachment to surfaces such as the skin, the lining of the mouth, and the cornea of the eye. If a controlled-release dosage form is introduced into the body and does not degrade with time, it must be removed surgically. For this reason biodegradable systems, such as the one shown in Figure 19–4, have been sought for the controlled release of biologically active agents. Today many polymer matrix and mem-

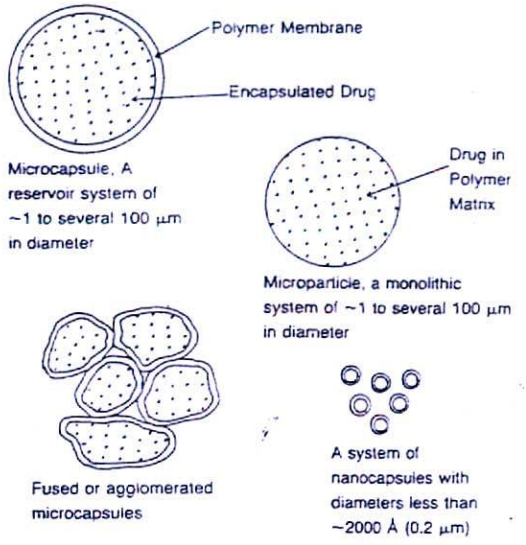


Fig. 19–3. Visualization of microcapsules, microparticles, and nanocapsules, and their approximate sizes. Nanoparticles, not shown, are approximately the same size as nanocapsules, but like microparticles they consist of a solid matrix through which the drug is dispersed.

brane materials are available that gradually degrade after the drug is released at the desired site in the body. With the use of biodegradable polymers, controlled-release implants and depot injections can be made with the assurance that the polymeric material will disappear from the body within a reasonable time. Examples of biodegradable polymers are poly(glycolic acid), poly(D,L-lactic acid), glutamic acid–ethyl glutamate copolymers, and polyacrylamides (hydrogels).

Studies on microcapsules, made from various polymers and used for different purposes, are introduced here, followed by a discussion of microparticles (microspheres), nanocapsules, and nanoparticles.

Microcapsules. In a symposium on microcapsules, Lim and Moss[21] defined microencapsulation as a process in which solids, liquids, or gases are enveloped in a membrane that may be impermeable or semipermeable. Activated charcoal, enzymes, hormones, antigens, and antisera are examples of materials that can be entrapped in microcapsules. The cells are formed by a process involving heat coagulation, by bringing an aqueous solution of the drug in contact with an organic solvent phase, or by polymerization and gelatin.

Invertase is an enzyme that catalyzes the hydrolysis of sucrose into fructose and glucose. Patients who cannot absorb sucrose are deficient in the enzyme invertase, and suffer microbial fermentation in the gut and severe diarrhea when sucrose is ingested. To overcome these digestive problems, Rambourg et al.[22] incorporated invertase into polyamide microcapsules, prepared by interfacial polymerization according to the method of Chang.[23] Interfacial polymerization is a polymerization reaction at the interface between an organic and an aqueous phase. An emulsification procedure was also tested in which the invertase was encapsulated in a cross-linked protein. In another report, Levy et al.[24] incorporated hemoglobin in microcapsules to produce a blood replacement fluid. The microcapsules were formed by linking hemoglobin, the protein, with various acylchlorides, such as terephthaloylchloride, as the cross-linking agent. Stable hemoglobin microcapsules were prepared 5 μm in diameter, that were able to carry out normal oxygen transfer but did not allow escape of the hemoglobin. A scanning electron micrograph of large, dehydrated microcapsules of hemoglobin, obtained in the early phase of the study, is shown in Figure 19–5. McGinity and associates[25] described the preparation and properties of nylon microcapsules containing three different matrices: formalized gelatin, calcium alginate, and calcium sulfate. The capsules were free-flowing and were approximately 50 to 150 μm in diameter. Various anionic, cationic, nonionic, quarternary, and amphoteric drugs were incorporated in the nylon microcapsules. Bala and

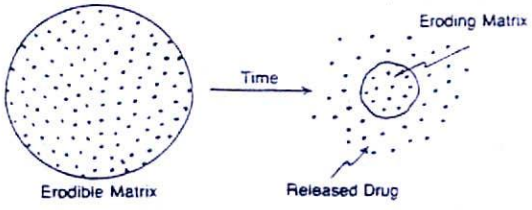


Fig. 19–4. Biodegradation of a microparticle. In time, the drug is completely released and simultaneously the degradable matrix erodes. Or the drug may be slowly released, and in a reasonable time thereafter the matrix, free of drug, gradually disappears.



Fig. 19–5. Scanning electron micrograph of hemoglobin microcapsules. (From M.-C. Levy, P. Rambourg, J. Levy and G. Potron, J. Pharm. Sci. 71, 759, 1982, reproduced with permission of the copyright owner.)

Vasudevan[26] designed a pH-sensitive microcapsule for the encapsulation of such agents as secretin, which is found in the upper intestinal tract and is activated when chyme, that is, the digestive secretions and partly digested food, enter the intestine. The microcapsules of polyacryloylchloride-lysine are spherical with diameters of 5 to 10 μm. The polymer dissolution and release of secretion depends on the pH of the solution in which the microcapsules are suspended. The drug is released following zero-order kinetics, which suggests the possible use of these pH-sensitive microcapsules for the delivery of drugs to the duodenum in the treatment of ulcers. The system should be useful for the delivery of drugs, in general, both under conditions of low pH and at pH values as high as 8.0, since the polymer may be eroded up to pH 8.

It has been observed that compression of microcapsules to form tablets shows the release rate and produces a sustained action. Nixon and Agyilirah[27] investigated the results of tableting microcapsules consisting of ethylcellulose shells or walls containing sodium phenobarbital in the cores. Dissolution from the capsules was found to depend on the core–wall ratio and the size of the dried microcapsule aggregates in the tablet. With a higher core-to-wall ratio the microcapsules have thinner walls so that the dissolution medium can enter the capsule more readily and the core solution can easily pass through the walls. The larger the microcapsules the greater the breakdown of the aggregates, providing additional surface for dissolution. Thus, both core-to-wall ratio and size of microcapsule aggregates increase the dissolution rate of the tableted microcapsules.

Early in the development of microcapsule technology (1966), Chang suggested the encapsulation of magnetic particles to direct entrained drug to specific sites in the body with the help of an external magnet. Povey et al.[28] suggested the addition of a suspension of magnetite, Fe_3O_4 (Ferrofluid EGM 705), to recover the magnetic microcapsules in the feces with an electromagnet for identification and study of reactive carcinogens captured from the intestinal tract. The results of their work show that magnetic polymer microcapsules are able in vitro to entrap a model carcinogen, *N*-methyl nitrosourea (NMN); and NMN can subsequently be released from the microcapsule mass by magnetic attraction for subsequent analysis. Gallo et al.[29] were able to alter the tissue distribution in the rat of adriamycin, an antineoplastic agent, by encapsulating the drug in magnetic albumin microcapsules prepared with a magnetite (Fe_2O_3) suspension and by directing the adriamycin microcapsules, following intraarterial administration, to the target site. The use of magnetic microspheres increased the drug's presence both at the target site and in the liver.

Microparticles (Microspheres). These devices differ from the reservoir system known as microcapsules in that they consist of a solid matrix throughout which the drug is distributed. Akbuga[30] prepared microspheres of furosemide, a potent diuretic, using various acrylic polymers (Eudragit, Rohm Pharma) as the microsphere matrix. These microparticles were spherical with diameters of 250 to 280 μm, and contained 75 to 80% by weight of furosemide. The release pattern of furosemide was altered by using different polymers, namely Eudragit L 100, S 100, RL 100, and RS 100. The results of dissolution experiments showed that the release of the drug followed the Higuchi[31] matrix model (p. 336). Gupta and associates[32] investigated the effects of albumin microspheres on the release rate of entrapped adriamycin (doxorubicin hydrochloride), a broad-spectrum antineoplastic agent. The behavior of albumin microspheres has been studied by a number of researchers[33] and found to be quite acceptable as polymeric carriers for the delivery of drugs in the living system.

Spenlehauer et al.[34] reported on the incorporation of cisplatin, a potent anticancer agent, into poly(D,L-lactide) microspheres by a process known simply as *solvent evaporation*. According to this method cisplatin was dispersed in methylene chloride and to this suspension was added the polymer, poly(D,L-lactide). The organic phase was emulsified in an aqueous solution of emulsifiers, namely polyvinyl alcohol and methylcellulose, and the pH was adjusted to 2 with HCl. The dispersion was stirred mechanically until the organic solvent, methylene chloride, was completely evaporated. The solid microspheres took up the cisplatin during evaporation and were collected on a filter and dried. The steps in the preparation of microspheres of cisplatin are illustrated in the flow chart shown in Figure 19–6. Cisplatin may be deposited in the polymer matrix by this process to the extent of about 45% by weight of the drug. The in vitro kinetics of cisplatin release was studied and found to depend on the amount of drug loaded into the microspheres; the greater the drug loading the faster was the drug release. Further work with microsphere entrapment of cisplatin may yield a targeted dosage form without the present side effects of nausea, vomiting, and renal disturbances.

Leucuta[35] proposed an ophthalmic drug delivery system consisting of gelatin or albumin microspheres designed to prolong the residence time of the drug in the eye and to provide improved bioavailability. Liposomes and nanoparticles have been used to obtain controlled drug delivery to the eye. Leucuta chose pilocarpine, a miotic which causes the pupil to contract and is used in the treatment of glaucoma. He prepared gelatin and albumin microspheres, containing pilocarpine nitrate, which were sufficiently large to be recognized as particles by the eye, yet not so large that they could not be readily flushed out of the eye by the natural flow of tears. The methods of preparation are described in detail in his report.[35] The release of pilocarpine from microspheres, as compared with the result with an aqueous solution of the drug, showed

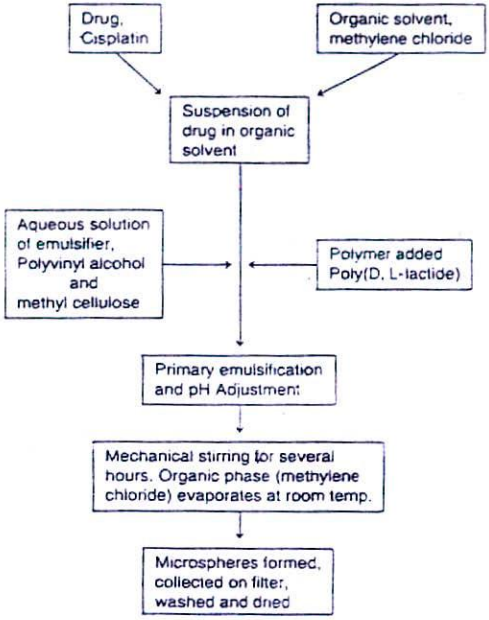


Fig. 19–6. Flow chart for the preparation of cisplatin microspheres by the solvent evaporation method.

extended contact of the microspheres at the corneal surface. Preliminary results suggested that microspheres provided a suitable dosage form to maintain water-soluble drugs such as pilocarpine nitrate in the area of the cornea.

Bodmeier and McGinity[36] evaluated the incorporation of various ionized and nonionized drugs in poly-(D,L-lactide) (PLA) microspheres. Poly(D-L-lactide) is a biodegradable polymer and its microparticles are ordinarily used as carriers for water-insoluble drugs. By adjusting the pH to minimize drug solubility, it was possible to increase the drug content in the microspheres for weakly ionizable drugs such as quinidine sulfate. The rate and amount of drug released was a strong function of the surface structure of the microspheres which, in turn, depended on the pH of the aqueous solution at the time of preparation of the microspheres. Thermal analysis (pp. 46–49) of the microspheres containing quinidine provided information regarding the glass transition temperature of the polymer and the melting and recrystallization of the drug, quinidine. The glass transition temperature T_g is a narrow temperature range over which a plastic changes on cooling from a very viscous rubbery melt to a glass state rather than from a liquid to a crystalline state (pp. 586–588).

In a second paper[37] Bodmeier and McGinity studied various methods of solvent selection in the preparation of PLA microspheres produced by the solvent evaporation method and containing the drugs quinidine and quinidine sulfate. A flow chart of the solvent evaporation method is presented in Figure 19–6. The steps in the preparation of drug-loaded microspheres as outlined in the figure should assist the reader to follow the arguments concerning the precipitation of the polymer, PLA, from the organic solvent phase, the dissolution of the drug in the aqueous phase, and concentration of the polymer in the organic phase. In the emulsification step the rate of diffusion of the organic solvent into the aqueous phase must be rapid, causing a high rate of precipitation of the polymer from the organic solvent. The use of an organic solvent of low water solubility results in slow polymer precipitation and a poor yield of microspheres. This is because the solvent solvates the polymer, PLA, and prevents its precipitation. The drug tends to escape entrapment in the microspheres, diffusing instead into the aqueous phase. Water-miscible solvents such as acetone, ethanol, and dimethyl sulfoxide should further favor precipitation of the polymer and increase the drug content in the microspheres; but this was found not to be the case. The authors found instead that the increase in the drug content with change of solvent could be explained by the effect of the solvent on the rate of precipitation of the polymer at the microdroplet interface. Rapid precipitation of PLA produced efficient entrapment of the drug in the matrix of the microspheres. The solvent methylene chloride possesses high water solubility, thus leaving the polymer to form microspheres containing the drug in its matrix. These workers[37] further found that the addition of cosolvents such as acetone or ethanol, together with the solvent methylene chloride, could increase the drug loading of the microspheres. The increased loading was attributed to the faster precipitation of PLA by the hydrophilic cosolvents, which assured the entrapment of quinidine sulfate, the drug.

Exposure to mercury compounds can result in serious poisoning, including organ damage and death. The antidote for mercury poisoning involves the administration of chelating agents such as dimercaprol, penicillamine, and polythiol resins, which bind mercury and excrete it in the feces. Margel and Hirsh[38] designed a polymercaptal microsphere that showed potential as an antidote against mercury poisoning. The microspheres were prepared by combining the mercury chelating agent pentaerythritol tetrathioglycolate with a sorbitan monolaurate surfactant to form an aqueous emulsion. Glutaraldehyde was added to the emulsion with stirring to form the microspheres, which were then separated by dialysis. By scanning electron microscopy, the diameter of the microspheres was determined to be 0.8 ± 0.02 μm and the surface area was calculated to be 8.04 $(\mu m)^2$. A suspension of the chelating microspheres was found to be free of aggregation after 1 year's storage. Both organic and inorganic mercury compounds are taken up, probably by the free thiol groups of the microspheres, over a broad range of pH. They compete strongly for mercury bound to albumin and cysteine. The effectiveness of chelating microspheres in

binding mercury in vitro is demonstrated in this study.

Morimoto, Natsume, and their colleagues[39,40] have prepared mitomycin C biodegradable albumin microspheres for use in a new procedure, *chemoembolization*, against liver tumors in rats. Chemoembolization is infusion of an anticancer drug into a solid malignant tumor, using a catheter that is passed directly into an artery of the tumor. Microspheres are used in this study as the drug carrier in the embolization procedure, and can be directed to target sites in the rat liver where the anticancer drug such as mitomycin C (MMC) is released slowly over several weeks. A schematic of the procedure is shown in Figure 19–7. The antitumor effects of the MMC microspheres were considerably greater (2.5 times) than those relating from the injection of saline solution alone (the control) or from infusion of MMC in saline solution. Chemoembolization was considered to be equally as effective as surgical removal of the malignancy.

Nanocapsules and Nanoparticles. These minute particles, about 100 Å (10 nm) to 2000 Å (0.2 μm) in diameter, were introduced by Kreuter and Speiser[41] in the 1970s as controlled-release drug carriers. The *nanocapsule* is a shell-like polymeric particle, a reservoir device, in which the drug is contained in an oily solution or colloidal suspension. A *nanoparticle* consists of a solid mass of polymer, a monolithic device, from which the drug is released by a leaching process. Nanoparticles may be distinguished from nanocapsules by subjecting them to ultracentrifugation; nanoparticles form a sediment at the bottom of a centrifuge tube whereas nanocapsules rise to form a layer at the top of the tube, as do the oil globules of an *o/w* emulsion.

Two main classes of polymerization—condensation and chain (addition) polymerization—are recognized along with several others of less importance in the preparation of nanocapsules, nanoparticles, and other microvesicles.[42] In *condensation polymerization*, the monomers react chemically through their functional groups to link the monomers in a step-wise manner to generate the polymer. In *addition (chain) polymerization* an initiator reacts with the monomer to form a free radical or an appropriate ionic site. The reactive monomers combine to initiate a chain, which grows as additional monomers are added to the polymer. The active site may be blocked at any stage and polymerization terminated (see p. 558 for the chemistry of condensation and addition [chain] polymerization).

Addition polymerization is conducted by several techniques: bulk, solution, suspension, and emulsion polymerization. *Bulk* polymerization involves only a monomer and a chain initiator, whereas *solution* polymerization involves the presence of a solvent together with the monomer and initiator. *Suspension* polymerization is conducted in aqueous solution with a water-insoluble monomer and initiator suspended in the solution; whereas in *emulsion* polymerization a monomer and a polymerization initator, soluble in water but insoluble in the monomer, are added to an aqueous solution of a surfactant. For emulsion polymerization to occur the surfactant must form micelles and therefore be sufficiently concentrated to remain above its cmc. Part of the monomer dissolves in the aqueous phase, part is solubilized in the micelles of the surfactant, and the remainder forms monomer droplets in the mixture.

The free radical initiation may be formed by heating a compound such as benzoyl peroxide:

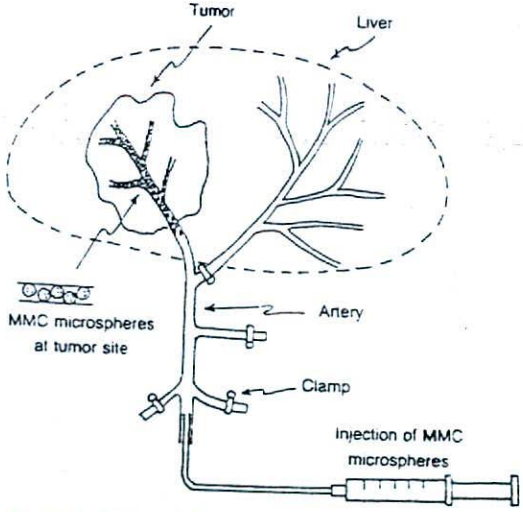
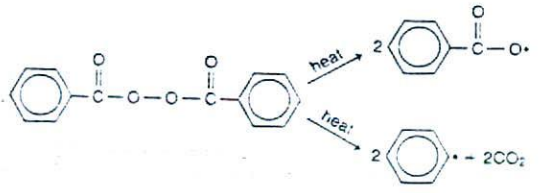
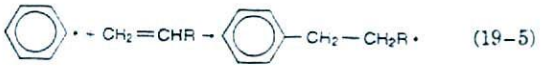


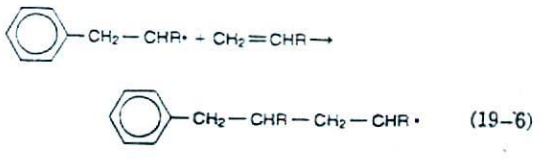
Fig. 19–7. Infusion of albumin microspheres by chemoembolization into the liver. (After Y. Morimoto et al., Int. J. Pharm. 54, 29, 1989, reproduced with permission of the copyright owner.)



(19–4)

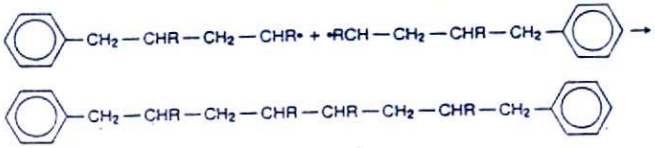


(19–5)



(19–6)

These steps show the *initiation*, *propagation*, and *termination* of the polymerization. Chain termination may occur by one of several processes, such as:



(19–7)

The end groups are then removed to yield the final polymer.

The polymer in its initial stage of formation enters the micelles where it grows rapidly in the presence of both solubilized monomer and free radicals R• that also enter the micelles. As more monomer is needed for continued growth of the polymer, monomer molecules leave the emulsified droplets in the aqueous medium and enter the micelles. As the process continues, the micelles are disrupted by the presence of the growing polymer molecules. The micelles essentially become "micellar swollen polymer particles," coated with surfactant and containing reacting monomer radicals.

The various species, monomers, micelles, surfactants, swollen polymer particles, and free radical initiators, together with the processes that occur in emulsion polymerization, are shown schematically in Figure 19–8.

To develop the mathematics of polymerization it is reasoned that the polymer chain reaction is begun with the formation of a free radical initiator (equations (19–4) and (19–5); the polymer is formed and grows in the propagation stage (equation 19–6) and continues until a second free radical molecule appears and terminates the chain reaction (equation (19–7)). There is a 50% chance at any moment that the $\bar{N}$ polymers will be terminated as in equation (19–7), and a 50% chance that the $\bar{N}$ micelles or swollen polymer particles are in readiness to receive another monomer and extend the polymer chains. The rate of polymerization, $\bar{R}_p$, is therefore proportional to one-half the number ($\frac{1}{2}\bar{N}$) of micelles or swollen polymer "factories." The rate of polymerization is also proportional to the concentration $[\bar{M}]$ of monomer present in the micelle-swollen polymer factories. Therefore, the rate of polymerization can be written

$$\bar{R}_p = k_p[\bar{M}]\left[\frac{\bar{N}}{2}\right] \qquad (19-8)$$

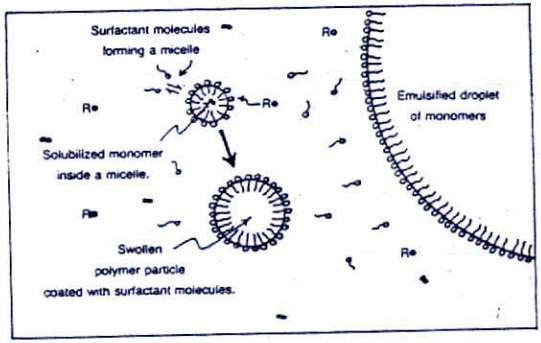


Fig. 19–8. A schematic of emulsion polymerization showing surfactant molecules, ⌒, and monomer molecules, ▬, in the aqueous phase; surfactant molecules on the surfaces of the monomer and the polymer droplets; surfactant molecules in the process of forming the micelle; monomer molecules solubilized in the core of the micelle; and free radical initiator molecules R• in the aqueous phase and entering the micelle. The dark arrow signifies conversion with time from the micelle containing solubilized monomer to the polymer droplet swollen with monomer and covered with surfactant molecules. (Modified from J. W. Vanderhof, E. B. Bradford, H. L. Tarkowski, J. B. Shaffer and R. M. Wiley, Adv. Chem. 34, 32, 1962.)

Example 19–2. Calculate the rate of polymerization $\bar{R}_p$ of a methyl methacrylate polymer that is undergoing emulsion polymerization with the free radical initiation provided by potassium persulfate as the initiator:

$$S_2O_8^{2-} + \text{acid} \rightarrow SO_4^{-\bullet}$$

The number of micelle-swollen polymer particles is $\bar{N} = 7.2 \times 10^{14}$ per liter, and the concentration of monomer, methyl methacrylate, in the micelle-swollen polymer "factories" is $[\bar{M}] = 3.5$ molar. The value k_p of the rate constant for emulsion polymerization was found experimentally to be 137.8 liters mole^{-1} sec^{-1}.

From equation (19–8):

$$\bar{R}_p = (137.8 \text{ liters mole}^{-1}\text{ sec}^{-1})(3.5 \text{ mole liter}^{-1})(7.2 \times 10^{14} \text{ particles liter}^{-1})(1/2)$$

$$= 1.74 \times 10^{17} \text{ liter mole}^{-1}\text{ sec}^{-1} \times \text{mole liter}^{-1} \frac{\text{particle}}{\text{liter}} \times \frac{\text{mole}}{6.022 \times 10^{23} \text{ particles}}$$

$$\bar{R}_p = 2.89 \times 10^{-7} \text{ (mole/liter)sec}^{-1}$$

The *kinetic chain length* $\bar{\nu}$ in a polymerization reaction is the rate of polymerization in the propagation stage divided by the rate of initiation, or $\bar{\nu} = \bar{R}_p/\bar{R}_i$. It is also the number of monomer molecules polymerized to produce a finished polymer chain and is therefore referred to in polymer science as the *degree of polymerization*, *DP* (see p. 558).

Example 19–3. Calculate the kinetic chain length $\bar{\nu}$ or degree of polymerization, *DP*, for the emulsion polymerization of methyl methacrylate of *Example 19–2*. The rate of initiation, $\bar{R}_i$ is 9.43×10^{-10} (mole/liter)sec^{-1}.

$$\bar{\nu} = DP = \frac{\bar{R}_p}{\bar{R}_i} = \frac{2.89 \times 10^{-7}\text{(mole/liter)sec}^{-1}}{9.43 \times 10^{-10}\text{(mole/liter)sec}^{-1}} = 306$$

It may appear that the number, 306, of monomers in the polymer is big, but the degree of polymerization for large polymer is big, but the degree of polymeriation for large polymers may actually be in the thousands or tens of thousands.

The preparation of new polymeric drug carriers has allowed the targeting of drugs to specific cells, tissues, and organs in the body, and has minimized toxic effects in healthy tissue. Rolland et al.[43] designed a new

site-specific drug delivery system consisting of polymethacrylic nanoparticles (nanospheres) prepared by the addition (chain) polymerization technique. The nanoparticles themselves have been found to show very low acute and subacute toxicities. Nanoparticles loaded with the antineoplastic agent doxorubicin, formerly known as adriamycin, are under clinical trials in human patients with liver carcinomas.

Nanoparticles and nanocapsules were prepared by N. Al Khouri Fallouh et al.[44] by interfacial polymerization with stirring of isobutyl cyanoacrylate in an aqueous medium containing dextran 70 and glucose in 0.001 molar HCl. The two different structures—nanocapsules and nanoparticles—were produced by varying the polymerization procedure. Nanocapsules may be used to enclose poorly water-soluble drugs that cannot be enclosed in nanoparticles. Drugs are liberated from nanocapsules by diffusion and passage through the thin wall of the capsule, whereas nanoparticles liberate the enclosed drug by erosion and leaching from the solid polymer mass. The authors[44] also considered the possibility of adsorbing drugs on the surface of nanoparticles as a possible carrier mechanism.

Gipps et al.[45] labeled polyhexylcyanoacrylate nanoparticles with carbon-14 and injected them into mice to ascertain the distribution of the particles in the body, using liquid scintillation counting. Following a single intravenous injection of 0.2 mL of the labeled nanoparticle preparation, 45% of the radioactive carbon remained in the body after 28 days. A large amount of the label was detected in the liver, with smaller amounts retained in the spleen and lungs. On repeated injection at intervals of 28 days, larger proportions of the nanoparticles accumulated in the spleen and lungs.

Studies have shown that improved anticancer activity and longer insulin response can be realized by entrapment of the active agent in polyalkylcyanoacrylate nanoparticles. It is therefore important to know the toxicity level of carriers such as nanoparticles, nanocapsules, microparticles, and liposomes. Kante et al.[46] found that the nanoparticles did not cause cellular damage until administered in high concentration in a cell culture medium. Neither nanoparticles nor their degradation products showed mutagenicity. Couvreur et al.[47] found that doxorubicin, an antineoplastic agent, when absorbed on nanoparticles reduced the weight loss and death rate of mice. Cardiotoxicity was also reduced because of the limited uptake of the drug-loaded nanoparticles by the myocardium.

A number of studies have been reported on the use of liposomes, microcapsules, and nanoparticles for the delivery of drugs to specific sites in the body. In addition to the investigations already mentioned—both research and applied—the references at the end of this chapter will be of assistance to workers entering the rapidly expanding field of controlled-delivery systems.

ROUTES OF ADMINISTRATION

Ocular Administration. Topical instillation is used in the treatment of local diseases affecting the eye. The absorption of drugs takes place through either the conjunctival sac or the corneal membrane (Fig. 19–9),

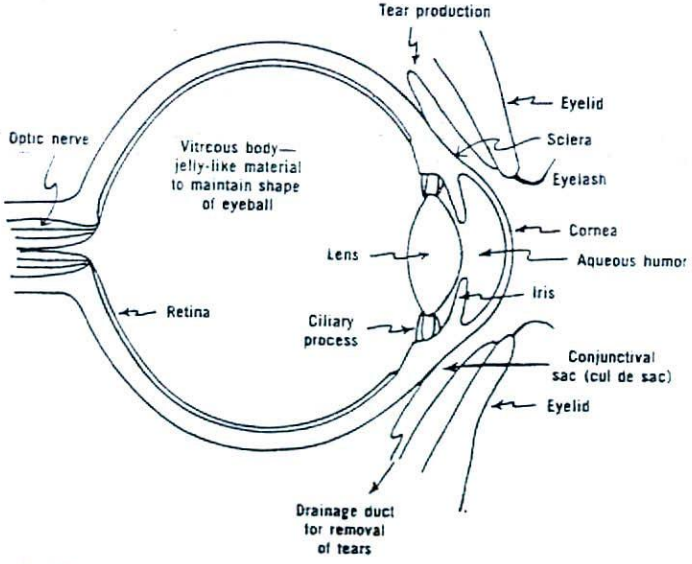


Fig. 19–9. A section of the eye showing the possible routes of drug administration.

the latter being a more effective barrier for drug absorption. The bioavailability of aqueous ophthalmic solutions is usually low owing not only to the barrier properties of the conjunctiva and cornea but also to the loss of drug by several processes. Precorneal loss of drug is due to tear turnover, drainage, systemic absorption, and in situ metabolism.[48] Tear turnover dilutes the drug, thus reducing the gradient of transport through the cornea. The difference between the pH of ophthalmic solutions of pilocarpine, between 4 and 5, and the pH of tears, about 7.47, causes increased lacrimation and loss of drug. An acidic pH is needed to increase the stability of pilocarpine. This drug is used as a topical miotic to reduce the intraocular pressure associated with glaucoma. Its ocular bioavailability is very low. About 1 to 3% of the instilled dose is absorbed into the eye; 50% of the dose is lost by systemic absorption from the conjunctiva.[49] The topical administration of beta-blocking agents such as propranolol is effective in the control of glaucoma.[50] The loss of levobunolol, also a beta-blocking agent, by systemic absorption is about 46%, and 12% is converted to dihydrolevobunolol in the ocular tissues.[51] The conjunctival and nasal mucosae play a role in the systemic absorption of ocularly applied drugs. The conjunctival mucosa has proteases capable of metabolizing peptides administered by the ocular route.[52]

Transport Through the Cornea. The corneal membrane is permselective, that is, it is able to discriminate between the transport of molecules having different charges. The electrical potential of this membrane, about 25 mV, is due to inward active Na^+ transport. At the isoelectric point (pH 3.2), the corneal membrane is electrically neutral and there is no ionic selectivity of positive or negative ions. At the tear pH of 7.47, the cornea is negatively charged and selectively permeable to cations, whereas at pH below 3.2 it is selectively permeable to anions.[53] Drug transport through the cornea is mainly a passive process. The corneal barrier can be considered as a laminated membrane consisting of the epithelial, stromal, and endothelial layers. Figure 19–10 shows the rate-limiting steps for the transport of hydrophilic and lipophilic drugs. For hydrophobic drugs, the stroma is the limiting region, whereas for hydrophilic drugs the epithelium gives the most resistance.

Grass and Robinson[54] used an in vitro perfusion technique to study the permeation of drugs through albino rabbit cornea. The total resistance to the drug transport, R, from the donor phase in the perfusion apparatus can be written as the summation of the resistance of the individual layers:

$$R = R_{a(d)} + \frac{R_m}{K} + R_{a(r)} \qquad (19-9)$$

where $R_{a(d)}$ and $R_{a(r)}$ represent the resistances of the aqueous diffusion layers on the donor side and the receptor side, respectively. The resistance of the stromal layer (aqueous) is included in the term, $R_{a(r)}$. R_m represents the resistance of the lipid membrane, that is, the corneal epithelial layer. Substituting resistances by the ratio of the thicknesses to the diffusion coefficients, in other words, h_i/D_i, equation (19–9) becomes

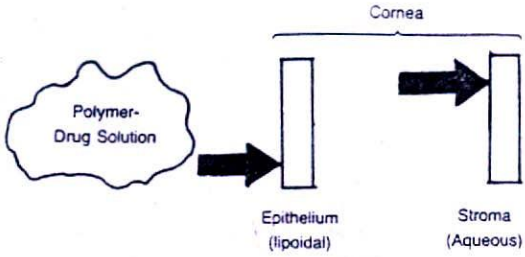


Fig. 19–10. Rate-limiting effect of corneal epithelium (lipid) and stroma (aqueous) for drugs with low *o/w* partition coefficients (arrow located low on the epithelium) and for drugs with high *o/w* partition coefficients (arrow located high on the stroma). (After G. M. Grass and J. R. Robinson, J. Pharm. Sci. 73, 1021, 1984, reproduced with permission of the copyright owner.)

$$R = \frac{h_{a(d)}}{D_a} + \frac{h_m}{KD_m} + \frac{h_{a(r)}}{D_a} \qquad (19-10)$$

where $h_{a(d)}$ and $h_{a(r)}$ represent the thickness of the aqueous layer in the donor and receptor phase, respectively, and h_m is the thickness of the epithelial layer. Therefore, the flux of the drug is defined as a combination of membrane control and diffusion layer control (Chapter 13, p. 338):

$$J = \frac{D_m K D_a C}{h_m D_a + h_a K D_m} \qquad (19-11)$$

From equation (19–11), when the diffusion through the aqueous medium is much faster than through the membrane (i.e., $h_m D_a >> h_a K D_m$), the diffusion is controlled by the membrane. On the other hand, when diffusion through the aqueous medium is much slower than that of the membrane (i.e., $h_m D_a << h_a K D_m$), the diffusion is controlled by the aqueous layer. These two limiting situations reduce equation (19–11) to equations (13–57) and (13–58) page 338. The lipophilic epithelial tissue can be viewed as a sieve in which the transport of drugs is hindered at a certain molecular size. Grass and Robinson[55] used transmission electron microscopy to visualize the actual pathway of drug transport through the cornea. The results indicated that hydrophilic compounds are preferentially located in the intercellular spaces, whereas hydrophobic compounds are present in the lipid structures of the tissue. The size of the intercellular space for diffusion of drugs was estimated to be smaller than 5 nm. Thus, the pore pathway is the main transport route for small hydrophilic molecules, as contrasted to the partition mechanism for large or lipophilic molecules.

The energy of activation E_a (pp. 295, 351, and 352) can be related to the transport mechanism.[54] This term is computed from the slope of a plot of ln P against $1/T$, where P is the permeability coefficient of the drug and T is the absolute temperature:

$$\ln P = -\frac{E_a}{R}\frac{1}{T} + \ln A \qquad (19-12)$$

The E_a values for hydrophilic molecules, such as ethanol, butanol and glycerol, ranged from 4.5 to 6.5 kcal/mole. These values are of the order of magnitude corresponding to the diffusion through an aqueous medium only. In contrast, hydrophobic molecules such as triamcinolone acetonide and hydrocortisone showed much larger E_a values, about 25 kcal/mole. These higher values result from drug transport by a partitioning mechanism.

Example 19–4. The permeability of hydrocortisone across rabbit cornea was determined at several temperatures:

$\frac{1}{T}$ (°K^{-1})	0.0032	0.0033	0.0034	0.0035
ln P	−11.630	−12.911	−14.196	−15.481

Compute the energy of activation E_a for the transport of hydrocortisone.

Using linear regression, one obtains

$$\ln P = -12838\frac{1}{T} + 29.45 \quad (r^2 = 0.999)$$

$$\frac{E_a}{R} = \text{slope} = -12838°\text{K}; \quad E_a = 12838°\text{K} \times 1.9872 \text{ cal °K}^{-1} \text{ mole}^{-1}$$

$$E_a = 25511 \text{ cal/mole} = 25.5 \text{ kcal/mole}$$

Schoenwald and Huang[56] found empirical correlations between the log of the permeability coefficient and the molecular weight, partition coefficient, and degree of ionization for beta-blocking agents (propranolol and related drugs). The expression is

$$\log P = 0.972 \log K - 0.112 (\log K)^2 - 2.71 \log MW - 9.26 \log \alpha + 0.219 \qquad (19-13)$$

where K is the octanol–water partition coefficient, MW is the molecular weight of the penetrant, and α is the degree or fraction of ionization. For weakly basic compounds,

$$\alpha = \frac{1}{1 + \text{antilog}(\text{pH} - \text{p}K_a)} \qquad (19-14)$$

Equation (13–78) on page 342 gives the fraction of ionization α multiplied by 100 to convert to percentage ionization.

Example 19–5. Compute the permeability coefficient, P (cm/sec) of the hypertensive agent propranolol across rabbit cornea at pH 7.65. The octanol–water partition coefficient K is 1640, the molecular weight of propranolol is 257, and the pK_a is 9.23.

The degree of ionization at pH 7.65 is

$$\alpha = \frac{1}{1 + \text{antilog}(7.65 - 9.23)} = 0.974$$

$$\log \alpha = -0.011$$

The permeability coefficient is

$$\log P = (0.972 \times 3.215) - (0.112 \times 10.34) - (2.71 \times 2.41) - [9.26(-0.011)] + 0.219$$

$$= -4.243$$

$$P = 5.7 \times 10^{-5} \text{ cm/sec}$$

Controlled Ocular Drug Delivery. The action of a drug for ocular delivery can be prolonged (1) by reducing drainage by the use of viscosity-enhancing agents, suspensions, emulsions, erodible, and nonerodible matrices and (2) by enhancing the corneal penetration by using prodrugs and liposomes (see pp. 513 to 515). The optimal viscosity range to reduce drainage loss is between 12 and 15 cps when polyvinyl alcohol[57] or methyl cellulose[58] is used as a viscosity enhancer. To minimize potential irritation, ophthalmic suspensions are prepared by micronization techniques. The dissolution rate of the large particles is smaller than that of small particles, so that the large particles may drain away before dissolution takes place, thus decreasing bioavailability.[59] Hui and Robinson[60] studied the effect of dissolution rate on ocular drug bioavailability. After instillation of a suspension, the drug penetrates into the cornea or conjunctiva from the saturated solution. Additional particles dissolve to maintain a reservoir of saturated solution. To obtain the desired bioavailability, the dissolution rate of the drug must be greater than the clearance of the dose from the conjunctival sac and approximately equal to the absorption rate. Many drugs cannot satisfy these requirements.

Precorneal retention and duration of action can be increased by using water-soluble matrices in which the drug is either dispersed or dissolved. The delivery of drugs from hydrophilic matrices is fast because the tear fluid rapidly penetrates into the matrix. The prolonged action is not controlled by the vehicle but is caused by the precorneal retention of the drug. The penetration of water into the matrix can be reduced using hydrophobic polymers such as alkyl half-esters of poly(methyl vinyl ether–maleic anhydride) (PVM–MA). The surface of the matrix is water-soluble above certain pH values, owing to the ionizable carboxylic groups. However, the hydrophobic alkyl ester groups avoid the penetration of water into the matrix. The diffusion of drug from the matrix is impeded so that it is released at the rate at which the polymer surface is dissolved. In one study, pilocarpine was released from PVM–MA polymers according to zero-order kinetics and was controlled by the erosion of the polymer surface.[49] Grass let al.[61] prepared erodible and nonerodible dry films for sustained delivery of pilocarpine. The polymers used in both cases were polyvinyl alcohol and carboxyl copoly-

mer (Carbomer 934). The release of drug from the films fitted either the Hixon–Crowell dissolution cube root equation (Chapter 13, pp. 333, 334) or the diffusion-controlled dissolution equation proposed by Cobby et al.[62] (see p. 534), the latter providing the best fit. The in vivo miotic response was delayed longer than that of pilocarpine solutions.

The ocular delivery of drugs from matrices can be improved by the use of bioadhesive polymers. Johnson and Zografi[63] measured the adhesion (adhesive strength) of hydroxypropyl cellulose to solid substrates as a function of dry film thickness. A "butt adhesion test" used by these workers provided a constant slow rate of film detachment to maintain the viscoelastic contribution of the film relative to the adhesion measurements as a constant. For thickness less than 20 μm, there is a linear relationship between the adhesive strength, Y (in g/cm^2) and the film thickness, h (in μm). The adhesive failure, Y_0, can be obtained by extrapolating the adhesive strength to zero film thickness.

Example 19–6. The adhesion, Y, of hydroxypropyl cellulose to polyethylene surfaces as a function of the film thickness (h) of the adhesive is

Y (g/cm^2)	3850	2800	1750	700
h (μm)	5	10	15	20

Compute the adhesive failure, Y_0. A regression of Y (dependent variable) against h (independent variable) gives

$$Y = -210\,h + 4900$$

The adhesive failure is given by the intercept, $Y_0 = 4900$ g/cm^2.

The *work of adhesion* W_a (pp. 368–369) of the dry film on the solid surface can be computed from the surface tension of the polymer and the solid surface[63]:

$$W_a = \frac{4\gamma_s^d\gamma_p^d}{\gamma_s^d + \gamma_p^d} + \frac{4\gamma_s^p\gamma_p^p}{\gamma_s^p + \gamma_p^p} \qquad (19-15)$$

where γ_s and γ_p are the surface tensions of the solid and the polymer, respectively. The superscripts d and p represent the contribution to the total surface tension from nonpolar and polar portions of the molecule.

Example 19–7. Compute the work of adhesion of hydroxypropyl cellulose films to a solid surface of polyethylene from the following data: $\gamma_s^d = 34.2$ erg/cm^2; $\gamma_s^p = 3.4$ erg/cm^2; $\gamma_p^d = 24.7$ erg/cm^2; $\gamma_p^p = 16.3$ erg/cm^2.

$$W_a = \frac{4 \times 34.2 \times 24.7}{34.2 + 24.7} + \frac{4 \times 3.4 \times 16.3}{3.4 + 16.3}$$

$$W_a = 68.6 \text{ erg/cm}^2$$

Ocusert System. The pilocarpine-containing device Ocusert, introduced in 1975 by Alza Corporation, was the first controlled topical dosage form marketed for use in the eye. The device (Fig. 19–11*a*) consists of a central core or reservoir of pilocarpine between two membrane surfaces, made of an ethylene–vinyl acetate copolymer, that control the rate of release of the drug. The oval device, slightly larger than a contact lens, is placed in the cul-de-sac under the upper or lower lid (Fig. 19–11*b*), where pilocarpine is released at a zero-order rate and is absorbed into the cornea of the eye. Two products are available: Ocusert P-20, which delivers a dose of 20 μg/hr, and Ocusert P-40, which delivers a dose of 40 μg/hr.

The ocular delivery system was designed to overcome the inefficient delivery of pilocarpine from ophthalmic drops. Because of the close contact with the eye and continuous release of drug from the Ocusert over a period of a week, only about one fourth as much pilocarpine must be administered as compared with the dropper technique, and this reduction in dose overcomes toxicity and side effects. The specialized medication system is expensive, however, and probably will be used only in patients who need continuous medication, can tolerate the presence of the disk in the eye, and can afford the therapy.

With drugs that are only sparingly soluble in water, such as chloramphenicol, release in the eye may be calculated from a form of Fick's law (Chapter 13):

$$M = \frac{SDKC_s}{h}\,t \qquad (19-16)$$

in which M is the accumulated amount released and t is the time. S is the surface area of the device in contact with the eye, D is the diffusion coefficient of the Ocusert membrane, K is a liquid–liquid partition coefficient between the Ocusert and the eye fluids, C_s is the solubility of the drug in water, and h is the Ocusert membrane thickness. As observed in Figure 19–12, a plot of accumulated drug release against time is linear, showing a break at point A (130 hr), then becoming horizontal, indicating that chloramphenicol is depleted and no more is release after 130 hours. A plot of *release rate*, rather than amount, versus time results in a straight horizontal line to point A, then tends toward zero (Fig. 19–12, inset). The curve does not fall vertically following point A, but descends parabolically as observed in the inset of Figure 19–12. These plots indicate that the release rate of a sparingly soluble drug is almost constant, that is, a zero-order release rate over most of the lifetime of the device, rather than a first-order release, which would represent a continuously decreasing rate with time.

Example 19–8. The diffusion coefficient of a new chloramphenicol derivative in the Ocusert device is 3.77×10^{-5} cm^2/hr. The surface area S of the Ocusert is 0.80 cm^2, the partition coefficient K between the Ocusert and ocular fluids is 1.03, the thickness of the membrane h is 0.007 cm, and the solubility C_s in water (25° C) of the new compound is 3.93 mg/cm^3. By use of equation (19–16), calculate the cumulative amount of drug released in 125 hours.

$$M = \frac{(0.80 \text{ cm}^2)(3.77 \times 10^{-5} \text{ cm}^2/\text{hr})(1.03)(3.93 \text{ mg/cm}^3)(125 \text{ hr})}{0.007 \text{ cm}}$$

$M = 2.18$ mg released in 125 hours

Pilocarpine is water soluble, and equation (19–16) is not an exact representation of the profile of the release

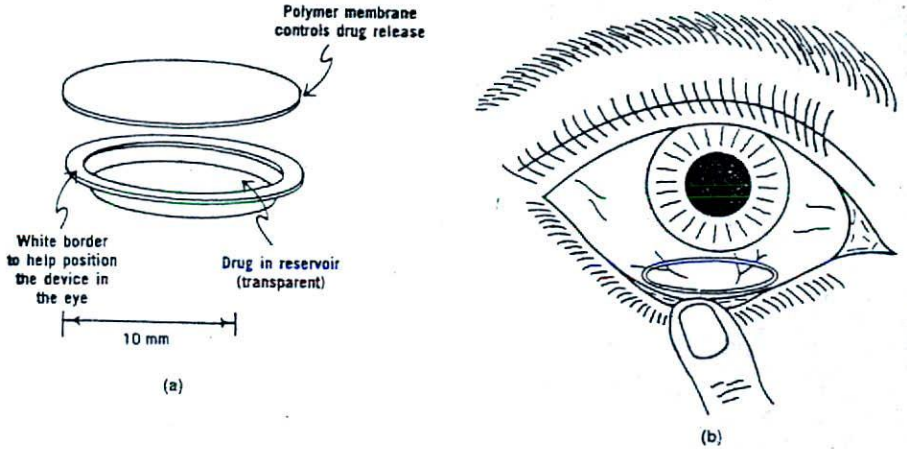


Fig. 19–11. (*a*) Schematic of Ocusert (Alza). (After K. Heilmann, *Therapeutic Systems*. Georg Thieme, Stuttgart, 1978, p. 67.) (*b*) Insertion of the Ocusert into the cul-de-sac of the eye. (ibid. p. 69: reproduced with permission of the copyright owner.)

rate with time for such a compound. The flux or rate per unit time for a water-soluble compound is not horizontal (Fig. 19–12 inset) but rather declines slowly as the release proceeds. By the proper choice of membranes for the Ocusert, however, the release rate of pilocarpine can be held essentially constant (near zero-order drug release) for up to 7 days of delivery.

Nasal Administration. The nose, Figure 19–13, consists of two openings (nostrils) that are separated by a median septum. The vestibule at the entrance of each nostril is covered with hairs, which prevent entrance of air-suspended particles. The nose cavity is divided by the septum into two chambers called *fossae*. They form passages for air movement from the nostrils to the nasopharyngeal space at the back of the nose. Each fossa consists of two parts, an olfactory region at the front of the nose and a respiratory region that accounts for the remainder of the fossae.

The nasal cavity is lined with a mucous membrane, called the *membrana mucosa nasi*, which is continuous with the skin of the nostrils. The respiratory portion of the nasal cavity contains ciliated (hair-like) projections consisting of columnar epithelial cells.

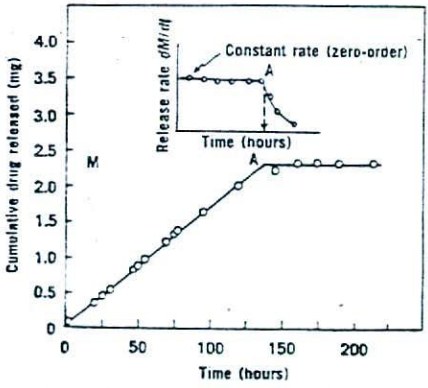


Fig. 19–12. Controlled drug release of chloramphenicol through the Ocusert membrane. The inset shows the relationship of the *release rate* rather than the cumulative amount released (main curve), versus time.

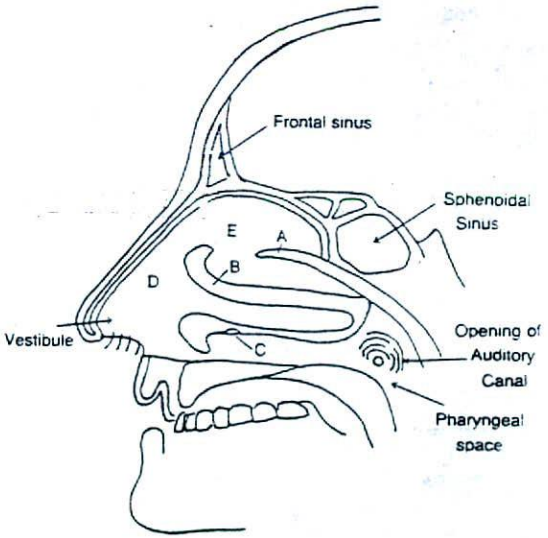


Fig. 19–13. Nasal anatomy. Modified from references 64 and 65. Key: A, upper meatus; B, middle meatus; C, opening of nasolacrimal duct on lower meatus; D, left fossa, olfactory region; E, left fossa, respiratory region.

The nasal cavity consists of three passageways or meatuses: upper, middle, and lower meatus. As observed in Figure 19–13 the nasolacrimal duct drains into the lower meatus. The nose is connected to the middle ear through the nasopharynx or postnasal space and through the auditory canal. The compartments of the nose are connected to the conjunctiva of the eye by way of the nasolacrimal and lacrimal ducts, and through several sinuses that drain into the nose. A portion of a drug administered into the conjunctiva of the eye may enter the nose through these ducts and sinuses, and may also pass into the esophagus.[64,65]

Nasal administration is widely used for local effects, but it is also a potential site for systemic drug absorption owing to its large surface area. The vascular bed of the nasal mucosa favors the rapid passage of fluids and dissolved compounds from the mucosa to the systemic circulation. The nasal route avoids the first-pass effect (that is, possible decomposition as the drug passes through the liver) and gastrointestinal degradation, providing an alternative route for oral administration. Most drug absorption occurs at the sinuses, where the mucous membrane is very thin and widely vascularized.[66] Lipophilic drugs such as propranolol produce blood levels similar to those observed after intravenous administration. Sustained nasal release formulations of propranolol result in prolonged drug levels.[67] Rapid absorption has been found for progesterone and testosterone.[68] Hydromorphone, a semisynthetic analgesic used for the relief of postoperative pain or severe chronic pain, is well absorbed by the nasal route.[69]

Huang et al.[70] developed an in situ rat technique to study nasal absorption. The drug solution is perfused at a constant rate through the nasal cavity of the rat. The extent of absorption is obtained by subtracting the initial amount of drug from that remaining in the perfusing solution. The nasal absorption of benzoic acid was found to depend on pH and followed first-order kinetics. At low pH values,

$$k_{obs} = k_{HA} \frac{[H^+]}{[H^+] + K_a} \qquad (19-17)$$

and at high pH values,

$$k_{obs} = k_{A^-} \frac{K_a}{[H^+] + K_a} \qquad (19-18)$$

where k_{obs} is the overall first-order absorption constant, and k_{HA} and k_{A^-} are the first-order absorption constants for the un-ionized and ionized species of benzoic acid, HA and A^-, respectively.

Example 19–9. (*a*) Compute the k_{obs} value at pH 2.4 and pH 7.19, where benzoic acid is predominantly in its nonionized and ionized forms, respectively. K_a is equal to 6.30×10^{-5}, k_{HA} is 9.75×10^{-3} min^{-1}, and k_{A^-} is 2.40×10^{-3} min^{-1}. (*b*) Compute the half-life for nasal absorption of benzoic acid in its nonionized form (pH 2.4) and ionized form (pH 7.19).

(*a*) From equation (19–17), at pH = 2.4

$$k_{obs} = 9.75 \times 10^{-3} \frac{3.98 \times 10^{-3}}{3.98 \times 10^{-3} + 6.3 \times 10^{-5}}$$

$$k_{obs} = 9.60 \times 10^{-3}\ min^{-1}$$

From equation (19–18) at pH 7.19

$$k_{obs} = 2.40 \times 10^{-3} \frac{6.30 \times 10^{-5}}{6.46 \times 10^{-8} + 6.3 \times 10^{-5}}$$

$$k_{obs} = 2.40 \times 10^{-3}\ min^{-1}$$

(*b*) From equation (12–18), page 288, the half-life for nasal absorption at 25° C is

(at pH 2.4) $t_{1/2} = \frac{0.693}{k_{obs}} = \frac{0.693}{9.60 \times 10^{-3}} = 72$ min for the nonionized form

(at pH 7.19) $t_{1/2} = \frac{0.693}{2.40 \times 10^{-3}} = 289$ min for the ionized form

Nasal administration is one of the most investigated routes for absorption of peptides and proteins. However, the bioavailability of these compounds is low due to their high molecular weight. Maitani et al.[71] studied the influence of molecular weight and charge on nasal absorption of neutral and positively charged (polycation) dextran derivatives in rabbits. These compounds were chosen as macromolecular models of water-soluble drugs. The plasma concentration resulting from nasal absorption of both neutral and charged dextrans decreased as the molecular weight of the compound increased. Additional information on nasal absorption of peptides and proteins is found in the two treatises by Chien et al.[72,73] Unfortunately, peptides are degraded at the site of administration by proteolytic enzymes, mainly aminopeptidases. Thus, the nasal dose needed for insulin is considerably greater than the parenteral dose required to produce a similar effect. Hussain et al.[74] found that even in concentrations as small as nanomolar (i.e., on the order of 10^{-9} molar), α-aminoboronic acid derivatives, which are potent inhibitors of aminopeptidases, greatly increase the absorption of leucine–enkephalin, a model peptide.

To improve the nasal absorption of peptides, various *permeability enhancers* have been investigated. Permeability enhancers are compounds that promote or enhance the absorption of drugs through the skin or mucosae, usually by reversibly altering the permeability of the membrane. Bile salts and other biologic agents have been shown to enhance drug permeability of the nasal mucosa. Thus, nasal absorption of enkephalin analogs increases from about 59% to 94% of the subcutaneous dose in the presence of 1% sodium glycholate.[75] The local antibiotic bacitracin, and sodium taurodihydrofusidate,[76] a derivative of the antibiotic fusidic acid but without antibiotic activity, markedly enhance the nasal absorption of peptides such as gonadorenin, a luteinizing hormone–releasing hormone and its agonist, buserelin. The properties of sodium salts of fusidic acid resemble those of the bile salts. It has been reported that bile salts may damage the

epithelial layer, which serves as a defense against infecting organisms. In addition to mucosal damage, some drugs for local and systemic use and some additives affect ciliary movement, which is the most important process in nasal mucociliary clearance. Some beta-adrenergic and cholinergic drugs stimulate ciliary movement and increase mucociliary clearance. On the other hand, local anesthetics, propranolol, and antihistamines, as well as some enhancers such as the bile salts, suppress ciliary movement. Thus, enhancers must be chosen carefully in the design of nasal drug formulation for systemic effects, particularly in drugs meant for use in long-term treatment.[77]

Dosage forms for nasal absorption must deposit and remain in the nasal cavity long enough to allow effective absorption. The standard methods of administration are sprays and drops. The particle size in aerosols is important in determining the site of deposition. Particles less than 0.5 μm in diameter may pass through the nose and reach the terminal bronchi and alveoli of the lungs. A nasal spray requires that the particles have a diameter larger than 4 μm to be retained in the nose and to minimize passage into the lungs. Harris et al.[78] studied the influence of the delivery system on drug deposition. The nasal spray deposits drug in the forward part of the nasal atrium, whereas nasal drops are dispersed throughout the nasal cavity. A spray clears more slowly than the drops since the spray is deposited in nonciliated regions. The bioavailability of desmopressin, a peptide derivative of 8-D-arginine vasopressin, is improved by administering it with a metered-dose inhaler* rather than by nasal drops.[79] (See Figure 19–14.)

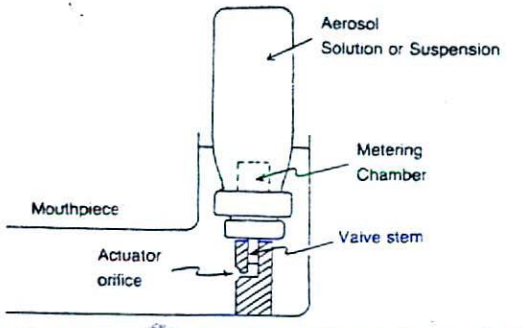


Fig. 19–14. Metered-dose device for drug administration to nasal and pulmonary regions. (From P. R. Byron, Ed., *Respiratory Drug Delivery*, CRC, Boca Raton, Fla., 1990, p. 171, reproduced with permission of the copyright owner.)

Buccal Administration. The absorption of drugs through the oral mucosa improves bioavailability of drugs that might otherwise be metabolized during their passage through the gastrointestinal tract or the liver, where the undesired first-pass effect occurs. The oral mucosa consists of stratified squamous epithelium; its thickness and degree of keratinization vary from one region to another and may affect the permeability of a drug.[80] Absorption is mainly a passive process that occurs through the buccal, sublingual, or gingival mucosa, the palatal and tongue mucosae being less permeable. In addition to circumventing first-pass metabolism, an advantage of the buccal route is its accessibility. A dosage form can easily be placed in and removed from the site of application,[81] and the buccal route is therefore used locally to administer antimicrobial and antiinflammatory agents, local anesthetics, and conventional pharmaceuticals including mouthwashes, oral gels or pastes, lozenges, and sublingual tablets. Buccal administration has been studied for the systemic delivery of peptides, polypeptides such as insulin, and nifedipine.[82]

The dosage forms should remain in contact with the oral mucosa to allow absorption of the drug. Therefore, taste is an important factor to be considered in the design of the product. Bitter taste can be masked by using an insoluble derivative of the drug so that the threshold taste concentration is not reached. Another approach is the use of prodrugs with acceptable organoleptic characteristics. Hussain et al.[83] prepared bitterness prodrugs of several opioid antagonists by esterification of their phenolic groups. The bitter taste of these compounds is due to the interaction of the phenolic groups with a taste receptor on the tongue. The rate of absorption of the prodrugs was greater than the rate of hydrolysis, so that the bitter taste did not develop.

Conventional dosage forms do not remain in contact with the oral mucosa long enough for controlled release to be achieved. Bioadhesive polymers that bind to mucin or the epithelial surface may be used to place the drug at a specific site on the mucosa, allowing prolonged delivery. Sodium carboxymethylcellulose, Carbopol 934, and hydroxypropylcellulose are examples of polymers for use in buccal dosage forms to produce adhesiveness. When the polymer is hydrated, it adheres to the oral mucosa and inhibits salivation, tongue movements, and swallowing for a period of time. Hydrophilic functional groups such as —OH, —COOH, and NH_3 on the polymers provide good wet adhesion.[82] The adhesiveness can be evaluated in vitro by tensile testing and other methods using isolated tissues of the gastrointestinal tract or mucous membrane. Park[84] used mucin molecules adsorbed on red colloidal gold. When the mucin–gold conjugates interact with the bioadhesive polymer, a red color is developed on the surface, and the adhesiveness can be quantitatively compared by measuring the intensity of the color. Rao and Buri[85] used an in situ method in the rat jejunum

*A metered-dose inhaler is a device which, when manually compressed, delivers an accurate and reproducible dose of the nasal (or bronchial) medication.

and stomach to evaluate the adhesiveness of drug particles coated with several polymers. Carboxymethylcellulose adhered more strongly to the mucus than hydroxypropylmethylcellulose (HPC). These authors suggested that the adhesion was promoted by relaxation of the polymer chains, which facilitated their interlinking with the glycoproteins of the mucus.

Adhesive patches are used to achieve sustained release. Anders and Merkle[81] prepared adhesive-laminated patches for buccal administration of oligopeptides. The device consists of an impermeable backing layer and a mucoadhesive polymer layer containing the drug. The shape and size can vary depending on the site of administration; whether at the buccal, sublingual, or gingival mucosa. The duration of mucosal adhesion, as determined in humans, depended on the polymer type and the amount and viscosity of the polymer used. The release of a model drug, sodium salicylate, from the patch was controlled by the dissolution kinetics of the polymer carrier rather than the drug diffusion out of the polymer. Collins and Deasy[82] prepared three-layer devices. The upper layer consisted of a nonadhesive and flavored waxy material containing the drug, and the middle layer was prepared from magnesium stearate (antiadhesive). The lower layer, made of a mixture of HPC and carbopol, was designed to adhere to the oral mucosa. The three-layered device showed constant salivary levels of the antiinfective agent cetylpyridinium chloride in human volunteers over the 3-hour period studied.

Pulmonary Administration.[86,87] The respiratory tract has a large surface area and is easily accessible for the treatment of respiratory diseases. The surface increases from the most exterior region (nasopharyngeal) to the tracheobronchial and pulmonary regions, the latter consisting of bronchioles and alveoli. The elements of the pulmonary route are illustrated in Figure 19–15. Aerosols are widely used to deliver drugs in the respiratory tract. The deposition mechanism of the particles depends on many factors, such as the inhalation regime and particle size, shape, density, charge, and hygroscopicity. The size of solid particles or liquid droplets in aerosols normally ranges from 1 to 10 μm, and is expressed as the *aerodynamic diameter*, $d_{ae} = \rho^{1/2}d$, where ρ is the density of the particle and d the observed diameter. Generally, the particles are delivered via mouth inhalation, to bypass the nasopharyngeal cavity. However, the total retention of particles is usually only 50 to 60% of the administered dose.

Larger particles (>5 μm) are usually deposited via inertial impaction in the upper airways. Moderate size particles (1–5 μm) can settle out from the airstream under gravitational influence. Submicron particles deposit as a result of Brownian movement (see p. 400) mainly in the lower airways (bronchial and alveolar regions).[88] The inhaled particles can be transported from one region to another within the respiratory tract. The duration of local therapeutic activity is

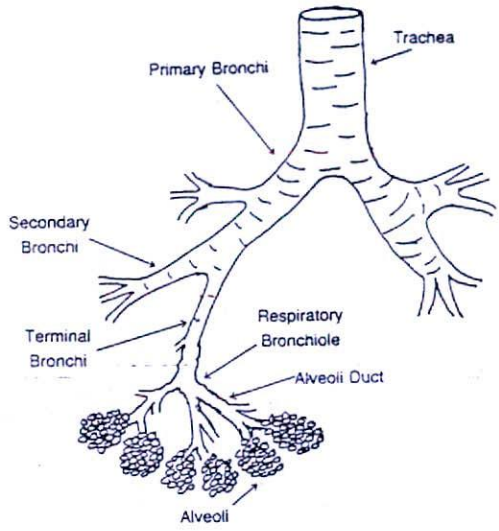


Fig. 19–15. Regions of the bronchial and pulmonary routes.

a complex function of particle deposition, mucociliary clearance, drug dissolution or release (for solid aerosols), absorption, tissue sequestration, and metabolism kinetics.

Byron[89] proposed a mathematical model to calculate drug residence times and dose fractions in the three functional portions of the respiratory tract: the nasopharyngeal region and the tracheobronchial and pulmonary (alveolar) regions. The deposition in the ciliated airways was largely unaffected by breath-holding, and the particles showed a maximum d_{ae} between 5 and 9 μm (slow inhalation) and 3 and 6 μm (fast inhalation). Alveolar deposition was dependent on the mode of inhalation and the breath-holding. The latter is a common practice and allows deposition of small particles which otherwise would be exhaled. To determine the effect of breath-holding on the deposition of particles, the *sedimentation efficiency*, S, was defined as

$$S = \frac{\text{distance the particle falls during breath-holding}}{\text{mean regional airway diameter}} \qquad (19-19)$$

The mean regional diameters for the three areas considered are 5 cm for the mouth, 0.2 cm for the tracheobronchial region, and 0.073 cm for the alveoli (pulmonary region). In cases where the sedimentation efficiency was >1, S was assigned a value of unity. A total lung volume after inhalation, V_t, of 3000 cm^3 was divided into 30, 170, and 2800 cm^3 for the mouth (M), tracheobronchial (TB) region, and alveolary (P) region, respectively. For each particle size, the *exhaled dose fraction* E is given by

$$E = 1 - (f_M + f_{TB} + f_P) \qquad (19-20)$$

where the terms f_M, f_{TB}, and f_P stand for the fractional deposition in each of the three regions. During breath-holding, additional fractions will sediment, depending on the sedimentation efficiency and the ratio of the regional volume to the total volume of the lungs. The *sedimentation dose fraction*, *SDF*, after breath-holding is calculated from the expression

$$SDF = E\left(\frac{SV_r}{V_t}\right) \qquad (19-21)$$

where V_r is the regional volume of the *M*, *TB*, or *P* regions and V_t the total volume after inhalation (3000 cm^3).

Example 19–10. For a 3-μm monodisperse aerosol inhaled at 22.5 L/min, the fractional depositions were found to be $f_M = 0.04$, $f_{TB} = 0.14$ and $f_P = 0.55$. Compute the undeposited or exhaled fraction *E*, and the additional sedimentation of the undeposited fraction in the mouth and tracheobronchial and alveolarly regions after 10 seconds of breath-holding. The velocity of sedimentation of the particles is 0.027 cm/sec.

From equation (19–20) the undeposited (exhaled) fraction is

$$E = 1 - (0.04 + 0.14 + 0.55) = 0.27$$

After 10 seconds of breath-holding, the distance of particle fall was 10 sec × 0.027 cm/sec = 0.27 cm. Substitution of this value and the mean diameter of the alveolary (*P*) region in equation (19–19) gives the sedimentation efficiency in the pulmonary region, S_P:

$$S_P = \frac{0.27}{0.073} = 3.70$$

since $S_P > 1$, a value of $S_P = 1$ is taken. From equation (19–21) the sedimentation dose fraction becomes

$$SDF_P = (0.27)(1)\frac{2800}{3000} = 0.252$$

Analogously, for the tracheobronchial zone (mean diameter 0.2 cm), a value of $S_{TB} > 1$ is obtained, so S_{TB} is taken equal to unity, and for the sedimentation dose fraction, one obtains

$$SDF_{TB} = (0.27)(1)\frac{170}{3000} = 0.0153$$

For the mouth region, *M*, the mean diameter is 5 cm,

$$S_M = \frac{0.27}{5} = 0.054$$

and

$$SDF_M = (0.054)\frac{30}{3000} = 5.4 \times 10^{-4}.$$

Thus, the total additional dose deposited after 10 seconds of breath-holding is

$SDF = SDF_P + SDF_{TB} + SDF_M = 0.252 + 0.0153 + (5.4 \times 10^{-4}) = 0.268$.

These results show that for 3-μm particles breath-holding is adequate to deposit particles in the alveolar region ($SDF_P = 0.252$); whereas breath-holding is inadequate to deposit these particles in the mouth ($SDF_M = 0.00054$) and in the tracheobronchial region ($SDF_{TB} = 0.0153$).

Byron et al.[90] used an isolated perfused rat lung preparation to study the deposition and absorption of disodium fluorescein from solid aerosols having an aerodynamic diameter of 3 to 4 μm. The aerosols were administered for 20 minutes under different inhalation regimes (respiration frequency *RF*, in cycles min^{-1}). The total dose administered *D* can be divided into a transferable amount *A* that diffuses into the perfusate according to a first-order rate constant *k*, and an untransferable amount *U* according to the scheme:

$$D \begin{cases} \nearrow U \\ \searrow A \xrightarrow{k} B \end{cases}$$

assuming instantaneous dissolution of *A* and first-order *k*. The amount in the perfusate, *B*, at any time, *t*, is given by the product of perfusate concentration and volume. The amount transferred to *B* can be computed from*

$$B = \frac{A}{20\,RF}\left[n - \frac{(1 - e^{-\frac{nk}{RF}})e^{-\frac{k}{RF}}}{1 - e^{-\frac{k}{RF}}}\right] \text{ for } t \le 20 \qquad (19-22)$$

and

$$B = B_{20} + A_{20}\,[1 - e^{-k(t-20)}] \text{ for } t > 20 \qquad (19-23)$$

where B_{20} is computed from equation (19–22) at time $t = 20$ min, and A_{20} is calculated using the following expression:

$$A_{20} = \left[\left(\frac{A}{20\,RF}\right)(1 - e^{-20k})e^{-\frac{k}{RF}}\right]\left(1 - e^{-\frac{k}{RF}}\right) \qquad (19-24)$$

The term, $A/20\,RF$, found in equations (19–22) and (19–24), is the transferable amount deposited after each inhalation. The inhalation or dose number, *n*, is equal to $t \times RF$ for $t \le 20$, where *RF* is the respiratory frequency.

The ratio (transferable amount/amount deposited) increased at high respiratory frequency *RF*, large tidal volume, and decreasing aerosol particle size. *Tidal volume* is the amount of air that enters the lungs with each inspiration or leaves the lungs with each expiration during normal breathing.

Example 19–11. Compute the transfer *B* of 3-μm particles at $t = 20$ min, knowing that the transferable amount *A* is 37.7 μg, the respiratory frequency *RF* is 28, and $k = 0.049$ min^{-1}.

The inhalation or dose number is $n = 20$ min × 28 cycles/min = 560 cycles; from equation (19–22)

$$B = \frac{37.7}{560}\left\{560 - \frac{\left[1 - \exp\left(\frac{-560 \times 0.049}{28}\right)\right] \times \exp\left(\frac{-0.049}{28}\right)}{1 - \exp\left(\frac{-0.049}{28}\right)}\right\}$$

$B = 13.69$ μg

The pulmonary route provides effective administration of beta-adrenergic agonists in asthma treatment.

*In personal correspondence, Byron has noted that *n* is incorrectly placed in equation (2) of the paper, J. Pharm. Sci. 75, 168, 1986. Equation (19–22) above is the correct expression.

Corticosteroids have been added to the therapeutic regime, in particular triamcinolone acetonide and beclomethasone, which are safe and effective in aerosol formulations.[91] However, this route has shown to be of limited usefulness for antimicrobial drugs. The pulmonary route is useful for controlled delivery of drugs to the respiratory tract, depending on the characteristics of the drug and the aerosol device. It is unlikely that this route will substitute for the administration of more conventional oral or parenteral drugs.

Gastrointestinal Administration. The Oral Route. Oral administration is perhaps the most widely used route for the delivery of drugs. Absorption from the gut depends on a number of factors, such as gastric emptying, intestinal motility, mucosal surface area, degradation of the drug in the stomach, and first-pass effect in the liver. The absorption varies from the stomach to the intestines owing to the increased surface area (about 4500 m^2) of the intestinal mucosa and to the greater velocity of blood (1000 mL/min) through the intestinal capillaries relative to the gastric capillaries.[92] The transport of drugs through the cellular barrier of the epithelia can be achieved through passive and carrier-mediated mechanisms. The former is mainly a diffusion process, while the latter requires the presence of a transport agent to ferry the drug across the membranes.

Sinko and Amidon[93] used a single-pass intestinal perfusion technique in rats to study the oral absorption of drugs via passive absorption and carrier-mediated mechanisms. For a passive process, the intrinsic permeability of the intestinal wall, P_w^*, is calculated as

$$P_w^* = \frac{P_{eff}^*}{\left(1 - \frac{P_{eff}^*}{P_{aq}^*}\right)} \qquad (19-25)$$

where P_{eff}^* is the effective permeability (see equation (19–27)) and P_{aq}^* is the aqueous permeability (see equation (19–28)). Solid stars, $\star$, indicate dimensionless permeabilities.* For example, P^* is defined as

$$P^* = \frac{PR}{D} \qquad (19-26)$$

in which P^* has the units of (cm/sec)cm(sec/cm^2) in which all units cancel. R is the radius of the intestine and D the aqueous diffusion coefficient. The values of P_{eff}^* and P_{aq}^*, respectively, are calculated from

$$P_{eff}^* = \frac{1 - (C_m/C_o)}{4\,Gz} \qquad (19-27)$$

and

$$P_{aq}^* = (A\,G_z^{1/3})^{-1} \qquad (19-28)$$

*See equation (13–11), page 327, for the definition of *permeability*.

C_o and C_m are the inlet and outlet perfusate concentrations and A is a constant. The *Graetz number*, G_z, is a dimensionless quantity that expresses the ratio of axial convection to radial diffusion times,

$$G_z = \frac{\pi DL}{2Q} \qquad (19-29)$$

D is the diffusion coefficient, L is the length of the intestine, and Q is the flow rate.

The constant A in equation (19–28) depends on the Graetz number as calculated from a film model approximation (see p. 648 in reference 93):

$$A = 10.00\,G_z + 1.01 \quad \text{for } 0.004 \le G_z \ge 0.01 \qquad (19-30)$$

$$A = 4.50\,G_z + 1.07 \quad \text{for } 0.01 \le G_z \ge 0.03 \qquad (19-31)$$

$$A = 2.5\,G_z + 1.13 \quad \text{for } 0.03 \le G_z \qquad (19-32)$$

Example 19–12. Compute the aqueous, effective, and intrinsic wall permeabilities for the passive transport of a drug in the rat jejunum from the following data: $L = 10$ cm, $D = 5 \times 10^{-6}$ cm^2/sec, and $Q = 0.25$ cm^3/min. The ratio C_m/C_o is 0.97.

The Graetz number for the experimental condition (equation 19–29)) is

$$G_z = \frac{3.1416 \times 5 \times 10^{-6}\ cm^2/sec \times 10\ cm}{2(0.25/60)\ cm^3/sec} = 0.0188$$

The A value is computed from equation (19–31):

$$A = (4.50 \times 0.0188) + 1.07 = 1.155$$

The aqueous permeability from equation (19–28) is

$$P_{aq}^* = [1.155(0.0188)^{1/3}]^{-1} = 3.25$$

The effective wall permeability from equation (19–27) is

$$P_{eff}^* = \frac{1 - 0.97}{4 \times 0.0188} = 0.399$$

and the intrinsic wall permeability, according to equation (19–25), is

$$P_w^* = \frac{0.399}{\left(1 - \frac{0.399}{3.256}\right)} = 0.455$$

For a carrier-mediated mechanism, the wall permeability P_w^* may be written in terms of the carrier uptake, $\frac{J_{max}^*}{K_m + C_w}$, and the passive membrane permeability, P_m^*, giving

$$P_w^* = \frac{J_{max}^*}{K_m + C_w} + P_m^* \qquad (19-33)$$

where J_{max}^* is the maximum flux (pp. 325–328), K_m is the intrinsic Michaelis constant (pp. 293–294), P_m^* is the intrinsic passive membrane permeability, and C_w is the concentration at the intestinal wall, calculated from

$$C_w = C_o\left(1 - \frac{P_{eff}^*}{P_{aq}^*}\right) \qquad (19-34)$$

where all the symbols have been defined previously. Note that the star on the P terms shows them to be dimensionless quantities. The carrier permeability, P_c^*, is defined as

$$P_c^* = \frac{J_{max}^*}{K_m} \qquad (19-35)$$

Substituting equation (19–35) into equation (19–33) yields

$$P_w^* = \frac{P_c^*}{1 + \left(\frac{C_w}{K_m}\right)} + P_m^* \qquad (19-36)$$

Sinko and Amidon[93] found that the jejunal absorption of several cephalosporins fitted equation (19–36) and the term P_m^* was negligible or zero. This indicates that the transport mechanism for these antibiotics is mainly a carrier-mediated process. The absorption of captopril in the rat intestine is also mediated by a carrier peptide with a small contribution of passive transport. Captopril is an angiotensin-converting enzyme inhibitor used in the treatment of hypertension and congestive heart failure.[94] Amidon et al.[95] found that the dose fraction, F, absorbed in humans correlated well with the effective permeability of the intestinal wall P_w^* in rats according to the expression,

$$F = 1 - e^{-2P_w^*} \qquad (19-37)$$

In equation (19–37) it is assumed that the aqueous permeability P_{aq}^* is not rate limiting, since its value is usually larger than unity (see example (19–12)). The authors were able to correlate F and P_w^* for a number of drugs (see *problem 19–18*).

An important factor in gastrointestinal (GI) absorption for ionizable drugs is the pH of the GI environment. The pH–partition theory (p. 343) states that the absorption is favored when the drug is nonionized and has an *o/w* partition coefficient larger than unity. Prieto et al.[96] studied the influence of the pH of beta-lactam antibiotics on their absorption through the rat intestinal tract using an in vivo perfusion technique. The absorption is due to a passive mechanism (diffusion) and a nonspecific carrier. The apparent rate constant, K_{app}, is transformed to metabolic weight units for the rat by introducing the term V_{app}, defined as

$$V_{app} = \frac{K_{app}}{(\text{living body weight})^{0.75}} \qquad (19-38)$$

where V_{app} is the apparent absorption rate constant per metabolic weight. The effect of pH on V_{app} was estimated from

$$V_{app} = \frac{V_o + V_{-1}\left(\frac{K_a}{[H^+]}\right)}{1 + \left(\frac{K_a}{[H^+]}\right)} \qquad (19-39)$$

where V_o and V_{-1} are the rate constant contributions of the nonionized and ionized forms, respectively, to the apparent absorption rate constant, V_{app}; and K_a is the dissociation constant of the drug.

Example 19–13. Compute V_{app} and K_{app} for a cephalosporin[96] in aqueous solution at pH 4.9 given that the drug's pK_a is 3.49, V_o is 25.072×10^{-3} min^{-1} g^{-1}, and V_{-1} is 2.946×10^{-3} min^{-1} g^{-1}. The mean weight of the rats is 246 g.

$$V_{app} = \frac{(25.072 \times 10^{-3}) + \left[(2.946 \times 10^{-3})\left(\frac{3.236 \times 10^{-4}}{1.259 \times 10^{-5}}\right)\right]}{1 + \left(\frac{3.236 \times 10^{-4}}{1.259 \times 10^{-5}}\right)}$$

$$V_{app} = 3.77 \times 10^{-3} \text{ min}^{-1} \text{ g}^{-1}$$

$$K_{app} = (3.77 \times 10^{-3} \text{ min}^{-1} \text{ g}^{-1})(246 \text{ g})^{0.75} = 0.234 \text{ min}^{-1}$$

Figure 19–16 shows the values of V_{app} against pH for several cephalosporins. At pH values much higher than the drug's pK_a, cephalosporins are fully ionized, and absorption takes place through aqueous channels on the membrane. Below pH 6.0 the absorption rate constant is increased significantly, the absorption rate of the nonionized fraction V_o depending for the most part on lipid solubility of the drug. The curves of Figure 19–16 show inflection points where the pH is equal to the pK_a of each drug. It should be noted from Figure 19–16 that the rate of absorption becomes constant for each of these three drugs at higher pH values.

The bioavailability of drugs administered by the oral route is greatly influenced by the physicochemical

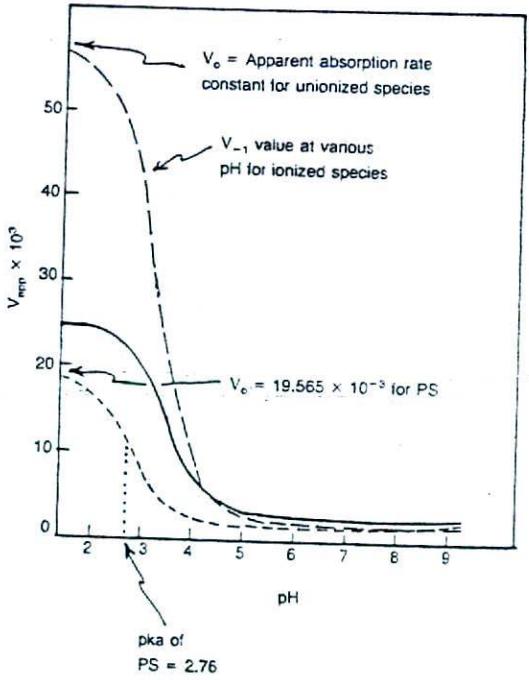


Fig. 19–16. Apparent absorption rate constant V_{app} plotted against pH using experimental data fitted to equation (19–39). Key: – – – NPADC; ——7FADCK; – – – PS. The antibiotic, abbreviated PS, is benzylpenicillin sodium, pK_a 2.76. (From J. G. Prieto et al., J. Pharm. Sci. 76, 596, 1987, reproduced with permission of the copyright owner.)

properties of the drug and the dosage form. One method to increase the oral bioavailability is to use prodrugs (p. 513). By this approach the functional group of the drug that could easily be metabolized during its passage through the liver is protected in the prodrug. The blocking or protecting substituent is then cleaved by enzymes in the blood to restore the parent compound. Hussain et al.[97] prepared prodrugs of estradiol in which the 3-phenolic hydroxyl group is protected. Use of the prodrug derivatives β-estradiol-3 acetylsalicylate and β-estradiol-3 anthranilate increased by 17-fold and by fivefold, respectively, the oral bioavailability of estradiol in dogs. Another approach to improve bioavailability is the use of *permeability enhancers* (see p. 541). Permeability enhancement is particularly useful for macromolecules and peptides against which the intestinal mucosa is largely impermeable. EDTA, bile salts, and ionic and nonionic surfactants have been studied as enhancers.

Peters et al.[98] found that 5-methoxysalicylate increased the absorption of several peptides in a rat gut preparation. (For a description of the rat gut preparation, see page 344). 5-Methoxysalicylate also enhances the gastrointestinal absorption of insulin and antibiotics. The authors suggested, however, that this adjuvant effect may occur as a result of undesirable damage that allows the peptidases of the lumen to penetrate the epithelial barrier. Mucosal damage by this and other mechanisms may discourage the search for appropriate enhancers for orally administered drugs.

Most of the oral extended-drug delivery systems are solid dosage forms: tablets, capsules, and granules. However, some extended-release liquid formulations, particularly suspensions, have also been formulated. Diffusion, dissolution, or a combination of both is the principal mechanism to achieve controlled delivery by the oral route. Several techniques for prolonging drug release are possible, based on the behavior of the dosage form in the GI tract and the properties of the excipients. The three basic approaches are (1) chemical or physicochemical bonding, (2) film coating, and (3) embedding.[99] A fourth class involves the principle of osmotic pressure.

Bonded Drug Systems. Extended release can be obtained by the use of salts or complexes of drugs (see Chapter 11) which are only slightly soluble in the GI fluids. The release occurs by slow dissolution of the salt or dissociation of the complex. The kinetics of drug delivery is usually first order, but under certain conditions may be zero order.

Another kind of physicochemical bonding is achieved when ionizable drugs are bound to water-insoluble polymers containing groups capable of exchanging ions (called *ion exchange resins*). Cation exchange resins have acidic groups such as phenolic, carboxylic, or sulfonic, whereas anion exchange resins contain basic groups such as amino or quaternary ammonium groups. A displacement reaction in the intestinal fluid involving a resin–drug complex ($R—SO_3^-\cdot NH_3^+—R'$) and a single acid–base species is illustrated in the equation[99]:

$$(R—SO_3^-\cdot NH_3^+—R') + (X^+Y^-) \rightleftarrows (R—SO_3^-\ X^+) + (NH_3^+—R'Y^-) \qquad (19\text{–}40)$$

where $R—SO_3^-$ is a sulfonic acid exchange resin, $NH_3^+—R'$ is a cationic (basic drug), X^+ is a cation such as H^+ or Na^+, and Y^- is ananion such as Cl^- in the GI fluids. The drug molecule is exchanged for the free cation, H^+ or Na^+ in solution, and the drug diffuses out of the resin into the bulk solution. The resins are characterized by the type of functional groups, degree of cross-linking, binding capacity, and particle size. The release rate can be further controlled by coating the drug–resin complex using microencapsulation techniques (p. 516). The dosage forms that serve as carriers for drug–resin complexes are tablets, capsules, suspensions, and microparticles. Hussain et al.[100] encapsulated phenylpropanolamine bound to a cross-linked sulfonated polystyrene ion-exchange resin in hollow fibers of polyurethane. Ion exchange resins have been used to deliver antitussives, antihistamines, central nervous system stimulants, antiarrhythmics, and other drugs.

Film-coated Dosage Forms. In the second procedure, a film surrounds the drug particles to allow delayed release. The mechanism and kinetics of drug delivery depend on the nature of the film. For insoluble membranes made of ethyl cellulose the principal mechanisms are diffusion and partitioning of the drug into the membrane. The release rate is controlled by the membrane and can be regulated by its porosity and thickness. The kinetics of delivery is usually zero order. Granules, pellets, microcapsules, and film-coated tablets are examples of coated dosage forms.

Soluble membranes such as cellulose acetate phthalate polymers of methacrylic acid are often used as enteric coating. The polymers are weak acids containing carboxyl groups and require pH values much higher than the acid values of the stomach for rapid dissolution. Ionizable drugs are frequently coated with acidic polymers. Thus, the dissolution of both the drug and the polymer becomes pH-dependent. Ozturk et al.[101] proposed a model to describe the dissolution kinetics of ionizable drugs. The method asumes that dissolution and ionization are limited to the stagnant film adjacent to the solid phase (drug surface), and that the overall process is diffusion limited. The dissolution rate, v, of a drug may be expressed (pp. 330–331) as:

$$v = S \cdot J = s\left[\frac{D}{h}(C_{T,s} - C_{T,b})\right] \qquad (19\text{–}41)$$

where J is the flux, S is the surface area, and $C_{T,s} - C_{T,b}$ are, respectively, the total solubility at the surface and the concentration of drug in the bulk. D is the diffusion coefficient and h is the thickness of the

diffusion layer. If the drug ionizes, the total solubility at the surface, $C_{T,s}$, is

$$C_{T,s} = [AH]_o \left(1 + \frac{K_a}{[H^+]_s}\right) \text{ for acidic drugs} \qquad (19-42)$$

$$C_{T,s} = [B]_o \left(1 + \frac{[H^+]_s}{K_a}\right) \text{ for basic drugs} \qquad (19-43)$$

where $C_{T,s}$ is the solubility at the solid–liquid surface at a particular pH value and $[H^+]_s$ is the concentration of hydrogen ions at the surface. $[AH]_o$ and $[B]_o$ are the intrinsic solubilities (i.e., solubilities independent of pH) of acidic and basic drugs, respectively. Equations (19–42) and (19–43) use the pH at the surface, which differs from the pH of the bulk phase. For a weakly acidic drug in unbuffered solution, the ionization reactions at the stagnant adjacent film are

$$HA \rightleftarrows A^- + H^+ \qquad (19-44)$$

$$H_2O \rightleftarrows OH^- + H^+ \qquad (19-45)$$

$$HA + OH^- \rightleftarrows A^- + H_2O \qquad (19-46)$$

According to the authors,[101] the concentration of HA at the solid–fluid interface is the *intrinsic solubility*, $[HA]_o$. The drug diffuses from the solid–fluid interface and is simultaneously ionized to give the conjugate base A^- and hydrogen ions (equation (19–44)). The bulk liquid at the outer surface of the stagnant layer is assumed to be well mixed, and the ionic species are assumed to be completely dissolved. The solution of the mass transfer equations gives an analytic form to calculate the surface pH and subsequently the surface concentrations driving the drug dissolution. For an acidic drug,

$$[H^+]_s = \frac{-b + \sqrt{b^2 + 4c}}{2} \qquad (19-47)$$

For a basic drug,

$$[H^+]_s = \frac{-b + \sqrt{b^2 + 4ac}}{2a} \qquad (19-48)$$

The expressions to compute the coefficients a, b, and c are given in Table 19–1.

Example 19–14. Compute the in vitro pH of a compact of benzoic acid at the solid–liquid interface and at pH 12 in unbuffered medium.[101] The ionization constant K_a of benzoic acid is 9.33×10^{-5} M ($pK_a = 4.03$); the intrinsic solubility $[HA]_o$ is 0.0216 M, and the diffusivities of the species are $D_{HA} = D_{A^-} = 9.6 \times 10^{-6}$ cm^2 sec^{-1} and $D_{H^+} = D_{OH^-} = 2.7 \times 10^{-5}$ cm^2 sec^{-1}. Assume sink conditions in the bulk, that is, $[HA]_b = [A^-]_b = 0$. The surface area, S, is 0.79 cm^2.

(*a*) If the hydrogen ion concentration in the bulk is $[H^+]_b = 10^{-12}$ mole/liter, the $[OH^-]_b$ concentration is

$$[OH^-]_b = \frac{K_w}{[H^+]_b} = \frac{1 \times 10^{-14}}{1 \times 10^{-12}} = 1 \times 10^{-2} \text{ mole/liter}$$

The coefficients γ in Table 19–1 are

$$\gamma_1 = \frac{D_{OH^-}}{D_{H^+}} = 1.0$$

$$\gamma_2 = \frac{D_{A^-}}{D_{H^+}} = \frac{9.6 \times 10^{-6}}{2.7 \times 10^{-5}} = 0.36$$

The constants b and c for acidic drugs, from Table 19–1, are

$$b = -(1 \times 10^{-12}) + (1)(1 \times 10^{-2}) + (0.36 \times 0) = 0.01 \text{ mole/liter}$$

$$c = (1)(1 \times 10^{-14}) + (0.36 \times 9.33 \times 10^{-5} \times 0.0216)$$
$$= 7.26 \times 10^{-7} \text{ (mole/liter)}^2$$

Therefore, from equation (19–48),

$$[H^+]_s = \frac{-0.01 + \sqrt{(-0.01)^2 + (4 \times 7.26 \times 10^{-7})}}{2}$$
$$= 7.20 \times 10^{-5} \text{ mole/liter}$$

The pH at the surface of the membrane is

$$(pH)_s = -\log(7.20 \times 10^{-5}) = 4.14$$

(*b*) Compute the dissolution rate, ν, and the solubility of the drug at the surface. It is observed that the pH, 4.14, at the surface of the solid drug is much lower than the pH within the bulk solution (pH = 12). The pH at the surface controls the dissolution rate, and the drug solubilities at pH 4.14 are used in equation (19–41) to compute ν.

From equation (19–42),

$$C_{T,s} = 0.0216 \left(1 + \frac{9.33 \times 10^{-5}}{7.20 \times 10^{-5}}\right) = 0.0496$$

$C_{T,b} = 0$ = sink conditions

From equation (19–41) for sink conditions $C_b = 0$ and

$$\nu = (0.79 \text{ cm}^2)\left(\frac{9.6 \times 10^{-6} \text{ cm}^2/\text{sec}}{0.01 \text{ cm}}\right)(4.96 \times 10^{-2}) \text{ mole/cm}^3$$
$$= 3.76 \times 10^{-5} \text{ mole/sec}$$

Embedded Dosage Forms. In the third procedure, the drug may be mixed with a carrier that acts as a release-rate controlling agent. Hydrophilic carriers

TABLE 19–1. *Equations for Surface pH Calculation and Related Constants (Unbuffered Medium)**

	Acidic Drug	Basic Drug
$[H^+]_s$	$(-b + \sqrt{b^2 + 4c})/2$	$(-b + \sqrt{b^2 + 4ac})/2a$
a		$K_a + \gamma_2[B]_o$
b	$-[H^+]_b + \gamma_1[OH^-]_b + \gamma_2[A^-]_b$	$(-[H^+]_b + \gamma_1[OH^-]_b - \gamma_2[BH^+]_b)K_a$
c	$\gamma_1 K_w + \gamma_2 K_a[HA]_o$	$\gamma_1 K_w K_a$
γ_1	D_{OH^-}/D_{H^+}	D_{OH^-}/D_{H^+}
γ_2	D_{A^-}/D_{H^+}	D_{BH^+}/D_{H^+}

*From S. S. Ozturk, B. O. Palsson and J. B. Dressman, Pharm. Res. 5, 272. 1988, reproduced with permission of the copyright owner.

include methylcellulose, sodium alginate, and other gel-forming materials. The drug diffuses from the viscous gel, and the release rate can be controlled by the degree of polymerization of the carrier and the ratio of drug to carrier. Wilson and Cuff[102] found that the optimum hydrogel concentration for sustained release of isomazole, an orally active cardiotonic, was 40 to 42%. Hydrophobic and digestible carriers include glycerides, waxes, fatty alcohols, and fatty acids. They constitute eroding tablets in which the release is achieved when the surface layer is continuously eroded by the GI fluids. Matrix tablets consist of insoluble and nondigestible materials, such as polyethylene, some waxes, and polyvinylchloride. The diffusion of a drug through this kind of matrix has been discussed in Chapter 13, pages 335 to 337. The kinetics of release is a function of the square root of time, and the release rate can be controlled by the tablet porosity, addition of soluble solids, and the ratio of drug to carrier.

Jambhekar and Cobby[103] prepared slow-release tablets using a polyvinylchloride–polyoxyethylene (PVC–PE) matrix and sodium salicylate as a model drug. The in vitro release of drug from a cylindrical PVC–PE matrix when all surfaces of the tablet are exposed to the dissolution fluid is described in the following equation:

$$f_t = (q + 2)K_r(t^{1/2} - t_o^{1/2}) - (2q + 1)[K_r(t^{1/2} - t_o^{1/2})]^2 + q[K_r(t^{1/2} - t_o^{1/2})]^3 \qquad (19-49)$$

where f_t is the fraction of drug released at time t, q is the ratio of tablet diameter to thickness, K_r is the rate constant, and t_o is the lag time. The rate constant, as well as the lag time, can be computed by fitting the fraction of drug released f_t to the cubic expression, equation (19–49), using a NONLIN program. Once k_r and t_o are known, the values of f_t at any time can be estimated.

Example 19–15. Compute the fraction released at 25° C of salicylate from insoluble matrices at 4:1 and 9:1 matrix-drug ratios and at t = 9 hours. The dissolution rate constants are $K_r = 0.116\ hr.^{-1/2}$ and $0.101\ hr.^{-1/2}$; the lag times are $t_o^{1/2} = 0.341\ hr.^{1/2}$ and $= 0.276\ hr.^{1/2}$. The ratio of tablet diameter to thickness in both cases is $q = 2.84$. For a matrix:drug ratio of 4:1, the fractional drug release is

$$f_t = (2.84 + 2)0.116(9.0^{1/2} - 0.341) - (2 \times 2.84 + 1)[0.116(9^{1/2} - 0.341)]^2 + 2.84[0.116(9^{1/2} - 0.341)]^3 = 0.941$$

For the matrix:drug ratio of 9:1,

$$f_t = (2.84 + 2)0.101(9.0^{1/2} - 0.276) - (2 \times 2.84 + 1)[0.101(9^{1/2} - 0.276)]^2 + 2.84[0.101(9^{1/2} - 0.276)]^3 = 0.885$$

Note that the fraction released depends on the matrix:drug ratio. The larger the ratio, the smaller the fraction released. Jambhekar and Cobby[103] showed that the release constant from this type of matrix was independent of the pH of the dissolution fluid and the flow rate of the fluid past the tablet, so that the in vivo behavior may be less subject to variations in the GI tract.

Osmotic Pump. The *elementary osmotic pump*, also known as Oros or Gastrointestinal Therapeutic System, was first described by Theeuwes and Yum and was introduced by Alza Corporation.[104] The dosage form has a semipermeable membrane on one surface to bring water by osmosis into the drug reservoir in the tablet. The device is shown in Figure 19–17(a). The hydrostatic pressure generated by the influx of water forces the release of a saturated solution of the drug through an opening in the tablet, as seen in Figure 19–17(b). The rate of drug release is constant (zero-order) until the excess undissolved drug is depleted. The release rate then decreases parabolically to zero (Fig. 19–18). Earlier sustained-release forms were markedly affected by physiologic pH changes. With the Oros system, the rates of release of phenobarbital, placed in both artificial gastric fluid at pH 2 and intestinal fluid at pH 7.5, were found to be independent of pH. The release rate of the device may be altered by changing the nature of the semipermeable membrane.

Sample Calculations. Theeuwes[105] first tested the elementary osmotic pump for drug delivery using potassium chloride to serve as both the osmotic agent and the drug model. In a later report, Theeuwes et al.[106] designed a therapeutic system, based on the principle of the osmotic pump, to deliver indomethacin

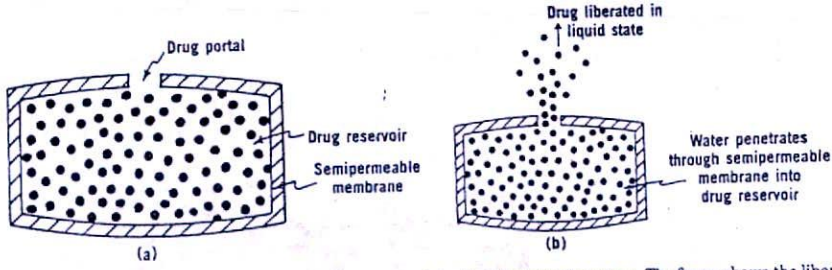


Fig. 19–17. The elementary osmotic pump, Oros (Alza), used as a gastrointestinal therapeutic system. The figure shows the liberation of the drug through the small orifice owing to osmosis of fluids through the semipermeable membrane and into the drug reservoir. (After K. Heilmann, *Therapeutic Systems*. Georg Thieme, Stuttgart, 1978. p. 49.; reproduced with permission of the copyright owner.)

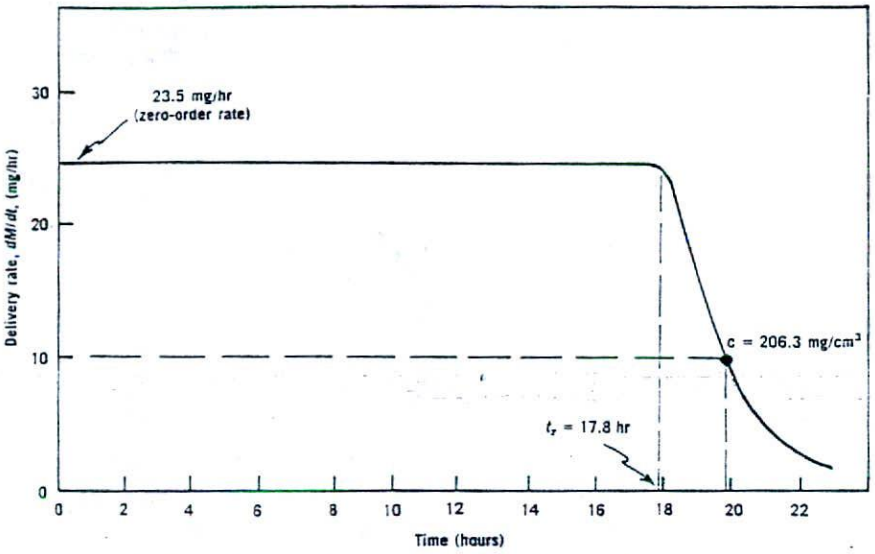


Fig. 19–18. Osmotically controlled drug delivery from Oros at zero-order release, then parabolic decrease in release rate. See the section on *Sample Calculations*.

at a constant zero-order rate. For zero-order delivery rate, these workers used the equation

$$\left(\frac{dM}{dt}\right)_z = \frac{S}{h} k' \pi_s C_s \qquad (19-50)$$

in which $(dM/dt)_z$ is the rate of delivery of the solute under zero-order conditions, S is the semipermeable membrane area (2.2 cm^2); h is the membrane thickness (0.025 cm); k' is a permeability coefficient, 2.8×10^{-6} cm^2/(atm hr), and π_s is the osmotic pressure, 245 atm, of the formulation under zero-order conditions (saturated solution) ($k'\pi_s = 0.686 \times 10^{-3}$ cm^2/hr). The concentration of the saturated solution, C_s, at 37° C is 330 mg/cm^3. The zero-order delivery rate for this system is calculated as follows.

$$\left(\frac{dM}{dt}\right)_z = \left(\frac{2.2 \text{ cm}^2}{0.025 \text{ cm}}\right)(0.686 \times 10^{-3} \text{ cm}^2/\text{hr})(330 \text{ mg/cm}^3)$$

$$\left(\frac{dM}{dt}\right)_z = 19.9 \text{ mg/hr}$$

Some of the drug is released from the device by simple diffusion through the membrane. Equation (19–50) therefore should be modified as follows:

$$\left(\frac{dM}{dt}\right)_z = \frac{S}{h} k' \pi_s C_s + \frac{S}{h} P C_s$$

or

$$\left(\frac{dM}{dt}\right)_z = \frac{S}{h} (k' \pi_s + P) C_s \qquad (19-51)$$

in which P is the permeability coefficient for passage of KCl across the semipermeable membrane (0.122×10^{-3} cm^2/hr). (See the footnote on page 327 for P given as cm^2/sec.)

$$\left(\frac{dM}{dt}\right)_z = \left(\frac{2.2 \text{ cm}^2}{0.025 \text{ cm}}\right)(330 \text{ mg/cm}^3)(0.686 \times 10^{-3} \text{ cm}^2/\text{hr} + 0.122 \times 10^{-3} \text{ cm}^2/\text{hr})$$

$$\left(\frac{dM}{dt}\right)_z = 23.5 \text{ mg/hr}$$

The time t_z in which the mass of the drug M_z is delivered (disregarding the start-up time required to reach equilibrium) is

$$t_z = M_t \left(1 - \frac{C_s}{\rho}\right) \frac{1}{(dM/dt)_z} \qquad (19-52)$$

in which M_t is the total mass of drug in the core (500 mg KCl) and ρ is the density of the drug (2 g/cm^3 or 2000 mg/cm^3):

$$t_z = (500 \text{ mg})\left(1 - \frac{330 \text{ mg/cm}^3}{2000 \text{ mg/cm}^3}\right) \frac{1}{23.5 \text{ mg/hr}}$$

$$t_z = 17.8 \text{ hr}$$

The zero-order delivery rate, $(dM/dt)_z = 23.5$ mg/hr, and the time, t_z, during which the drug is being delivered are shown in Figure 19–18.

Beyond t_z, the drug is delivered under non-zero conditions. For a drug that is released by both osmotic pumping action and passive diffusion through the membrane, the rate beyond t_z is given by

$$\frac{dM}{dt} = \frac{F_s}{S}C^2 + \left(\frac{S}{h}P\right)C \qquad (19-53)$$

in which F_s is a volume flux (cm^3/hr) used to represent the quantity $(S/h)k'\pi_s$ = (2.2 cm^2/0.025 cm)(0.686 × 10^{-3} cm^2/hr), or 0.0604 cm^3/hr. C is the concentration of drug in the dispensing fluid (mg/cm^3). At t values beyond t_z, the saturation concentration, C_s, has fallen to a subsaturation concentration. Let us calculate C when dM/dt in Figure 19–18 has fallen to 10 mg/hr on the parabolic descending curve. Equation (19–53) is written in the quadratic form:

$$\frac{F_s}{C_s}C^2 + \left(\frac{S}{h}P\right)C - \left(\frac{dM}{dt}\right) = 0 \qquad (19-54)$$

$$C = \frac{-b \pm \sqrt{b^2 - 4ac}}{2a} \qquad (19-55)$$

in which $a = F_s/C_s$ = 1.829 × 10^{-4} cm^6/(mg hr); $b = SP/h$ = 0.0107 cm^3/hr; and $c = -dM/dt$ = −10 mg/hr as shown at point C in the figure. (Only the positive root of the quadratic equation is applicable.)

$$C = \frac{-0.0107 + \sqrt{(0.0107)^2 - 4(1.829 \times 10^{-4})(-10)}}{2(1.829 \times 10^{-4})}$$

$$C = 206.4 \text{ mg/cm}^3$$

To plot the calculated line of Figure 19–18 to the right of t_z, one needs the values of t for each value of dM/dt. For dM/dt = 10 mg/hr used previously in this example, we obtain t using the expression[105]

$$t - t_z = \left(\frac{Vh}{SP}\right)\ln\frac{\left(\frac{F_sC}{C_s}\right) + \frac{SP}{h}}{\left(F_s + \frac{SP}{h}\right)\frac{C}{C_s}} \qquad (19-56)$$

in which V is the volume of the drug and is obtained from mass and density as

$$V = \frac{500 \text{ mg}}{2000 \text{ mg/cm}^3} = 0.250 \text{ cm}^3$$

$$t - t_z = \left(\frac{(0.250 \text{ cm}^3)(0.025 \text{ cm})}{(2.2 \text{ cm}^2)(0.122 \times 10^{-3} \text{ cm}^2/\text{hr}}\right) \times$$

$$\ln\frac{(0.0377 \text{ cm}^3/\text{hr}) + (0.0107 \text{ cm}^3/\text{hr})}{(0.0604 \text{ cm}^3/\text{hr} + 0.0107 \text{ cm}^3/\text{hr})\left(\frac{206.3 \text{ mg/cm}^3}{330 \text{ mg/cm}^3}\right)}$$

$$t - t_z = (23.286 \text{ hr}) \ln 1.0889 = 1.98 \text{ hr}$$

$$t = 1.98 \text{ hr} + t_z = 19.8 \text{ hr}$$

This point (dM/dt = 10 mg/hr, t = 19.8 hr) is shown as a black circle on the downward-sloping curve of Figure 19–18. By calculating a sufficient number of such points, the parabolic portion of the curve is plotted.

Another interesting quantity is the maximum size of the orifice or portal (Fig. 19–17) for delivery of the drug from the osmotic pumping system. The maximum cross-sectional area is given by

$$S_{max} = \frac{L}{f}\left(\frac{dM}{dt}\right)_z \frac{1}{DC_s} \qquad (19-57)$$

in which D is the diffusivity (see Chapter 13) of the drug delivered through the orifice (D = 2 × 10^{-5} cm^2/sec or 0.072 cm^2/hr), L the path length of this opening (25 × 10^{-4} cm), and f a dimensionless sizing factor, taken to have a value of 50. The sizing factor specifies how many times greater is the zero-order pumping rate than the free diffusion rate.

We use equation (19–57) to estimate the port size for drug delivery and to convert D to cm^2/hr:

$$S_{max} = \frac{25 \times 10^{-4} \text{ cm}}{50}(23.5 \text{ mg/hr}) \cdot \frac{1}{(0.072 \text{ cm}^2/\text{hr})(330 \text{ mg/cm}^3)}$$

$$S_{max} = 4.945 \times 10^{-5} \text{ cm}^2 \text{ or } 4945 \ \mu\text{m}^2 \text{ area}$$

(*Note:* 1 cm = 10^4 μm; therefore, 1 cm^2 = $10^4 \times 10^4$ = 10^8 μm^2.) The area is equal to πr^2, and the radius of the orifice is obtained as follows:

$$4945 \ \mu\text{m}^2 = 3.14159 \ r^2$$

$$r = 39.675 \ \mu\text{m}$$

$$\text{orifice diameter} = 79 \ \mu\text{m}$$

Advancements in drug design centered on the osmotic pump principle continues to be reported in the pharmaceutical literature; examples are the work of Amidon et al.[107] and Haslam et al.[108] dealing with a lipid osmotic pump and Lindstedt et al.[109] on osmotic pumping and membrane-coated dosage forms. To release a drug from its dosage form at a constant rate, soluble tablet cores have been coated with microporous membranes to control the diffusion. Bodmeier and Paeratakul[110] used a latex consisting of poly(ethacrylate-methylmethacrylate) and containing a *pore-forming agent* insoluble in the latex but which leaches out of the membrane to form minute holes in the tablet surface when it comes in contact with the gastrointestinal fluids. (A *latex* is an aqueous dispersion of a polymer produced by emulsion polymerization.) Dicalcium phosphate, $CaHPO_4$, is insoluble in the latex but soluble in the acidic gastric fluid, and was found to yield the desired microporous tablet coating. Release of the test drug, theophylline, was linear with time and the rate could be adjusted by varying the concentration of the pore-forming agent, $CaHPO_4$, and the thickness of the latex coating.

Rectal Administration. Rectal delivery is an alternative to the oral route to avoid the gastric irritation caused by some drugs and to minimize hepatic first-pass metabolism. The mechanism of absorption is similar to that of the gastrointestinal tract—mainly by passive diffusion.[111] However, the absorption is less extensive and

slower because the surface area of the rectal mucosa available for absorption is limited, being about 1/10,000 the surface area of the small intestine.

The bioavailability of a drug depends on the site of absorption in the rectal mucosa. The upper rectal (hemorrhoidal) veins drain into the portal system and the lower veins drain into the inferior vena cava.[111] Generally, drugs administered rectally are considered to be absorbed mainly in the lower hemorrhoidal veins, thus avoiding the first pass through the liver. de Boer et al.[112] showed that rectal absorption of lidocaine is greater than oral absorption, supporting the hypothesis that the rectal route can result in a bypass of the liver. This route can be useful for drugs that, like lidocaine, undergo first-pass metabolism where they are substantially decomposed by liver and/or gut wall metabolism. The bioavailability of poorly absorbable drugs can be increased by the use of enhancers in the rectal formulations. As in the case of the nasal route, rectal administration may be an alternative to the parenteral route for peptides and proteins. A number of workers have investigated enhancers and dosage formulations to promote the absorption of these macromolecules. Liversidge et al.[113] found that sodium salicylate enhances the absorption of insulin suppositories. Nishihata et al.[114] studied the promoting effect of glyceryl esters of acetoacetic acid on the rectal absorption of insulin. A decrease in the glucose level was observed in rabbits after the administration of suppositories containing the adjuvant. The addition of calcium gluconate or magnesium chloride to the suppositories markedly diminished the efficacy of the enhancer. This suggested that the promoting effect is related to the interaction of the enhancers with calcium and magnesium ions located in the rectal membrane. Calcium ions are important to preserve a tight intercellular structure. The interaction of the enhancer with calcium may cause temporary change in the integrity of the rectal barrier, increasing the permeability of the drug. This mechanism was also suggested by Morimoto et al.[115] for the rectal absorption of calcitonin, a hypocalcemic peptide hormone, from a polyacrylic acid aqueous gel. The absorption was larger at lower pH values of the gel base and was concentration-dependent in the range of 0.01 to 0.1% *w/v* polyacrylic acid. This acid has chelating properties toward calcium and was found not to damage the surface of the rectal mucosa. Permeability enhancers for the rectal absorption of ampicillin, such as bile salts, fatty acids, saponines, *N*-acyl derivatives of collagen peptide, and *N*-acyl derivatives of amino acids, also have the capacity to sequester calcium ions.[116]

Using an in situ perfusion of rat rectum, Nishihata et al.[117] found that salicylate and 5-methoxysalicylate enhanced the disappearance of phenylalanine and phenylalanylglycine from the perfusate. Nishihata et al.[118] reported that the rectal absorption of theophylline was increased in the presence of salicylate. These authors compared the enhancer effects of a surfactant, sodium lauryl sulfate, and salicylate in perfused rat rectum. The effect of salicylate was eliminated by washing out the rectum, whereas the effect of the surfactant was not eliminated. This suggested that the action of salicylate does not produce a permanent change in the membrane, whereas the surfactant seems to damage the barrier.[119] Sodium salicylate also enhances the rectal absorption of the antibiotics gentamicin sulfate[120] and ampicillin.[121] Other enhancers for rectal administration of cephalosporins include medium-chain monoglycerides and fatty acids.[122] Fatty acids may increase the transcellular permeability by perturbing membrane lipids. The intercellular enhancing effect may be due to the affinity of the fatty acids for calcium, which results in widening of closely connected conjunctions.

Fix et al.[123] investigated the use of short-chain alkyl esters of levodopa (L-dopa) as prodrugs for rectal administration. L-dopa is the drug of choice in Parkinson's disease, and significant bioavailability was obtained by these workers in dogs and rats using short-chain alkyl ester prodrugs such as L-dopa methyl ester, L-dopa isopropyl ester, and L-dopa 4-hydroxybutyl ester. When the prodrug enters the systemic circulation, the ester group is removed by enzymatic hydrolysis to yield the parent compound, L-dopa. Most of the esters enhanced rectal absorption considerably. The 4-hydroxybutyl ester produced a slower absorption rate, which the workers considered a possible advantage in the design of a sustained release L-dopa product, free of elevated plasma concentration and untoward side effects.

Buur and Bundgaard[124] prepared lipophilic derivatives of 5-fluorouracil, an antitumor agent, to avoid the first-pass metabolism in the GI tract and liver and to facilitate membrane permeability of the drug in its passage to the target site in the body. The prodrugs, 1-methoxy and 1-butoxy 5-fluorouracil, showed rapid and extensive absorption, and their conversion in plasma to the active parent 5-fluorouracil was rapid and complete. Tomita et al.[125] found that the colonic absorption of cefmetazole was greatly increased by 1% sodium caprate, sodium laurate, and mixed micelles composed of sodium oleate and sodium taurocholate. The increased absorption of cefmetazole across the intercellular route was considered to be a result of the increase in the pore size of the membrane produced by the enhancers. The colonic pore radius r may be computed from the following expression:

$$r = -a_w + (2a_w^2 + \lambda)^{\frac{1}{2}} \qquad (19-58)$$

where a_w, the radius of the water molecule, is 1.5 Å and λ (cm^2) is defined by the following equation:

$$\lambda = \left[\frac{8\eta_w D_w}{(RT/V_w)}\right]\left[\left(\frac{P_f}{P_d}\right) - 1\right] \qquad (19-59)$$

D_w is the diffusion coefficient of water, η_w is the water viscosity, R is the gas constant, V_w is the molar volume

of water, and T is the absolute temperature. The term P_f/P_d represents the ratio of the osmotic water permeability coefficient, P_f, to the permeability coefficient P_d of tritiated water through the colonic membrane. The osmotic water permeability is calculated from a plot of the osmotically induced water flux J_o through the colonic membrane against the osmotic difference, $\Delta\pi$, between the two sides of the membrane as seen in the expression:

$$J_o = \frac{V_\pi}{A} = -(P_f \cdot \Delta\pi) \qquad (19-60)$$

in which it is assumed that the area A of the colonic membrane is known. J_o (equation (19–60)) is the osmotically induced water flux (mole min^{-1} cm^{-2}), V_π is the volume rate in mole min^{-1}, A is the area of the membrane in cm^2, P_f is the osmotic water permeability coefficient (cm min^{-1}), and $\Delta\pi$ is the osmotic difference in mOsm/kg.

Example 19–16. Compute the percent increase in pore radius of the colonic membrane at 37° C after treatment with mixed micelles of sodium oleate and sodium taurocholate. The ratio P_f/P_d is 26.48 and the water viscosity is 6.915×10^{-3} dyne sec cm^{-2} (poise). The diffusion coefficient of water is 3.24×10^{-5} cm^2 sec^{-1} and the molar volume of water is 18.14 cm^3 $mole^{-1}$ at 37° C. The initial radius of the mucosal pores is 7.9 Å.

From equation (19–59),

$$\lambda = \left[\frac{8 \times 6.915 \times 10^{-3} \text{ dyne sec/cm}^2 \times 3.24 \times 10^{-5} \text{ cm}^2\text{/sec}}{(8.3143 \times 10^7 \text{ g cm}^2\text{/sec}^2 \text{ deg mole} \times (310°\text{K}/18.14 \text{ cm}^3\text{/mole})}\right] \times (26.48 - 1)$$

$$\lambda = 3.21 \times 10^{-14} \text{ cm}^2$$

From equation (19–58), in which $a_w = 1.5 \times 10^{-8}$ cm,

$$r = -1.5 \times 10^{-8} \text{ cm} + [2(1.5 \times 10^{-8} \text{ cm})^2 - (3.21 \times 10^{-14} \text{ cm}^2)]^{1/2}$$

$$= 16.5 \times 10^{-8} \text{ cm} = 16.5 \text{ Å}$$

The percent increase in the radius is

$$\frac{16.5 - 7.9}{7.9} \times 100 = 109\%$$

owing to the action of the enhancer, composed of mixed micelles of sodium oleate and sodium taurocholate.

Transdermal Administration. The skin has been used for centuries as the administration site of drugs in local treatment, but only recently has it been used as a pathway for systemic effects. The barrier function of the skin prevents both water loss and the entrance of external agents; however, some drugs are able to penetrate the skin layers in sufficient concentration to produce systemic action. The transdermal route is of particular interest for drugs that have a short elimination half-life and undergo extensive first-pass metabolism, therefore requiring frequent dosing.

The most exterior layer of the skin, the epidermis, consists of three main layers, the stratum corneum, the granular layer, and the basal layer. The stratum corneum is considered the most important barrier to drug transport. It is a heterogeneous nonliving structure, formed by keratinized cells, protein-rich cells, and intercellular lipid layers. The lipid composition among the epidermal layers is very different. Polar phospholipids, which are usual components of the membrane of living cells, are absent in the stratum corneum. These lipids form bilayers and their acyl chains can exist as "gel" and as "liquid crystalline" states. The transition between these two states occurs at certain temperatures without loss of the bilayer structure.[126] The principal lipids of the stratum corneum are ceramide (50%) and fatty acids (25%). Although the stratum corneum does not contain phospholipids, the mixture of ceramides, cholesterol, and fatty acids is capable of forming bilayers. These lipid bilayers are considered to provide the barrier function of the stratum corneum.[126]

To study the percutaneous transport of drugs the skin can be considered as a bilaminate membrane consisting of the dead stratum corneum (lipophilic layer) and the viable tissue (aqueous layer) which comprises the granular and basal layers of the epidermis, and the dermis, Figure 19–19. Diffusion of polar drugs is much faster through the viable tissue than across the stratum corneum.[127] The permeability coefficient through the skin, P, can be expressed as[128]

$$P = \frac{D_v D_s}{K\ell_v D_s + \ell_s D_v} \qquad (19-61)$$

where K is the partition coefficient of the drug between the stratum corneum (s) and the viable tissue (v), and ℓ_v, ℓ_s, D_v, and D_s are the diffusion path lengths and diffusion coefficients, respectively. The subscripts s and v refer to the stratum corneum and the viable tissue, respectively. If the drug diffuses slowly through the stratum corneum, $K\ell_v D_s \ll \ell_s D_v$, and equation (19–61) becomes

$$P = \frac{D_s}{\ell_s} \qquad (19-62)$$

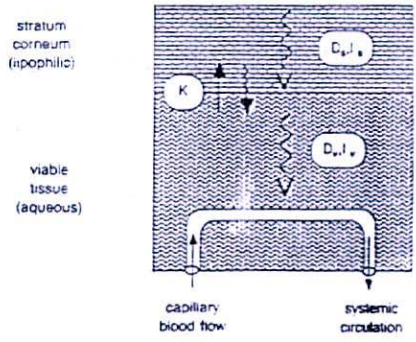


Fig. 19–19. The skin represented as two layers: the dead stratum corneum, s, and the viable or living tissue, v, (dermis and part of epidermis). The diffusion coefficients and the diffusion path lengths, ℓ_s and ℓ_v, together with the partition coefficient, K, control the transport of the penetrant through the two layers. (From R. H. Guy and J. Hadgraft, Pharm. Res. 5, 753, 1988, reproduced with permission of the copyright owner.)

In this case the skin permeability is controlled by the stratum corneum alone. If the diffusion through the stratum corneum is fast, $Kh_v D_v > \ell_v D_v$, and equation (19–61) becomes

$$P = \frac{D_v}{\ell_v K} \qquad (19-63)$$

In this case, the partition coefficient may be influential in the permeability. As K increases, the transport from the stratum corneum to viable epidermis becomes less favorable and slower. At large K values, partitioning of the drug is the rate-limiting step.[128]

Example 19–17. Compute the permeability of a drug across the skin assuming that D_v is 10^{-10} cm^2 sec^{-1} and D_v is 10^{-7} cm^2 sec^{-1}. The path lengths are ℓ_v = 350 μm and ℓ_v = 150 μm. The large value for ℓ_v is due to the fact that the molecules follow a tortuous pathway through the intercellular spaces. The value for ℓ_v is the distance from the underside of the stratum corneum to the upper capillary region of the dermis. The partition coefficient is taken to be K = 1.

Since diffusion through the stratum corneum is very slow (D_v = 10^{-10} cm^2 sec^{-1}), and the product $K\ell_v\ell_v = 1.0 \times 150 \times 10^{-4} \times 10^{-10} < \ell_v D_v = 350 \times 10^{-4} \times 10^{-7}$, therefore, $1.5 \times 10^{-4} \ll 3.5 \times 10^{-9}$ From equation (19–62),

$$P = \frac{10^{-10}\ \text{cm}^2/\text{sec}}{350 \times 10^{-4}\ \text{cm}} = 2.86 \times 10^{-9}\ \text{cm/sec}$$

Using equation (19–61), we arrive at a similar order of magnitude:

$$P = \frac{(10^{-7}\ \text{cm}^2/\text{sec})(10^{-10}\ \text{cm}^2/\text{sec})}{(1.0 \times 350 \times 10^{-4} \times 10^{-10}) + (10^{-7} \times 150 \times 10^{-4})} = 6.7 \times 10^{-9}\ \text{cm/sec}$$

Tojo[129] proposed a random brick model for the transport of drugs across the stratum corneum. As shown in Figure 19–20, the stratum corneum is represented by the cells rich in proteins separated from one another by thin-layer intercellular lipids. The side length of the cells varies, but the total average surface area is constant. The thickness of the cells and the lipid layer are also assumed to be constant. According to this model, the transport of a drug is divided into three parallel pathways: (1) across the cellular–intercellular regions in series, (2) across the lipid intercellular spaces, and (3) across thin lipid layers sandwiched between flattened protein cells of the stratum corneum.

According to the brick model, the effective diffusion coefficient, $\overline{D}$, across the skin is

$$\overline{D} = 2\,\epsilon(1-\epsilon)D_1 + \epsilon^2 D_2 + (1-\epsilon)^2 D_3 \qquad (19-64)$$

The first, second, and third right-hand terms represent the three possible routes (1), (2), and (3) (Fig. 19–20), D_1, D_2, and D_3 being the difusivities across routes (1), (2), and (3); ϵ and $(1-\epsilon)$ are the average fraction of diffusion area of the lipid and protein on the skin surface, respectively. Substituting D_1, D_2, and D_3 by their corresponding expressions, equation (19–64) becomes

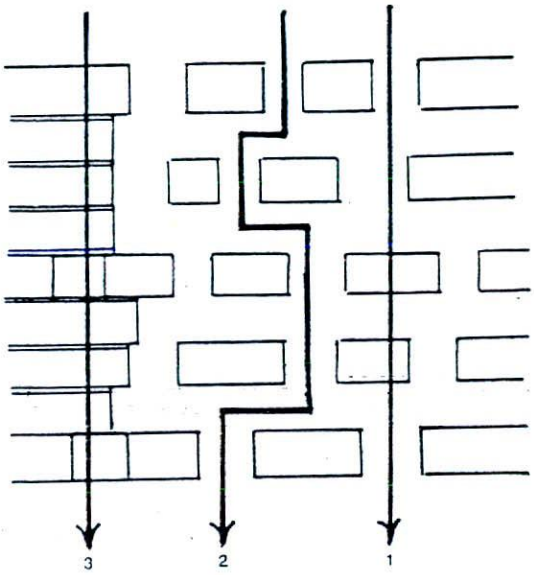


Fig. 19–20. Random brick model for the stratum corneum. Arrows 1, 2, and 3 show three possible routes of drug diffusion. (From K. Tojo, J. Pharm. Sci. 76, 889, 1987, reproduced with permission of the copyright owner.)

$$\overline{D} = \frac{2\epsilon(1-\epsilon)(2n+4)}{\left(\frac{n}{D_p} + \frac{n+4}{K D_\ell}\right)} + \epsilon^2 K D_\ell + \frac{(1-\epsilon)^2(2n+4)}{\left(\frac{2n}{D_p} + \frac{4}{K D_\ell}\right)} \qquad (19-65)$$

The term n is related to the volume fraction of lipids in the skin and the average fraction of diffusion area of the lipids, ϵ; K is the lipid–protein partition coefficient and D_p and D_ℓ are the diffusion coefficients across the protein layer and the lipid layer, respectively.

The flux across the skin is given by the following expression:

$$J = \frac{dQ}{dt} = \frac{\overline{D}\,C_p}{h} \qquad (19-66)$$

where C_p is the concentration of drug in the protein cell layer, h the thickness of the skin, and $\overline{D}$ is defined by equation (19–65).

*Example 18.** Compute the flux at the steady state, dQ/dt, of a new drug from the following data: $D_\ell = 1 \times 10^{-10}$ cm^2/sec, $D_p = 1 \times 10^{-7}$ cm^2/sec, C_p = 10 mg/cm^2, ϵ = 0.02, h = 0.0020 cm, K = 0.1, and n = 14.3. Use the random brick model.

$$\overline{D} = \frac{(2)(0.02)(1-0.02)[(2 \times 14.3) + 4]}{\left[\left(\frac{14.3}{1 \times 10^{-7}}\right) + \frac{(14.3+4)}{(0.1)(10^{-10})}\right]} + (0.02)^2(0.1)(10^{-10}) +$$

*This example was provided by K. Tojo, Kyushu Institute of Technology, Japan.

$$\frac{(1 - 0.02)^2[(2 \times 14.3) + 4]}{\left[\frac{(2 \times 14.3)}{1 \times 10^{-7}} + \frac{4}{(0.1)(1 \times 10^{-7})}\right]} = 4.564 \times 10^{-6} \text{ cm}^2/\text{sec}$$

The flux is

$$J = \frac{(4.564 \times 10^{-6})(1 \times 10^4 \ \mu\text{g/cm}^3)}{0.0020 \text{ cm}} = 0.228 \ \mu\text{g/(cm}^2 \text{ sec)}$$

Factors Affecting Permeability: Hydration. The permeability of a drug depends on the hydration of the stratum corneum; the higher the hydration the greater the permeability. The dermal tissue is fully hydrated, while the concentration of water in the stratum corneum is much lower, depending on ambient conditions. Hydration may promote the passage of drugs in the following way. Water associates through hydrogen bonding with the polar head groups of the lipid bilayers present in the intercellular spaces. The formation of a hydration shell loosens the lipid packing so that the bilayer region becomes more fluid.[130] This facilitates the migration of drugs across the stratum corneum. From the rate of transpiration (passage of water from inner layers to the stratum corneum) and diffusivity of water in the stratum corneum, the amount of water in the tissue can be obtained.[131]

Solubility of the Drug in the Stratum Corneum. Using the experimental results obtained from intact skin and stripped skin (layers of stratum corneum removed using Scotch tape), the solubility C of a drug in the stratum corneum was calculated from the following expression:[132]

$$C = \frac{1 - 3\tau + 2\eta\tau}{(1 + 2\eta)(1 - \eta)} \cdot \frac{6t_2}{h_2}\left(\frac{dQ}{dt}\right)_2 \qquad (19-67)$$

where $(dQ/dt)_2$ is the steady-state permeation across the intact skin, τ is the ratio of the two time lags, (t_1/t_2), and η is the ratio $(dQ/dt)_2/(dQ/dt)_1$. The subscripts 1 and 2 refer to the stripped and intact skin, respectively; h_2 is the thickness of the stratum corneum.

Example 19–15. Compute the solubility of progesterone in the stratum corneum. The lag times across the intact and stripped skin are $t_2 = 5.49$ and $t_1 = 1.55$ hr, and the permeation rates across the intact and stripped skin are $(dQ/dt)_2 = 2.37$ μg/(cm² hr) and $(dQ/dt)_1 = 3.62$ μg/(cm² hr). The thickness of the stratum corneum is 10 μm (10×10^{-4} cm).

$$\tau = \frac{t_1}{t_2} = \frac{1.55}{5.49} = 0.28$$

$$\eta = \frac{(dQ/dt)_2}{(dQ/dt)_1} = \frac{2.37}{3.62} = 0.65$$

From equation (19–67),

$$C = \frac{1 - (3 \times 0.28) + (2 \times 0.65 \times 0.28)}{[1 + (2 \times 0.65)](1 - 0.65)} \cdot \frac{6 \times 5.49}{10 \times 10^{-4}} \cdot 2.37$$

$C = 50816.8$ μg/mL = 50.8 mg/mL

Excipients. Common solvents and surfactants can affect penetration of drugs though the skin. Sarpotdar and Zatz[133] studied the penetration of lidocaine through hairless mouse skin in vitro from vehicles containing various proportions of propylene glycol and polysorbate 20. Propylene glycol is a good solvent for lidocaine and reduces its partitioning into the stratum corneum, lowering the penetration rate. In this study, the effect of the surfactants depended on the concentration of propylene glycol in the vehicle. The decrease of flux for 40% *w/w* propylene glycol concentration may be explained by micellar solubilization of lidocaine. It is generally assumed that only the free form of the drug is able to penetrate the skin. Thus, the micellar solubilization of lidocaine reduces its thermodynamic activity in the vehicle and retards its penetration. At higher propylene glycol concentrations, 60% and 80%, an increase in flux was observed, possibly owing to an interaction of the surfactant with propylene glycol.

Influence of pH. According to the pH–partition hypothesis (p. 343) only the un-ionized form of the drug is able to cross the lipoidal membranes in significant amounts. However, in studies of isolated intestinal membranes, both the ionized and un-ionized forms of sulfonamides permeated the membrane. The diffusion of ionized drug through the skin may be nonnegligible, particularly at pH values at which a large number of ionized molecules are present.[134] Fleeker et al.[135] studied the influence of pH on the transport of clonidine, a basic drug, through hydrated shed snakeskin. The contribution to the total flux, J, in μg cm^{-2} hr^{-1} of the nonionized and ionized species for a basic drug can be written as

$$J = J_B + J_{BH^+} \qquad (19-68)$$

where B and BH^+ represent the basic (nonionized) and protonated forms, respectively. The dissociation of the protonated form is represented as

$$[BH^+] \overset{K_a}{\rightleftharpoons} [B] + [H^+] \qquad (19-69)$$

and

$$K_a = \frac{[B][H^+]}{[BH^+]} \qquad (19-70)$$

Taking the logarithm of both sides of equation (19–70), and rearranging it, the concentration of the protonated form is

$$[BH^+] = \frac{10^{(pK_a - pH)}}{1 + 10^{(pK_a - pH)}}[T] \qquad (19-71)$$

where [T] represents the total concentration of both the charged and uncharged species.

$$[T] = [B] + [BH^+] \qquad (19-72)$$

The concentration of nonionized form, [B], can be computed from equation (19–72). The total flux (equation (19–68)) can also be written in terms of the permeability coefficients times the concentrations of each species:

$$J = P_B[B] + P_{BH^+}[BH^+] \qquad (19-73)$$

From equations (19–71) and (19–73), provided $P_B \equiv P_{BH^+}$,

(a) when pK_a = pH, [B] = [BH^+] and both species B and BH^+ will contribute to the total flux.

(b) When pH ≫ pK_a, [B] ≫ [BH^+] and the total flux, $J \cong P_B[B]$, and

(c) When pH ≪ pK_a, [B] ≪ [BH^+] and $J \cong P_{BH^+}[BH^+]$

Equation (19–73) allows one to compute the permeabilities of both species from the total experimental flux and the values of [B] and [BH^+] from equations (19–71) and (19–72).

Example 19–20. Compute the permeability coefficients P_B and P_{BH^+} corresponding to the nonionized and protonated forms of clonidine. The total fluxes at pH 4.6 and pH 7 are 0.208 and 0.563 μg/(cm² hr), respectively. The pK_a of the protonated form is 7.69. The total concentration* of the two species [T] = 4×10^3 μg/uv where μg/uv stands for microgram/unit volume.

At pH 4.6,

$$[BH^+] = \frac{10^{(7.69-4.6)}}{1 + 10^{(7.69-4.6)}}(4 \times 10^3) = 3.996 \times 10^3 \ \mu g/uv$$

$$[B] = (4 \times 10^3) - (3.996 \times 10^3) = 4.0 \ \mu g/uv$$

At pH 7,

$$[BH^+] = \frac{10^{(7.69-7)}}{1 + 10^{(7.69-7)}}(4 \times 10^3) = 3.322 \times 10^3 \ \mu g/uv$$

$$[B] = (4 \times 10^3) - (3.322 \times 10^3) = 678 \ \mu g/uv.$$

From equation (19–73) with the flux, J, expressed in μg cm^{-2} hr^{-1} and the permeability coefficient, P, in units of cm hr^{-1}, at pH 4.6:

$$0.208 \ \mu g \ cm^{-2} \ hr^{-1} = P_B \ (4 \ \mu g \ cm^{-3}) + P_{BH^+}(3996 \ \mu g \ cm^{-3})$$

At pH 7,

$$0.563 \ \mu g \ cm^{-2} \ hr^{-1} = P_B \ (678 \ \mu g \ cm^{-3}) + P_{BH^+} \ (3322 \ \mu g \ cm^{-3})$$

P_B and P_{BH^+} are calculated by solving the two equations simultaneously:

$$P_B = (0.208 - 3996 \ P_{BH^+})/4$$

$$0.563 = 678\left(\frac{0.208 - 3996 \ P_{BH^+}}{4}\right) + 3322 \ P_{BH^+}$$

$$P_{BH^+} = \frac{-34.693}{-674000} = 5.15 \times 10^{-5} \text{ cm hr}^{-1}$$

$$P_B = 0.208 - (5.15 \times 10^{-5} \times 3996)/4 = 5.5 \times 10^{-4} \text{ cm hr}^{-1}$$

It will be noted that the values found for P_{BH^+} and P_B do not change with pH, whereas the fluxes, J, are markedly different at pH 4.6 and pH 7.0.

Equations (19–70) and (19–73) can be combined to give

$$\frac{J}{[B]} = \frac{P_{BH^+}}{K_a}[H^+] + P_B \qquad (19–74)$$

From equation (19–74), the permeability coefficients of the ionized [BH^+] and nonionized [B] forms can be computed from the slope and intercept of a plot of J/[B] against [H^+]. The corresponding equation for acids is

$$\frac{J}{[A^-]} = \frac{P_{HA}}{K_a}[H^+] + P_{A^-} \qquad (19–75)$$

*"Concentration," expressed in μg/uv was obtained by using four-tenths milliliter of an appropriate concentration of clonidine solution.

From equation (19–75), the permeability coefficients of the nonionized [HA] and ionized [A^-] forms are computed from the slope and the intercept of a plot of J/[A^-] against [H^+] (see *Problem 19–24*). Swarbrick et al.[134] found that both the ionized and nonionized forms of four chromone-2 carboxylic acids permeated skin, although the permeability of the nonionized form was about 10^4 times greater.

Binding of Drug to the the Skin. The skin may act as a reservoir for some drugs that are able to bind to macromolecules. The drug fraction bound is not able to diffuse, and binding hinders the initial permeation rate of molecules, resulting in larger lag times. Banerjee and Ritschel[136] studied the binding of vasopressin and corticotropin to rat skin. Penetration of large molecules such as collagen, used in cosmetic formulations, is questionable, but partial hydrolysates of collagen are able to reach the deeper skin layers. The sorption process can be represented by the Langmuir equation (pp. 380–383):

$$\frac{c}{(x/m)} = \frac{1}{bY_m} + \frac{c}{Y_m} \qquad (19–76)$$

where c represents the equilibrium concentration of the drug, x is the amount of drug adsorbed per amount of adsorbent, m (the skin proteins in this case), b is the affinity constant, and Y_m is the maximum adsorption capacity, $(x/m)_{max}$. The sorption isotherm was obtained by Banerjee and Ritschel by equilibration of a measured weight of rat epidermis with a known concentration of radiolabeled vasopressin solution and was analyzed by scintillation counting (measured radioactivity). The small value for the adsorption constant in equation (19–76), $b = 6.44 \times 10^{-4}$ mL/μg, suggests low affinity of vasopressin for the binding sites in the skin.

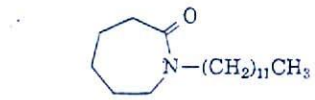
Drug Metabolism in the Skin. The metabolism of drugs during transport through the skin affects bioavailability and can produce significant differences between in vivo and in vitro results. Oxidation, reduction, hydrolysis, and conjugation are kinetic processes that compete with the transport of drugs across the skin. Guzek et al.[137] and Potts et al.[138] found differences in the in vitro and the in vivo extent of enzymatic cleavage in the skin and in the distribution of the metabolites of a diester derivative of salicylic acid. The authors suggested that the in vitro measurements overestimated the metabolism because of the increased enzymatic activity and/or decreased removal of the drug in the absence of capillaries. The fact that the skin contains esterases and other enzymes is useful for the administration of prodrugs. The solubility and absorption can be improved and the prodrug can be cleaved by the enzymes to give the active parent compound in the skin.[139]

Enhancers for Percutaneous Absorption. The transport of molecules through the skin can be increased by the use of certain adjuvants known as *enhancers*. Ionic surfactants enhance transdermal absorption by disordering the lipid layer of the stratum corneum and by

denaturation of the keratin. Enhancers may increase penetration by causing the stratum corneum to swell and/or leach out some of the structural components, thus reducing the diffusional resistance and increasing the permeability of the skin.[140]

Nishihata et al.[141] proposed a mechanism for the enhancing effect of reducing agents such as ascorbate and dithiothreitol. The poor permeability of the skin is due to the ordered layer of intercellular lipids and to the low water content. Proteins in keratinized tissue are rich in cysteine residues, and the strong disulfide bonds may be the reason for the insoluble nature of this protein. The reducing agents cause a decrease in the number of disulfide bridges, thus increasing the hydration of the proteins, which results in increased permeability.

Azone or laurocapram (1-dodecyl-azacycloheptan-2-one) is one of the most efficient enhancers of percutaneous absorption. It greatly improves the penetration of hydrophilic and hydrophobic compounds, the latter to a smaller degree. Wiechers et al.[142] studied the absorption and elimination of azone in healthy volunteers. Azone is an oily liquid, insoluble in water but freely soluble in organic solvents. Most of the azone applied remains on the skin surface; the small fraction absorbed is located mainly in the stratum corneum. Azone does not form reservoirs in the skin and is rapidly cleared from the circulation by the kidneys. This fact, together with the nontoxicity of this compound in animals, indicates that azone is probably safe for human use. The compound has been found to be the most effective enhancer in the percutaneous absorption of dihydroergotamine, a drug widely used in the prevention and/or treatment of migraine.[140] Azone can be incorporated into a drug formulation, or the skin can be treated previously with the enhancer. The effect of azone increases in the presence of propylene glycol.[143] A possible mechanism of azone is its fluidization of the intercellular lipid lamellar region of the stratum corneum. As shown in Figure 19–21, azone, a very nonpolar molecule, enters the lipid bilayers and disrupts their structure. In contrast, a strongly dipolar solvent, dimethyl sulfoxide (DMSO), enters the aqueous region and interacts with the lipid polar heads to form a large solvation shell and to expand the hydrophilic region between the polar heads. As a result, both azone and DMSO increase the lipid fluidity, thus reducing the resistance of the lipid barrier to the diffusion of drugs. From differential scanning calorimetry experiments, the lipid transition temperature from an ordered structure to a fluid state is lowered.[130] Alcohol derivatives of *N*,*N*-disubstituted amino acids and hexamethylene lauramine also enhance the permeability of drugs.[144]



Azone (1-Dodecyl-azacycloheptan-2-one)

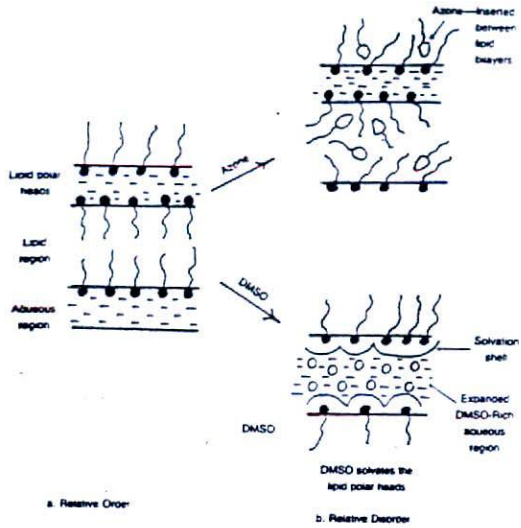


Fig. 19–21. Schematic diagram of the interaction of the enhancers, azone and DMSO, with the intercellular lipids of the stratum corneum. (*a*) Relatively ordered structure of the lipid bilayers. (*b*) Relative disorder of the lipid array due to the action of azone and DMSO. (Modified from B. W. Barry, Int. J. Cosmet. Sci. 10, 281, 1988, reproduced with permission of the copyright owner.)

Membrane-Controlled Systems for the Percutaneous Absorption Route. A transdermal device is a laminated structure consisting of four layers, as shown in Figure 19–22. It consists of (1) an impermeable backing membrane, which is the mechanical support of the system; (2) an adjacent polymer layer, which serves as the drug reservoir; (3) a microporous membrane filled with a nonpolar material (e.g., paraffin); and (4) an adhesive film to make close contact with the skin and maintain the device in the desired position. Grenger et al.[145] used a computer program to calculate the drug transport through a laminated device and across the skin. In this model, all the layers except the backing membrane allow drug diffusion and transport. The authors give a description of the drug transport together with the concentration profiles of drug within each layer, as computed by the program.

Guy and Hadgraft[146] proposed a model for the transport of clonidine across the skin (Fig. 19–23) from a membrane-controlled adhesive system. The constant k_0 represents the zero-order rate constant for the membrane-controlled leaching of the drug, and k_R represents the partition between the patch and the skin surface. The system should be designed so that the partitioning favors the skin, and k_R remains negligibly small. The first-order constants k_1 and k_2 in Figure 19–23 are for drug transport across the stratum corneum and the living part of the epidermis. These constants are directly proportional to the diffusion

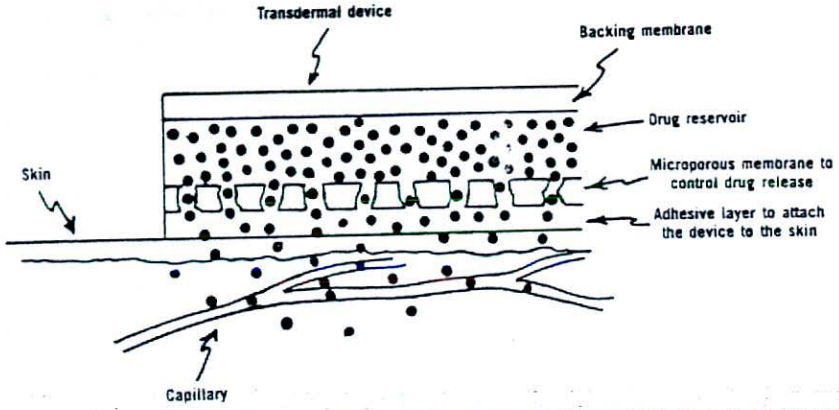


Fig. 19–22. A schematic of the Transdermal Therapeutic System. (After K. Heilmann, *Therapeutic Systems*, Georg Thieme, Stuttgart, 1978, p. 53.)

coefficients for passage through the layers of the skin, and therefore inversely proportional to the penetrant molecular weight as observed from the Stokes–Einstein equation (p. 401):

$$D = \frac{RT}{6\pi\eta N}\sqrt[3]{\frac{4\pi N}{3M\bar{v}}} \qquad (19-77)$$

The rate constant k_3 of Figure 19–23 is included to express any tendency for reverse drug transport from epidermis to the stratum corneum and, in conjunction with k_2, may be considered as a partition coefficient. The authors computed the values of k_1 and k_2 for benzoic acid and used them to compute these rate constants for other drug molecules using the appropriate molecular weights. The expressions are

$$k_1 = k_1^{BA}\left(\frac{M^{BA}}{M}\right)^{\frac{1}{3}} \qquad (19-78)$$

$$k_2 = k_2^{BA}\left(\frac{M^{BA}}{M}\right)^{\frac{1}{3}} \qquad (19-79)$$

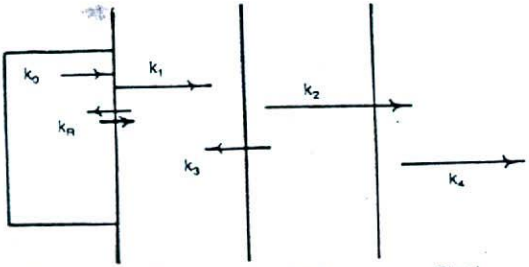


Fig. 19–23. Transdermal delivery of clonidine from a membrane-controlled patch. (From R. H. Guy and J. Hadgraft, J. Pharm. Sci. 74, 1016, 1985, reproduced with permission of the copyright owner.)

where k_1^{BA}, k_2^{BA}, and M^{BA} are the rate constants and molecular weight of benzoic acid, and M is the molecular weight of the drug for which the constants k_1 and k_2 are calculated. The ratio k_3/k_2 was found to be a function of the octanol–water partition coefficient, K:

$$K \cong 5(k_3/k_2) \qquad (19-80)$$

Using this model, the constants k_1, k_2, and k_3 can be predicted from the physicochemical properties of the drug. The rate constant k_4 in Figure 19–23 represents the first-order elimination of the drug from the blood, and cannot be predicted. It must be measured experimentally.

Example 19–21. (*a*) Compute the rate constants k_1, k_2, and k_3 for the transport of clonidine from a membrane-controlled patch. The first-order rate constants k_1^{BA} and k_2^{BA} are 5.11×10^{-5} sec^{-1} and 80×10^{-5} sec^{-1}, respectively. The octanol–water partition coefficient of clonidine is $K = 6.7$. The molecular weight of benzoic acid is 122.12 g/mole, and the molecular weight of clonidine is 230.10 g/mole.

$$k_1 = 5.11 \times 10^{-5}(122.12/230.10)^{1/3} = 4.14 \times 10^{-5}\ \text{sec}^{-1}$$

$$k_2 = 80 \times 10^{-5}(122.12/230.10)^{1/3} = 64.77 \times 10^{-5}\ \text{sec}^{-1}$$

From equation (19–80)

$$k_3 = \frac{K\,k_2}{5} = \frac{6.7 \times 64.77 \times 10^{-5}\ \text{sec}^{-1}}{5} = 8.68 \times 10^{-4}\ \text{sec}^{-1}$$

(*b*) The steady-state plasma concentration of clonidine, C^{ss}, can be computed from

$$C^{ss} = Ak_0V_dk_4 \qquad (19-81)$$

where A is the area of the patch, k_0 is the zero-order rate constant for the delivery of clonidine from the patch, and V_d is the *volume of distribution*,* that is, the amount of drug in the body divided by the plasma concentration. For the most efficient membrane-controlled patch, which contains 2.5 mg of clonidine, A, the area of the patch, is 5 cm^2, and k_0 is 1.6 μg/(cm^2 hr). The volume of distribution V_d for

*To understand V_d, the volume of distribution, consider the following: If an amount of drug, say 1.5 μg, is distributed in the body plasma to give a drug concentration of 9.38×10^{-3} μg/mL, the volume of plasma containing this amount (1.5 μg) of drug is 1.5 μg/(9.38×10^{-3} μg/mL) = 160.000 mL, or V_d = 160 liters.

clonidine is 147 liters and the first-order constant, k_e, is 0.08 hr^{-1}. From equation (19–81),

$$C^{ss} = \frac{5\ cm^2 \times 1.6\ \mu g\ cm^{-2}\ hr^{-1}}{147{,}000\ cm^3 \times 0.08\ hr^{-1}} = 6.8 \times 10^{-4}\ \mu g/mL$$

Examples of membrane-controlled systems are the Transderm-Nitro (Ciba and Alza) for the delivery of nitroglycerin, Transderm-Scōp (Alza and Ciba-Geigy) for scopolamine,[147] and Catapress TTS (Alza/Boehringer Ingelheim) for clonidine.[148]

Adhesive Diffusion-Controlled Systems. The basic difference between this system and the previously described one is that the microporous membrane is absent. Figure 19–24 is a schematic of the adhesive system. The device consists of an impermeable plastic barrier on the top, a drug reservoir in the middle, and several rate-controlling adhesive layers next to the skin. The rate of drug release dQ/dt depends on the partition coefficient K of the drug between the reservoir (r) and the adhesive layers (a), the diffusion coefficient, D_a, the sum of the thicknesses of the adhesive layers, h_a, and the concentration C_r of the drug in the reservoir layer[147]:

$$\frac{dQ}{dt} = \frac{KD_aC_r}{h_a} \qquad (19\text{–}82)$$

Examples of these devices are the Nitrodisc (Searle) and Deponit (Pharma-Swartz) for the delivery of nitroglycerin. The in vitro release of drug as well as the in vivo permeation are zero-order processes.

Matrix-Controlled Devices. In a matrix-controlled device, the drug reservoir consists of a hydrophilic or hydrophobic polymer containing the dispersed drug, attached to a plastic backing that is impermeable to the drug. The drug reservoir is in direct contact with the skin, and the release of drug is matrix-controlled, that is, it is a function of the square root of time (see p. 336, equation (13–43). To obtain zero-order release of the drug across the skin using a matrix-controlled system, the stratum corneum must control the rate of drug delivery. This can be achieved if the release rate of the drug from the device is much greater than the rate of skin uptake. Noonan et al.[149] studied the transdermal penetration of 2% nitroglycerin formulated in a polymer gel matrix (Nitro-Dur system; Key and Schering Co's). The pharmacokinetics of delivery from these matrix systems has been studied by Berner.[150]



Fig. 19–24. Schematic of an adhesive diffusion-controlled transdermal drug delivery system. (From Y. W. Chien, in *Controlled Drug Delivery*, 2nd Edition, J. R. Robinson and V. H. L. Lee, Eds., Marcel Dekker, N.Y., 1987, p. 534, reproduced with permission of the copyright owner.)

Iontophoresis. This technique is used to enhance the transdermal transport of drugs by applying a small current through a reservoir that contains ionized species of the drug. Positive or negative electrodes are placed between the drug reservoir and the skin. Positive ions are introduced in the skin from a positive electrode, and negative ions from a negative electrode. Figure 19–25 shows an iontophoresis circuit with the active electrode being negative. A second electrode, positive in this case, is placed a short distance away on the body to complete the circuit, and the electrodes are connected to a power supply. When the current flows, the negatively charged ions are transported across the skin, mainly through the pores (see Fig. 13–22, p. 347, for a discussion of pores). Pore transport during iontophoresis can be visualized by using a microscope and a fluorescein probe as the dye.[151] The use of this method in various diseases has been reviewed by Tyle.[152]

The isoelectric point of the skin is between 3 and 4 pH units; below pH 3 the pores are positively charged and above pH 4 they have a negative charge. Owing to the negative charge in the upper skin layers, basic drugs are relatively easy to introduce. In vitro systems designed to study iontophoretic transport involve the use of diffusion cells in which a skin membrane is placed vertically between the two halves of the cell. The "active" electrode, say the positive electrode for the transport of positive ions, is placed on the epidermal side. The other side of the cell contains a passive (oppositely charged) electrode in a conductive fluid. Glikfeld et al.[153] described an improved diffusion cell and reported iontophoretic enhancement of clonidine and morphine delivery across full-thickness hairless mouse skin. Iontophoresis enhances the transdermal absorption of insulin. At a pH below the isoelectric point of insulin (pH 5.3) the drug acts as a positive electrode, while at a pH above the isoelectric point the drug reservoir acts as a negative electrode. The greatest transport of insulin was found at pH 3.68 rather than at 7 or 8 owing possibly to low aggregation and a high charge density of insulin at pH 3.68.[154] The rate of skin permeation depends on the drug concentra-

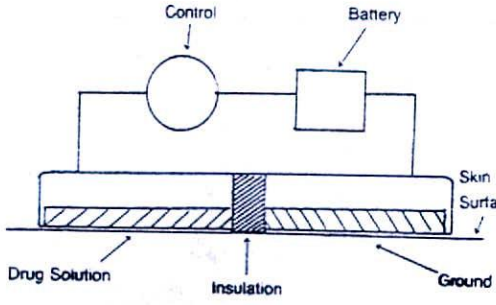


Fig. 19–25. A schematic of the iontophoresis apparatus in place on the skin.

tion, the ionic strength of the buffer solution, the magnitude of current applied, and the duration of iontophoresis.[154] Del Terzo et al.[155] found that in a series of n-alkanols, the iontophoretic transport of the more hydrophobic derivatives was decreased as compared with passive diffusion. These authors suggested that the transport of both nonionized and ionized molecules through the skin pores may be enhanced by iontophoresis, whereas the lipoidal pathway is inhibited by the use of this technique. Iontophoresis is a promising method to deliver peptides through the skin. Burnette and Marrero[156] showed that the flux of both ionized and nonionized species of thyrotropin releasing hormone were greater than the flux obtained by passive diffusion alone. The increased flux was proportional to the applied current density. Transport through the pores is favored for positive ions whereas transport of negative ions is probably smaller owing to electrostatic repulsion across the negatively charged skin membrane.

Faraday's law states that equal quantities of electricity will deposit equivalent quantities of ions at either electrode. However, the correlation between that predicted by Faraday's law and the experimental values is not good, owing to the many factors involved in iontophoretic transport. Kasting et al.[157] used an electrodiffusion model to study the transport of etidronate disodium, a negatively charged bone resorption agent, through excised human skin. At steady state, the flux J_i of drug through the membrane is given by the Nernst–Planck flux equation[158]:

$$J_i = -D_i \frac{dc_i}{dx} + \frac{D_i z_i e E c_i}{kT} \qquad (19-83)$$

where D_i is the diffusion coefficient for the ion i (in the x direction), z_i its charge, and c_i its concentration. The term kT is the thermal energy of the system where k is the Boltzmann constant and T is the absolute temperature. The Goldman approximation[158] provides a solution of equation (19–83):

$$J_i = \frac{-D_i K \nu}{h} \frac{c_i - c_o e^{-\nu}}{1 - e^{-\nu}} \qquad (19-84)$$

where K is the partition coefficient, h the thickness of the membrane, and c_i and c_o the concentrations at both sides of the membrane. Assuming that the concentration $c_o = 0$, in the limit as $\nu \to 0$, equation (19–84) becomes the flux passive diffusion, J_o (see equation (13–57), p. 338):

$$J_i = \frac{-D_i K c_i}{h} \qquad (19-85)$$

The term ν is a dimensionless driving force, defined as

$$\nu = \frac{z_i e V}{kT} \qquad (19-86)$$

where e is the electronic charge, z is the charge on the drug, k the Boltzmann constant, T the absolute temperature, and V the applied voltage across the membrane. The *iontophoretic enhancement factor*, J_i/J_o, is

$$\frac{J_i}{J_o} = \frac{\nu}{1 - e^{-\nu}} \qquad (19-87)$$

That is, equation (19–87) measures the increase in transport of a drug relative to the passive diffusion, due to the electrical current applied. For positive values (z_i and V of the same sign in equation (19–86),), equation (19–84) predicts that the enhancement in flux is proportional to ν. For negative ν values, the flux will fall exponentially with increasing magnitude of ν.

Example 19–22. (*a*) Compute the iontophoretic enhancement factor, J_i/J_o, across human excised skin for a 10% etidronate solution. The voltage applied is 0.25 V, the average number of charges, z, per ion is 2.7. The charge on the electron is 1 eV. The value kT at 25° C is 0.025 eV.

From equation (19–86),

$$\nu = \frac{2.7 \times 1 \times 0.25}{0.025} = 27$$

Using equation (19–87) the iontophoretic enhancement factor is

$$\frac{J_i}{J_o} = \frac{27}{1 - e^{-27}} = 27$$

Thus we see that the flux for the drug promoted by iontophoresis is 27 times that expected for passive diffusion.

(*b*) Compute the flux, under the driving force of iontophoresis, knowing that the passive permeability coefficient P of the drug is 4.9×10^{-6} cm/hr and the concentration, c, is 1.02×10^5 μg/cm³.

Since $P = DK/h$ cm/hr from equation (19–85),

$$J_o = 4.9 \times 10^{-6} \times 1.02 \times 10^5 = 0.5 \text{ μg/(cm}^2 \text{ hr)}$$

From equation (19–87), using the value, 27, obtained in part (*a*) for J_i/J_o,

$$J_i = 0.5 \times 27 = 13.5 \text{ μg/(cm}^2 \text{ hr)}$$

Kasting et al.[157] found that equation (19–84) applies up to 0.25 V. At higher voltages, the flux of etidronate disodium rises much faster than the predicted values, owing to alteration of the membrane and because the diffusion coefficient is no longer a constant value, as assumed in equation (19–84). Burnette and Bagniefski[159] determined the skin electrochemical resistance R after iontophoresis. The decrease in resistance suggested that the current may alter the ion-conducting pathways of the skin even at the clinically acceptable current densities, leading to tissue damage.[151] (For electrochemical resistance R, see page 127.)

Topical Administration in Cattle. Pitman and Rostas[160] reviewed the topical administration of drugs to cattle and sheep with emphasis on a description of the absorption barriers and the mechanism of absorption, and they described the drug delivery studies on cattle and sheep that have appeared in the literature.

Parenteral Administration. The intravenous, intramuscular, subcutaneous, and intraperitoneal routes are the common avenues for parenteral administration of a drug. Advances in genetic engineering have provided a number of peptide drugs and proteins such as insulin that are orally inactive and must be given by the

parenteral route. Although other routes have been investigated, such as the nasal, gastrointestinal, rectal and transdermal routes (see these sections in this chapter), parenteral administration remains the more viable route for peptides and some other drugs.[161] Controlled release can be achieved by continuous intravenous infusion, the amount of drug administered being equal to the amount of drug eliminated from the body. However, this method requires hospitalization during treatment.[162] The intravenous route is used occasionally to deliver sustained or controlled dosage forms such as liposomes, erythrocytes, nanoparticles, and small microcapsules (see pp. 513–521). Of the parenteral avenues, the subcutaneous and intramuscular routes are preferred for the controlled delivery of a drug. A number of physicochemical and physiologic factors affect the rate of release from the dosage form, as enumerated in Table 19–2. The absorption rate can be limited by the release rate from the delivery system. Figure 19–26 illustrates the rate-limiting step using several approaches such as complexation, dispersion, dissolution, adsorption, and partitioning to retard drug delivery.[163]

The drug release from aqueous solution can be prolonged by adding viscosity-increasing agents. These agents consist of water-soluble materials such as methylcellulose, sodium carboxymethylcellulose, and povidone. The increased viscosity of the medium reduces the diffusion of the drug (see the Stokes–Einstein equation, p. 401). Complex formation (Chapter 11) may prolong the delivery as long as the dissociation of the complex is slow. These same macromolecules employed as viscosity-promoting agents are used to prepare

TABLE 19–2. *Factors Influencing Parenteral Drug Absorption

A. Drug and dosage form related factors
   1. Drug's pK_a, molecular size, solubility, dissolution rate, diffusivity, partition coefficient, etc.
   2. Type of dosage form, i.e., solution (type of solvent), suspension, etc.
   3. Physical-chemical properties of dosage form (pH, osmotic pressure, viscosity, etc.)
   4. Volume of injection
   5. Initial drug concentration in dosage form
B. Physiologic factors
   1. Site of administration
      a. Local circulation
      b. Local temperature
   2. Body movement
   3. Tissue injury

*From L. Krowczynski, *Extended-Release Dosage Forms*, CRC, Boca Raton, Fla., 1987, p. 60, reproduced with permission of the copyright owner.

complexes with drugs for intramuscular injection. The release of drugs from oily solutions depends on the partition coefficient of the drug between oil and aqueous fluids of the body and also depends on the viscosity of the vehicle. Depo-Estradiol (Upjohn) is an example of an oleaginous injectable, the active principle being dissolved in a mixture of benzyl alcohol and vegetable oil.

Suspensions usually produce a more extended release in comparison with solutions. A drug in aqueous suspension injected subcutaneously must first dissolve in the tissue fluids surrounding the particle agglomerate, diffuse into the intercellular spaces or intracellular regions of the connective tissues, then permeate the vascular membranes of the bloodstream. By mixing particles of different size, the rate of dissolution can be

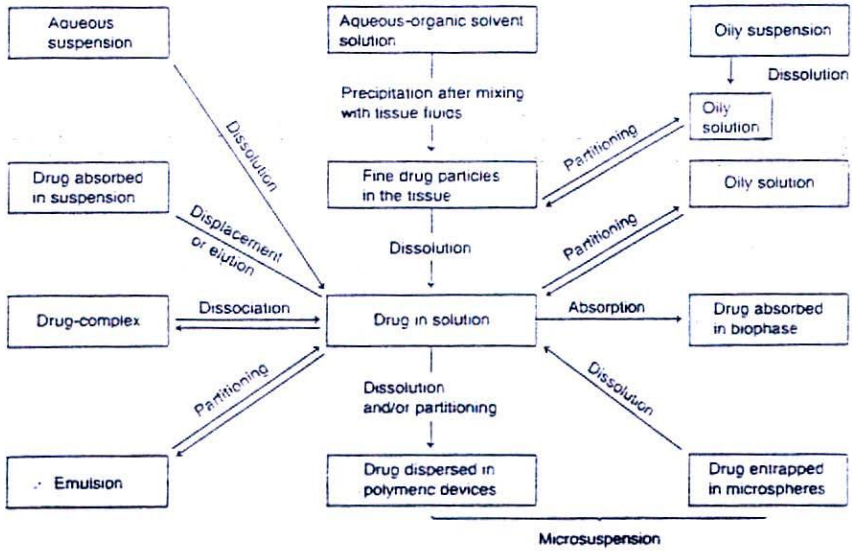


Fig. 19–26. Various approaches to achieving sustained drug action with parenteral medication. (From L. Krowczynski, *Extended-Release Dosage Forms*. CRC, Boca Raton, Fla., 1987, p. 60, reproduced with permission of the copyright owner.)

varied. Commercial zinc insulin suspensions use this approach to modulate the action of the drug. Hirano and Yamada[164] proposed a cube root expression relating the fraction of dose remaining at the subcutaneous injection site to the time,

$$\left(\frac{W}{W_o}\right)^{\frac{1}{3}} = 1 - kt \qquad (19-88)$$

where W_o is the initial amount and W is the amount of drug at time t; k is a rate constant for absorption from the depot site. The authors found that for suspensions having particle sizes between 3 and 4 μm the in vitro solubility C_s was related to the absorption constant k according to

$$\log k = 0.525 \log C_s - 0.578 \qquad (19-89)$$

where C_s is the aqueous solubility (see *Problem 19–28*). Microcapsules and microspheres, including magnetic microspheres, have been investigated as carrier suspensions for controlled delivery (see the earlier Section on microcapsules). Parenteral oil-in-water and water-in-oil emulsions can also be used as delivery systems. Examples of drug release from emulsions have been considered in Chapter 18, pages 504–506. Implants are placed subcutaneously to bring about drug delivery by way of drug diffusion, polymer dissolution, or a combination of both mechanisms. Sterile disks or cylinders (pellets) containing the drug are prepared by fusion (melting) or compression. Silicone capsules (see Chapter 13, pp. 341–342) have been used for the delivery of contraceptive hormones, L-dopa, and tranquilizers.[165] The rate of delivery is controlled by the thickness of the wall (membrane-controlled release), and produces zero-order release. The kinetics of drug delivery from matrix-type devices, on the other hand, is not zero-order, as desired. The release is proportional to the square root of time (see pp. 335, 336). The hydrophobic polymers used in the matrix-type (monolithic) devices are derived from the co-(ethylene/vinyl acetate) (EVA) polymers. The mechanism of release is not concerned with dissolution or swelling of the polymer, but rather involves diffusion of the drug through narrow channels (Fig. 19–27). Although zero-order kinetics is not usually obtained with the matrix-type systems, nearly zero-order release can be achieved by changing the geometry of the device. For example, in vitro release of bovine serum albumin is zero-order from an inward-releasing hemisphere.[161] The release from hydrogels, as contrasted to hydrophobic polymers, depends on the swelling and the degree of hydration of the polymer (pp. 497–498). Hydrogels of hydroxyethyl methacrylate (HEMA) are used as membranes for diffusion-controlled delivery of water-soluble drugs, glucose, insulin, cytochrome, and albumin.[166]

Self-regulating delivery systems have been studied for the controlled release of insulin.[167] The system is based on the competitive binding between glucose and glycosylated insulin to the specific sites of concanavalin A (Con A). Glycosylated insulin is an insulin derivative.

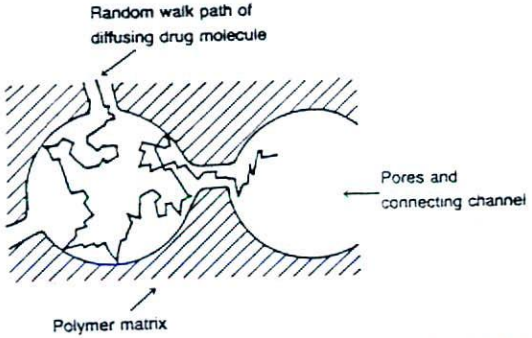


Fig. 19–27. Release of a macromolecular drug from a polymer matrix based on diffusion through narrow channels connecting larger pores. (From R. A. Siegel and R. Langer, Pharm. Res. 1, 1, 1984, reproduced with permission of the copyright owner.)

succinyl amido phenyl-α-D glucopyranoside insulin, (SAPG-insulin). Con A is a plant protein capable of binding erythrocytes, carbohydrates, insulin, and other large biologic agents. The competitive reaction is written:

$$\text{glucose} + \text{SAPG-insulin–Con A} \rightleftarrows \text{glucose–Con A} + \text{SAPG-insulin} \qquad (19-90)$$

Under conditions of hyperglycemia, glucose enters the insulin delivery device, Figure 19–28, implanted in the body and releases SAPG-insulin from its Con A binding

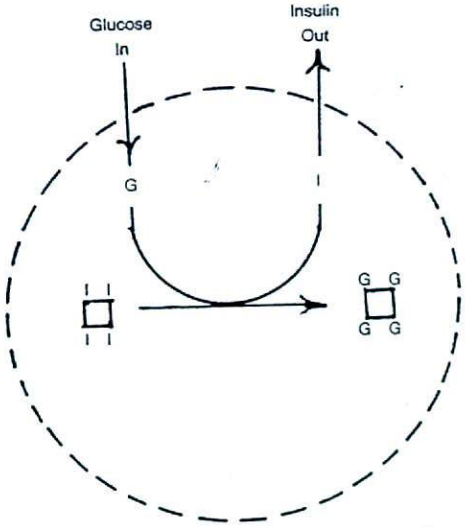


Fig. 19–28. Visualization of the insulin delivery process. Glucose, G, enters the device during bouts of hyperglycemia, displacing SAPG-insulin from the binding sites on Con A, □, forming the complex, glucose–Con A. (After S. Y. Jeong, S. W. Kim, M. J. D. Eenink and J. Feijen, J. Controlled Release 1, 37, 1984, reproduced with permission of the copyright owner.)

sites in accordance with equation (19–90). The SAPG-insulin escapes through the membrane of the delivery system to counteract the hyperglycemia. Because of its high molecular weight (~110,000 daltons), Con A cannot pass through the membrane and is retained in the device. Similar self-regulating systems under development are based on the reaction

glucose + glucose oxidase →

gluconic acid + H_2O (19–91)

In these systems, the formation of gluconic acid is accompanied by a reduction of pH, promoting the permeability of the membrane and increasing the delivery of insulin in response to an increase in glucose concentration.[168] Additional reference sources dealing with drug product design and controlled delivery are listed following the section on **References and Notes**.

References and Notes

1. T. Higuchi and V. Stella, Eds., *Prodrugs as Novel Drug Delivery Systems*, American Chemical Society, Washington, D.C., 1975.
2. H. Seki, T. Kawaguchi and T. Higuchi, J. Pharm. Sci. 77, 855, 1988.
3. R. P. Waranis and K. B. Sloan, J. Pharm. Sci. 77, 210, 1988.
4. H. Bundgaard, M. Johansen, V. Stella and M. Cortese, Int. J. Pharm. 10, 181, 1982.
5. H. Bundgaard and J. Moss, J. Pharm. Sci. 78, 122, 1989.
6. Y. Takakura, Y. Kaneko, T. Fujita, M. Hashida, H. Maeda and H. Sezaki, J. Pharm. Sci. 78, 117, 1989; Y. Takakura, M. Kitajima, S. Matsumoto, M. Hashida and H. Sezaki, Int. J. Pharm. 37, 135, 1987.
7. K. Sato, K. Itakura, K. Nishida, K. Takakura, M. Hashida and H. Sezaki, J. Pharm. Sci. 78, 11, 1989.
8. A. D. Bangham and R. W. Horne, J. Mol. Biol. 8, 660, 1964; A. D. Bangham, M. M. Standish and J. C. Watkins, J. Mol. Biol. 13, 238, 1965.
9. F. J. Martin, in *Specialized Drug Delivery Systems*, P. Tyle, Ed., Marcel Dekker, N.Y., 1990. Chapter 6.
10. C. Pidgeon and C. A. Hunt, J. Pharm. Sci. 70, 173, 1981
11. D. Lichtenberg and T. Markello, J. Pharm. Sci. 73, 122, 1984.
12. M. A. Schwartz and H. M. McConnell, Biochemistry 17, 837, 1978.
13. H. Sasaki, T. Kakutani, M. Hashida and H. Sezaki, J. Pharm. Sci. 75, 1166, 1986.
14. R. M. Abra, C. A. Hunt and D. T. Lau, J. Pharm. Sci. 73, 203, 1984.
15. R. Mezei and V. Gulasekharam, Life Sci. 26, 1473, 1980.
16. J. H. Wiessner, H. Mar, D. G. Baskin and K. J. Hwang, J. Pharm. Sci. 75, 259, 1986.
17. M. Guzman, A. Abeger and E. Sellés, Pharm. Acta Helv. 62, 163, 1987.
18. N. I. Payne, P. Timmins, C. V. Ambrose, M. D. Ward and F. Ridgway, J. Pharm. Sci. 75, 325, 1986; N. I. Payne, I. Browning and C. A. Haynes, J. Pharm. Sci. 75, 330, 1986.
19. G. Gregoriadis, Ed., *Liposome Technology*, Vol. I, II, III, CRC, Boca Raton, Fla., 1984.
20. R. Baker, *Controlled Release of Biologically Active Agents*, Wiley, N.Y., 1987, pp. 14, 15.
21. F. Lim and R. D. Moss, J. Pharm. Sci. 70, 351, 1981.
22. P. Rambourg, J. Levy and M.-C. Lévy, J. Pharm. Sci. 71, 753, 1982.
23. T. M. S. Chang, Science 146, 524, 1964.
24. M.-C. Lévy, P. Rambourg, J. Lévy and G. Potron, J. Pharm. Sci. 71, 759, 1982.
25. J. W. McGinity, A. Martin, G. W. Cuff and A. B. Combs, J. Pharm. Sci. 70, 372, 1981.
26. K. Bala and P. Vasudevan, J. Pharm. Sci. 71, 960, 1982.
27. J. R. Nixon and G. A. Agvilirah, J. Pharm. Sci. 73, 52, 1984.
28. A. C. Povey, H. Bartsch, J. R. Nixon and I. K. O'Neill, J. Pharm. Sci. 75, 831, 1986.
29. J. M. Gallo, P. K. Gupta, C. T. Hung and D. G. Perrier, J. Pharm. Sci. 78, 190, 1989; P. K. Gupta, C. T. Hung and N. S. Rao, J. Pharm. Sci. 78, 290, 1989.
30. J. Akbuğa, Int. J. Pharm. 53, 99, 1989.
31. T. Higuchi, J. Pharm. Sci. 52, 1145, 1963; R. W. Baker and H. K. Lonsdale, in *Controlled Release of Biologically Active Agents*, A. C. Tanquary and R. E. Lacey, Eds., Plenum, N.Y. 1974, pp. 15–71.
32. P. K. Gupta, F. C. Lam and C. T. Hung, Int. J. Pharm. 51, 253, 1989.
33. J. M. Gallo, C. T. Hung and D. C. Perrier, Int. J. Pharm. 22, 63, 1984.
34. G. Splenlehauer, M. Veillard and J.-P. Benoit, J. Pharm. Sci. 75, 750, 1986.
35. S. E. Leucuta, Int. J. Pharm. 54, 71, 1989.
36. R. Bodmeier and J. W. McGinity, Pharm. Res. 4, 465, 1987.
37. R. Bodmeier and J. W. McGinity, Int. J. Pharm. 43, 179, 1988.
38. S. Margel and J. Hirsh, J. Pharm. Sci. 71, 1030, 1982.
39. Y. Morimoto, H. Natsume, K. Sugiboyashi and S. Fujimoto, Int. J. Pharm. 54, 27, 1989.
40. H. Natsume, K. Sugibayashi, K. Juni, Y. Morimoto, T. Shibata and S. Fujimoto, Int. J. Pharm. 58, 79, 1990.
41. J. Kreuter, Pharm. Acta Helv. 53, 33, 1978; G. Birrenbach and P. P. Speiser, J. Pharm. Sci. 65, 1763, 1976; P. P. Speiser, in *Microencapsulation: New Techniques and Applications*, T. Kondo, Ed., Techno Inc., Tokyo, Japan, 1979; J. Kreuter and E. Liehl, J. Pharm. Sci. 70, 367, 1981.
42. P. C. Hiemenz, *Polymer Chemistry, The Basic Concepts*, Marcel Dekker, N.Y., 1984. Chapter 6; J. R. Robinson and V. H. L. Lee, Eds., *Controlled Drug Delivery, Fundamentals and Applications*, 2nd Edition, Marcel Dekker, N.Y., Chapter 3.
43. A. Roland, B. Collet, R. Le Verge and L. Toujas, J. Pharm. Sci. 78, 481, 1989.
44. N. Al Khouri Fallouh, L. Roblot-Treupel, H. Fessi, J. P. Devissaguet and F. Puisieux, Int. J. Pharm. 28, 125, 1986; P. Couvreur, M. Roland and P. Speiser, U. S. Patent, 4329 332 1982.
45. E. M. Gipps, P. Groscurth, J. Kreuter and P. P. Speiser, J. Pharm. Sci. 77, 208, 1988; E. M. Gipps, R. Arshady, J. Kreuter, P. Groscurth and P. P. Speiser, J. Pharm. Sci. 75, 256, 1986.
46. B. Kante, P. Couvreur, G. Dubois-Krack, C. de Meester, P. Guiot, M. Roland, M. Mercier and P. Speiser, J. Pharm. Sci. 71, 786, 1982.
47. P. Couvreur, B. Kante, L. Grislain, M. Roland and P. Speiser, J. Pharm. Sci. 71, 790, 1982.
48. A. G. Thombre and K. J. Himmelstein, J. Pharm. Sci. 73, 219, 1984.
49. A. Urtti, L. Salminen and O. Miinalainem, Int. J. Pharm. 23, 147, 1985.
50. A. Hussain, S. Hirai and J. Sieg, J. Pharm. Sci. 69, 735, 1980.
51. D. D.-S. Tang-Liu, S. Liu, J. Neff and R. Sandri, J. Pharm. Sci. 76, 780, 1987.
52. R. E. Stratford, Jr., L. Wulf-Carson, S. Dodda-Kashi and V. H. L. Lee, J. Pharm. Sci. 77, 838, 1988.
53. Y. Rojanasakul and J. R. Robinson, Int. J. Pharm. 55, 237, 1989.
54. G. M. Grass and J. R. Robinson, J. Pharm. Sci. 77, 3, 1988.
55. G. M. Grass and J. R. Robinson, J. Pharm. Sci. 77, 15, 1988.
56. R. D. Schoenwald and S. H. Huang, J. Pharm. Sci. 72, 1266, 1983.
57. T. F. Patton and J. R. Robinson, J. Pharm. Sci. 64, 1312, 1975.
58. S. S. Chrai and J. R. Robinson, J. Pharm. Sci. 63, 1218, 1974.
59. R. D. Schoenwald and P. Stewart, J. Pharm. Sci. 69, 391, 1980.
60. H.-W. Hu and J. R. Robinson, J. Pharm. Sci. 75, 280, 1986.
61. G. M. Grass, J. Cobby and M. C. Makoid, J. Pharm. Sci. 73, 618, 1984.
62. J. Cobby, M. Mayersohn and G. C. Walker, J. Pharm. Sci. 63, 725, 1974.
63. B. A. Johnson and G. Zografi, J. Pharm. Sci. 75, 529, 1986.
64. H. Gray and C. M. Moss, *Anatomy of the Human Body*, 29th Edition, Lea & Febiger, Philadelphia, 1972, pp. 1114–1119.
65. Y. W. Chien, K. S. E. Su and S-F. Chang, *Nasal Systemic Drug Delivery*, Marcel Dekker, N.Y., 1989, Chapter 1.

66. V. H. K. Li, J. R. Robinson and V. H. L. Lee, in *Controlled Drug Delivery*, 2nd Edition, J. R. Robinson and V. H. L. Lee, Eds., Marcel Dekker, N.Y., 1987, pp 44–45.
67. A. Hussain, S. Hirai and R. Bawarshi, J. Pharm. Sci. 69, 1411, 1980.
68. A. A. Hussain, S. Hirai and R. Bawarshi, J. Pharm. Sci. 70, 466, 1981; A. A. Hussain, R. Kimura and C. H. Huang, J. Pharm Sci. 73, 1300, 1984.
69. S.-F. Chang, L. Moore and Y. W. Chien, Pharm. Res. 5, 718, 1988.
70. C. H. Huang, R. Kimura, R. B. Nassar and A. Hussain, J. Pharm. Sci. 74, 608, 1985.
71. Y. Maitani, Y. Machida and T. Nagai, Int. Pharm. J. 49, 23, 1989.
72. Y. W. Chien, Ed., *Transdermal Systemic Medication*, Elsevier, N.Y., 1985, Chapters 7, 9.
73. Y. W. Chien, K. S. E. Su and S-F. Chang, *Nasal Systemic Drug Delivery*, Marcel Dekker, N.Y., 1989, Chapter 4.
74. M. A. Hussain, A. B. Shenvi, S. M. Rowe and E. Shefter, Pharm. Res. 6, 186, 1989.
75. K. S. E. Su, K. M. Campanaie, L. G. Mendelsohn, G. A. Kerchner and C. L. Gries, J. Pharm. Sci. 74, 394, 1985.
76. S. C. Raehs, J. Sandow, K. Wirth and H. P. Merkle, Pharm. Res. 5, 689, 1988; J. P. Longenecker, A. C. Moses, J. S. Flier, R. D. Silver, M. C. Carey and E. J. Dubovi, J. Pharm. Sci. 76, 351, 1987.
77. W. A. J. J. Hermens and F. W. H. M. Merkus, Pharm. Res. 4, 445, 1987.
78. A. S. Harris, I. M. Nilsson, Z. G.-Wagner and U. Alkner, J. Pharm. Sci. 75, 1085, 1986.
79. A. S. Harris, M. Ohlin, S. Lethagen and I. M. Nilsson, J. Pharm. Sci. 77, 337, 1988.
80. Y. Kurosaki, S. Hisaichi, L.-Z. Hong, T. Nakayama and T. Kimura, Int. J. Pharm. 49, 47, 1989; K. W. Garren and A. J. Repta, J. Pharm. Sci. 78, 160, 1989.
81. R. Anders and H. P. Merkle, Int. J. Pharm. 49, 231, 1989.
82. A. E. Collins and P. B. Deasy, J. Pharm. Sci. 79, 116, 1990.
83. M. A. Hussain, B. J. Aungst, C. A. Koval and E. Shefter, Pharm. Res. 5, 615, 1988.
84. K. Park, Int. J. Pharm. 53, 209, 1989.
85. K. V. R. Rao and P. Buri, Int. J. Pharm. 52, 265, 1989.
86. P. R. Byron, Ed., *Respiratory Drug Delivery*, CRC, Boca Raton, Fla., 1990.
87. V. H. K. Li, J. R. Robinson and V. H. L. Lee, in *Controlled Drug Delivery*, 2nd Edition, J. R. Robinson and V. H. L. Lee, Eds., Marcel Dekker, N.Y., 1987, pp. 45–49.
88. R. L. Juliano, in *International Encyclopedia of Pharmacology and Therapeutics*, Section 120, Methods of Drug Delivery, G. M. Ihler, Ed., Pergamon Press, Oxford, 1986, p. 141.
89. P. R. Byron, J. Pharm. Sci. 75, 433, 1986.
90. P. R. Byron, N. S. R. Roberts and A. R. Clark, J. Pharm. Sci. 75, 168, 1986.
91. P. R. Byron, Ed., *Respiratory Drug Delivery*, CRC, Boca Raton, Fla., 1990, pp. 225–227.
92. L. Krowczynski, *Extended-Release Dosage Forms*, CRC, Boca Raton, Fla., 1987, Chapter 6.
93. P. J. Sinko and G. L. Amidon, Pharm. Res. 5, 645, 1988.
94. M. Hu and G. L. Amidon, J. Pharm. Sci. 77, 1007, 1988.
95. G. L. Amidon, P. J. Sinko and D. Fleisher, Pharm. Res. 5, 651, 1988.
96. J. G. Prieto, L. Santos, J. P. Barrio and M. L. Alonso, J. Pharm. Sci. 76, 596, 1987.
97. M. A. Hussain, B. J. Aungst and E. Shefter, Pharm. Res. 5, 44, 1988.
98. G. E. Peters, L. E. F. Hutchinson, R. Hyde, C. McMartin and S. B. Metcalfe, J. Pharm. Sci. 76, 857, 1987.
99. L. Krowczynski, *Extended-Release Dosage Forms*, CRC, Boca Raton, Fla., 1987, pp. 104–110; ibid. p. 105.
100. M. A. Hussain, R. C. Diluccio and E. Shefter, Pharm. Res. 6, 49, 1989.
101. S. S. Ozturk, B. O. Palsson and J. B. Dressman, Pharm. Res. 5, 272, 1988; ibid. p. 281.
102. H. C. Wilson and G. W. Cuff, J. Pharm. Sci. 78, 582, 1989.
103. S. S. Jambhekar, and J. Cobby, J. Pharm. Sci. 74, 991, 1985.
104. F. Theeuwes and S. I. Yum, Ann. Biomed. Eng. 4, 343, 1976; Alzet Mini-Osmotic Pump Bibliography, Alza Corp. 1981; F. Theeuwes, in *Directed Drug Delivery*, R. T. Borchardt, A. J. Repta and V. J. Stella, Eds., Humana Press, Clifton, N.J., 1985, pp. 121–146.
105. F. Theeuwes, J. Pharm. Sci. 64, 1987, 1975.
106. F. Theeuwes, D. Swanson, P. Wong, P. Bonsen, V. Place, K. Heimlich and K. C. Kwan, J. Pharm. Sci. 72, 253, 1983.
107. G. L. Amidon, T. Higuchi and J. B. Dressman, U.S. Patent, 4 685 918 (1987).
108. J. L. Haslam, A. E. Merfeld and G. S. Rork, Int. J. Pharm. 56, 227, 1989.
109. B. Lindstedt, G. Ragnarsson and J. Hjärtstam, Int. J. Pharm. 56, 261, 1989.
110. R. Bodmeier and O. Paeratakul, J. Pharm. Sci. 79, 925, 1990.
111. V. H. K. Li, J. R. Robinson and V. H. L. Lee, in *Controlled Drug Delivery*, 2nd Edition, J. R. Robinson and V. H. L. Lee, Eds., Marcel Dekker, N. Y., 1987, p. 43.
112. A. G. de Boer, D. D. Breimer, J. Pronk and J. M. Gubens-Stibbe, J. Pharm. Sci. 69, 804, 1980.
113. G. G. Liversidge, T. Nishihata, K. K. Engle and T. Higuchi, Int. J. Pharm. 23, 87, 1985.
114. T. Nishihata, S. Kim, S. Morishita, A. Kamada, N. Yata and T. Higuchi, J. Pharm. Sci. 72, 280, 1983.
115. K. Morimoto, H. Akatsuchi, R. Aikawa, M. Morishita and K. Morisaka, J. Pharm. Sci. 73, 1366, 1984.
116. W. M. Wu, T. Murakami, Y. Higashi and N. Yata, J. Pharm. Sci. 76, 508, 1987; W. M. Wu, T. Murakami, A. Yamajo, Y. Higashi and N. Yata, J. Pharm. Sci. 78, 499, 1989.
117. T. Nishihata, C.-S. Lee, M. Yamamoto, J. H. Rytting and T. Higuchi, J. Pharm. Sci. 73, 1326, 1984.
118. T. Nishihata, J. H. Rytting and T. Higuchi, J. Pharm. Sci. 69, 744, 1980.
119. T. Nishihata, J. H. Rytting and T. Higuchi, J. Pharm. Sci. 70, 71, 1981.
120. J. A. Fix, P. S. Leppert, J. A. Porter and L. J. Caldwell, J. Pharm. Sci. 72, 1134, 1983.
121. T. Nishihata, S. Kawabe, M. Miyake, S. Kim and A. Kamada, Int. J. Pharm. 22, 147, 1984.
122. Y. Watanabe, E. J. van Hoogdalem, A. G. de Boer and D. D. Breimer, J. Pharm. Sci. 77, 847, 1988; E. J. van Hoogdalem, M. A. Hardens, A. G. de Boer and D. D. Breimer, Pharm. Res. 5, 453, 1988.
123. J. A. Fix, J. Alexander, M. Cortese, K. Engle, P. Leppert and A. J. Repta, Pharm. Res. 6, 501, 1989.
124. A. Buur and H. Bundgaard, J. Pharm. Sci. 75, 522, 1986.
125. M. Tomita, M. Shiga, M. Hayashi and S. Awazu, Pharm. Res. 5, 341, 1988.
126. W. Curatolo, Pharm. Res. 4, 271, 1987.
127. R. L. Bronaugh and R. F. Stewart, J. Pharm. Sci. 75, 487, 1986.
128. R. H. Guy and J. Hadgraft, Pharm. Res. 5, 753, 1988.
129. K. Tojo, J. Pharm. Sci. 76, 889, 1987.
130. B. W. Barry, Int. J. Cosmet. Sci. 10, 281, 1988.
131. M.-S. Wu, J. Pharm. Sci. 72, 1421, 1983.
132. K. Tojo, C. C. Chiang and Y. W. Chien, J. Pharm. Sci. 76, 123, 1987.
133. P. P. Sarpotdar and J. L. Zatz, J. Pharm. Sci. 75, 176, 1986.
134. J. Swarbrick, G. Lee, J. Brom and N. P. Gensmantel, J. Pharm. Sci. 73, 1352, 1984.
135. C. Fleeker, O. Wong and J. H. Rytting, Pharm. Res. 6, 443, 1989.
136. P. S. Banerjee and W. A. Ritschel, Int. J. Pharm. 49, 189, 1989.
137. D. B. Guzek, A. H. Kennedy, S. C. McNeill, E. Wakshull and R. O. Potts, Pharm. Res. 6, 33, 1989.
138. R. O. Potts, S. C. McNeill, C. R. Desbonnet and E. Wakshull, Pharm. Res. 6, 119, 1989.
139. S. Y. Chan and A. L. W. Po, Int. J. Pharm. 55, 1, 1989.
140. E. M. Niazy, A. M. Molokhia and A. S. El Gorashi, Int. J. Pharm. 56, 181, 1989.
141. T. Nishihata, J. H. Rytting, K. Takahashi and K. Sakai, Pharm. Res. 5, 738, 1988.
142. J. W. Wiechers, B. F. H. Drenth, J. H. G. Joknman and R. A. de Zeeuw, Pharm. Res. 4, 519, 1987.
143. P. K. Wotton, B. Mœllgaard, J. Hadgraft and A. Hoelgaard, Int. J. Pharm. 24, 19, 1985; R. A. Patel and R. C. Vasavada, Pharm. Res. 5, 116, 1988; P. Agrawala and W. A. Ritschel, J. Pharm. Sci. 77, 776, 1988; P. Catz and D. R. Friend, Int. J. Pharm. 55, 17, 1989.
144. O. Wong, J. Huntington, T. Nishihata and J. H. Rytting,

Pharm. Res. 6, 286, 1989; D. D.-S. Tang-Liu, J. Neff, H. Zolezio and R. Sandri, Pharm. Res. 5, 477, 1988.
145. G. Gienger, A. Knoch and H. P. Merkle, J. Pharm. Sci. 75, 9, 1986.
146. R. H. Guy and J. Hadgraft, J. Pharm. Sci. 73, 883, 1984; R. H. Guy and J. Hadgraft, J. Pharm. Sci. 74, 1016, 1985.
147. Y. W. Chien, in *Controlled Drug Delivery*, 2nd Edition, J. R. Robinson and V. H. L. Lee, Eds., Marcel Dekker, N.Y., 1987, p. 533, 534.
148. D. Arndts and K. Arndts, Eur. Clin. Pharmacol. 26, 79, 1984;
149. P. K. Noonan, M. A. Gonzalez, R. Ruggirello, J. Tomlinson, E. Babcock-Atkinson, M. Ray, A. Golub and A. Cohen, J. Pharm. Sci. 75, 688, 1986.
150. B. Berner, J. Pharm. Sci. 74, 718, 1985.
151. R. R. Burnette and B. Ongpipattanakul, J. Pharm. Sci. 77, 132, 1988.
152. P. Tyle, Pharm. Res. 3, 318, 1986.
153. P. Glikfeld, C. Cullander, R. Hinz and R. H. Guy, Pharm. Res. 5, 443, 1988.
154. O. Siddiqui, Y. Sun, J.-C. Liu and Y. W. Chien, J. Pharm. Sci. 76, 341, 1987.
155. S. Del Terzo, C. R. Behl and R. A. Nash, Pharm. Res. 6, 85, 1989.
156. R. R. Burnette and D. Marrero, J. Pharm. Sci. 75, 738, 1986.
157. G. B. Kasting, E. W. Merrit and J. C. Keister, J. Membrane Sci. 35, 137, 1988.
158. G. B. Kasting and J. C. Keister, J. Controlled Release 8, 195, 1989.
159. R. R. Burnette and T. M. Bagniefski, J. Pharm. Sci. 77, 492, 1988.
160. I. H. Pitman and S. J. Rostas, J. Pharm. Sci. 70, 1181, 1981.
161. C. G. Pitt, Int. J. Pharm. 59, 173, 1990.
162. V. H. K. Li, J. R. Robinson and V. H. L. Lee, in *Controlled Drug Delivery*, 2nd. Edition, J. R. Robinson and V. H. L. Lee, Eds., Marcel Dekker, N.Y., 1987, p. 37.
163. L. Krowczynski, *Extended-Release Dosage Forms*, CRC, Boca Raton, Fla., 1987, p. 59.
164. K. Hirano and H. Yamada, J. Pharm. Sci. 71, 500, 1982.
165. L. Krowczynski, *Extended-Release Dosage Forms*, CRC, Boca Raton, Fla., 1987, p. 84.
166. S. Sato and S. W. Kim, Int. J. Pharm. 22, 229, 1984.
167. L. A. Seminoff, G. B. Olsen and S. W. Kim, Int. J. Pharm. 54, 241, 1989.
168. S. Y. Jeong, S. W. Kim, M. J. D. Bennink and J. Feijen, J. Controlled Release 1, 57, 1984.
169. S. Benita, D. Babay, A. Hoffman and M. Donbrow, Pharm. Res. 5, 178, 1988.
170. A. A. Hussain, R. Barawshi-Nassar and C. H. Huang, "Physicochemical Considerations of Intranasal Drug Administration," in *Transnasal Systemic Medication*, Y. C. Chien, Ed., Elsevier, New York, 1985, pp. 128–129.
171. B. Hoener and L. Z. Benet, *Modern Pharmaceutics*, Banker and Rhodes, Eds., Marcel Dekker, N.Y., 1990, p. 165.
172. D. S. Roy and G. L. Flynn, Pharm. Res., 6, 147, 1989.

Additional References

A. C. Tanquary and R. E. Lacey, *Controlled Release of Biologically Active Agents*, Plenum Press, N.Y., 1974.
D. R. Paul and F. W. Harris, Eds., *Controlled Release Polymeric Formulations*, American Chemical Society, Washington, D.C., 1976.
S. K. Chandrasekaran and J. E. Shaw, "Design of Transdermal Systems, in *Contemporary Topics in Polymer Science*, Vol. 2, Plenum Press, N.Y., 1977.
G. Gregoriadis, Ed., *Drug Carriers in Biology and Medicine*, Academic Press, N.Y., 1979.
R. Baker, Ed., *Controlled Release of Bioactive Materials*, Academic Press, N.Y., 1980.
R. Juliano, Ed., *Drug Delivery Systems*, Oxford Press, N.Y., 1980.
A. F. Kydonieus, Ed., *Controlled Release Technologies: Methods, Theory and Applications*, CRC, Boca Raton, Fla., 1980.
S. Yolles and M. P. Sartori, *Drug Delivery Systems*, Oxford Press, N.Y., 1980.
H. Bundgaard, A. B. Hansen and H. Kofod, Eds., *Optimization of Drug Delivery*, Munksgaard, Copenhagen, 1981.
D. H. Lewis, Ed., *Controlled Release of Pesticides and Pharmaceuticals*, Plenum Press, N.Y., 1981.
L. F. Prescott and W. S. Nimmo, Eds., *Drug Absorption*, ADIS Press, Balgowlah, Australia and New York, 1981.
Y. W. Chien, *Novel Drug Delivery Systems*, Marcel Dekker, N.Y., 1982.
C. Gregoriadis, J. Senior and A Trouet, Eds., *Targeting of Drugs*, Plenum Press, N.Y., 1982.
M. Ostro, Ed., *Liposomes*, Marcel Dekker, New York, 1983.
T. J. Roseman and S. Z. Mansdorf, Eds., *Controlled Release Delivery Systems*, Marcel Dekker, N.Y., 1983.
S. S. Davis, L. Illum, J. G. McVie and E. Tomlinson, Eds., *Microspheres and Drug Therapy*, Elsevier, N.Y., 1984.
P. D. Deasy, *Microencapsulation and Related Drug Processes*, Marcel Dekker, N.Y., 1984.
R. S. Langer and D. L. Wise, Eds., *Medical Applications of Controlled Release*, Vol. I, *Classes of Systems*, Vol. II, *Applications and Evaluation*, CRC, Boca Raton, Fla., 1984.
R. T. Borchardt, A. J. Repta and V. J. Stella, Eds., *Directed Drug Delivery: A Multi-disciplinary Problem*, Humana Press, Clifton, N.J., 1985.
Y. W. Chien, Ed., *Transdermal Systemic Medications*, Elsevier, N.Y., 1985.
L. F. Prescott and W. S. Nimmo, Eds., *Rate Control in Drug Therapy*, Churchill Livingstone, N.Y., 1985.
V. Smolen, Ed., *Controlled Drug Bioavailability*, Wiley, N.Y., 1985.
P. Guiot and P. Couvreur, *Polymeric Nanoparticles and Microspheres*, CRC, Boca Raton, Fla., 1986.
G. M. Ihler, *Methods of Drug Delivery*, Pergamon Press, N.Y., 1986.
N. A. Peppas, Ed., *Hydrogels in Medicine and Pharmacy*, CRC, Boca Raton, Fla., 1986.
H. A. J. Struyker-Boudier, *Rate-Controlled Drug Administration and Action*, CRC, Boca Raton, Fla., 1986.
Y. W. Chien, Ed., *Transdermal Controlled Systemic Medications*, Marcel Dekker, N.Y., 1987.
A. F. Kydonieus and B. Berner, Eds., *Transdermal Delivery of Drugs*, Vols. I, II, and III, CRC, Boca Raton, Fla., 1987.
P. I. Lee and W. R. Good, Eds., *Controlled Release Technology*, ACS Symposium Series, No. 348, American Chemical Society, Washington, D.C., 1987.
J. R. Robinson and V. H. L. Lee, Eds., *Controlled Drug Delivery, Fundamentals and Applications*, 2nd Edition, Marcel Dekker, N.Y., 1987.
A. Rembaum and Z. A. Tokes, *Microspheres: Medical and Biological Applications*, CRC, Boca Raton, Fla., 1988.
P. Tyle, Ed., *Drug Delivery Devices, Fundamentals and Applications*, Marcel Dekker, N.Y., 1988.
P. R. Byron, *Respiratory Drug Delivery*, CRC, Boca Raton, Fla., 1989.
Y. W. Chien, K. S. E. Su and S.-F. Chang, *Nasal Systemic Drug Delivery*, Marcel Dekker, N.Y., 1989.
L. T. Fan and S. K. Singh, *Controlled Release—A Quantitative Treatment*, Springer-Verlag, New York, 1989.
U. Gundert-Remy and H. Mollier, *Oral Controlled Release Products*, CRC, Boca Raton, Fla., 1989.
R. Gurney and H. E. Junginger, *Bioadhesion Possibilities and Future Trends*, CRC, Boca Raton, Fla., 1989.
J. Hadgraft and R. H. Guy, Eds., *Transdermal Drug Delivery*, Marcel Dekker, N.Y., 1989.
J. G. Hardy, S. S. Davis and C. G. Wilson, Eds., *Drug Delivery to the Gastrointestinal Tract*, Wiley, N.Y., 1989.
V. M. Lenaerts and R. Gurney, *Bioadhesive Drug Delivery Systems*, CRC, Boca Raton, Fla., 1989.
D. W. Osborne and A. H. Amann, Eds., *Topical Drug Delivery Formulations*, Marcel Dekker, N.Y., 1989.
J. Kost, Ed., *Pulsed and Self-Regulated Drug Delivery*, CRC, Boca Raton, Fla., 1990.

*Problems**

19–1. (a) Calculate the volume VW_s of total water encapsulated in a three-lamella ($n = 3$) liposome having a radius $R = 0.0447$ μm and

*Note that the definition of the symbols of Lichtenberg and Markello in this problem are not the same as those of Pidgeon and Hunt (*Problem 19–1*). For example, i of R_i does not have the same meaning for these authors.

a volume of phospholipid, VL_3 (which constitutes the three bilayers) of 15.2 μm^3. See *Example 19–1*, page 514.

(b) The liposomal preparation is found to contain a homogeneous population of $N = 52.7 \times 10^{14}$ liposome particles. The total volume of phospholipid, TVL_3 in the N liposomes of this three-lamellar preparation is calculated[10] knowing N and VL_3. The total volume of water TVW_3 entrapped in the N liposomes of this three-lamellar liposomal population is calculated using $N \times VW_3$.

(c) Calculate E, the *encapsulation ratio* of water to phospholipid (see p. 514, *Example 19–1*).

(d) Calculate the total surface area TSA_3 for the homogeneous population of three-lamella liposomes. The equation required is

$$TSA_3 = 4\pi N_3 R_3^2$$

The value for R_3 is 0.0447 and for N_3 is 52.7×10^{14}, as found in the accompanying table.

Data for *Problem 19–3:*

Parameters Used to Calculate Homogeneous Liposome Populations**

n	1	2	3
R (μm)	0.0225	0.0336	0.0447
$VL_n \times 10^5$ μm³	1.99	6.68	15.2
$LW_n \times 10^5$ μm³	2.78	9.21	22.2
E	1.40	1.38	1.46
$N \times 10^{-14}$	404	120	52.7
$TSA \times 10^{-13}$ μm²	25.7	17.0	13.2
$TVW \times 10^{-12}$ μm³	1.12	1.11	1.17

**The table and equations in this problem are from reference 10.

Answers: (a) $VW_3 = 2.22 \times 10^{-4}$ μm³; (b) $TVL_3 = 8.01 \times 10^{21}$ μm³; (c) $E = 1.46$; (d) $TSA_3 = 1.32 \times 10^{14}$ μm²

19–2. Lichtenberg and Markello[11] calculated the dimensions of a liposome in a way somewhat different from that used by Pidgeon and Hunt (*Problem 19–1*). For a multilamellar vesicle—a liposome—of five bilayers (Fig. 19–29), the radius R_i of the outer surface of any of the bilayers, $i = 1$ to $i = 5$, is given by the equation of Lichtenberg and Markello[11]

$$R_i = R_1 - [(i - 1)(45.7 + d)] \qquad (19-92)$$

in which R_1, the outermost radius of the liposome, is 5000 Å, the value 45.7 is the thickness in angstroms of each phospholipid bilayer, and $d = 60.0$ Å is the thickness of each aqueous shell separating the bilayers.

As observed in Figure 19–29, the serial number i of each bilayer is counted inward from the outermost bilayer, designated R_1.

(a) Using equation (19–92), obtain the values in angstroms for the radius of each of the phospholipid bilayers, R_2, R_3, R_4, and R_5.

PE, the *percent exposure*, is defined as the external surface area of the outermost bilayer, $4\pi R_1^2$, divided by the sum of the surface areas of the five bilayers, and multiplied by 100. The equation for *percent exposure* is

$$PE = \frac{R_1^2}{\sum_{i=1}^{n} [R_1 - (i - 1)(45.7 + d)]^2} \times 100 \qquad (19-93)$$

Counting from the outer phospholipid bilayer of radius R_1, the innermost bilayer radius is R_n, in which $n = 5$.

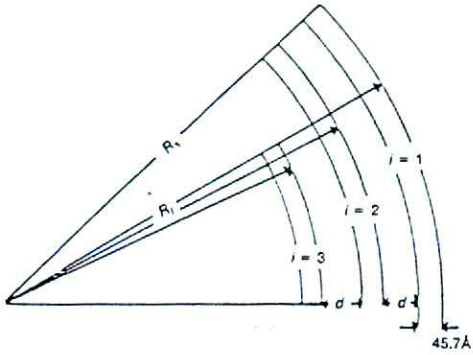


Fig. 19–29. Model of a liposome showing multilamellar (multilayer) structure of the lipid bilayers. R_1 stands for the outermost radius of the liposomal vesicle, i is the serial number of the bilayers running from $i = 1$ for the outermost bilayer, and d is the thickness of the aqueous layers interposed between the lipid bilayers. The authors have assumed that the thickness of each hydrated phospholipid bilayer is 45.7 Å, as shown at the bilayer labeled $i = 1$. (After D. Lichtenberg and T. Markello, J. Pharm. Sci. 73, 122, 1984, reproduced with permission of the copyright owner.)

(b) Calculate the percent exposure PE for this liposome in which d is 60 Å. Note that a value 4π appears in both the numerator and denominator to obtain the surface area. These terms cancel and so do not appear in equation (19–93).

(c) The aqueous core of the liposome has a radius

$$R_n = R_5 = R_1 - [(45.7 \times n) + d(n - 1)] \qquad (19-94)$$

in which $R_1 = 5000$ Å and $d = 60$ Å and the volume

$$V_n = V_5' = (4/3)\pi R_5'^3$$

Calculate the radius R_5' and the volume V_5' of the aqueous core of the liposome.

Answers: (a) $R_2 = 4894$ Å, $R_3 = 4789$ Å, $R_4 = 4683$ Å, $R_5 = 4577$ Å; (b) $PE = 4.36\%$; (c) $R_5' = 4532$ Å, $V_5' = 3.90 \times 10^{11}$ Å$^3 = 0.39$ μm³

19–3. (a) The mean diameter of an ethylcellulose microsphere containing indomethacin was found by Benita et al.[168] using a projection microscope to be 340 μm (340×10^{-4} cm). What is the volume of the microsphere assuming it is roughly spherical?

(b) The density of the microsphere is 1.15 g/cm³; calculate its mass in micrograms.

(c) The amount of indomethacin in the microsphere is 22.5% by weight. What is the total amount of the drug that can be released in 0.5 mL of buffer solution from the microsphere?

Answers: (a) 2.058×10^{-6} cm³; (b) 23.67 μg; (c) 5.33 μg/0.5 mL or 10.66 μg/mL

19–4. The polymer polylactide was used as a biodegradable controlled-release microcapsule for delivery of the narcotic antagonist cyclazocine. The molecular weight of polylactide in g/mole (daltons) may be determined using the Mark–Houwink equation

$$[\eta] = K M^a$$

in which $[\eta]$ is the intrinsic viscosity, 17.50 dL/g at 25° C, and the values of K and a for this class of polymers have been reported to be $K = 1.69 \times 10^{-3}$ dL/g and $a = 0.950$, respectively.

What is the molecular weight of the polylactide used to prepare the microcapsule? (*Note:* 1 dL = 0.1 liter = 100 mL.)

Answer: The molecular weight of this polylactide is 16,845 daltons = 16,845 g/mole = 17,000 gram/mole.

19–5. The diffusion coefficient D of a new pilocarpine derivative in ocular fluid is 9.2×10^{-5} cm²/sec. The surface area S of an Ocusert is

0.80 cm², the liquid–liquid partition coefficient K between the fluids of the Ocusert and the eye is 1.81, and the thickness of the Ocusert membrane, h, is 0.01 cm. The solubility of the drug in water, C_s, is 8.0 mg/cm³. Calculate the cumulative amount of pilocarpine released from an Ocusert in milligrams per 24-hour day. See *Example 19–8*.

Answer: 0.931 mg

19–6. The transcorneal permeation of pilocarpine at several pH values was studied at 34° C using an in vitro rabbit corneal preparation. The fraction of un-ionized pilocarpine, f_B, as a function of pH is found in the following table:

Data for *Problem 19–6**

pH	4.67	5.67	6.24	6.40
f_B	0.01	0.09	0.27	0.35

*Data from A. K. Mitra and T. J. Mikkelson, J. Pharm. Sci. 77, 771, 1988.

The permeability coefficient of the nonionized form P_B is 9.733×10^{-6} cm/sec and the permeability coefficient of the ionized form is $P_{BH^+} = 4.836 \times 10^{-6}$ cm/sec. The concentration of pilocarpine in the donor compartment is constant, $C_d = 3.69 \times 10^{-5}$ mole cm^{-3}.

(a) Compute the total permeability coefficient, $P = P_B f_B + P_{BH^+} f_{BH^+}$ and the total flux, $J = J_B + J_{BH^+} = PC_d$ for pilocarpine under steady-state conditions at the various pH values studied.

(b) Compute the amount of penetrant, M, through the corneal membrane at 30, 60, and 150 min at pH 6.4 for the ionized and the nonionized forms of pilocarpine. The diffusional area is $S = 0.95$ cm². The thickness of the membrane is $h = 0.022$ cm. *Hint:* Use the equations given in Chapter 13 to solve parts (b) and (c).

Partial Answer: (a) At pH 4.67, $P = 4.885 \times 10^{-6}$ cm/sec; $J = 1.80 \times 10^{-10}$ mole/(cm² sec); (b) At $t = 30$ min, $M_B = 2.15 \times 10^{-7}$ mole; $M_{BH^+} = 1.98 \times 10^{-7}$ mole; (c) $t_L = 13$ min

19–7. The nasal absorption of benzoic acid is influenced greatly by pH, the percent absorbed being large at low pH, i.e., pH 2 to 4, and the percent absorbed being small at high pH, i.e., pH 6 to 8. The observed absorption constant k_{obs} at low pH is given by equation (19–17), and at high pH values k_{obs} is given by equation (19–18). The ionization constant of benzoic acid $K_a = 6.30 \times 10^{-5}$, $pK_a = 4.2$. At a pH of 2.4, the observed first-order absorption rate constant,[170] k_{obs}, is 9.60×10^{-3} min^{-1}, and at pH 7.19, k_{obs} is 2.40×10^{-3} min^{-1}.

(a) Calculate k_{HA} and k_{A^-}, the specific first-order nasal absorption rate constants at pH 2.4 where benzoic acid is in the totally nonionized form, and at pH 7.19 where benzoic acid is in the totally ionized form.

(b) Using k_{HA} and k_{A^-} obtained in (a) above, calculate k_{obs} for the nasal absorption of benzoic acid at pH 8.2 and for absorption at pH = 3.0.

Answers: (a) $k_{HA} = 9.75 \times 10^{-3}$ min^{-1}; $k_{A^-} = 2.40 \times 10^{-3}$ min^{-1}; (b) k_{obs} at pH 3.0 $= 9.17 \times 10^{-3}$ min^{-1}; k_{obs} at pH 8.2 $= 2.40 \times 10^{-3}$ min^{-1}.

19–8. Nasal absorption has been considered to be facilitated by a carrier mechanism and therefore to follow the Michaelis–Menten scheme (pp. 293, 294). The Lineweaver–Burk equation (equation (12–68), p. 294),

$$\frac{1}{V} = \frac{1}{V_m} + \frac{K_m}{V_m}\frac{1}{S}$$

may be used for nasal absorption. V is the rate or velocity of absorption of a drug substance, V_m is the maximum velocity of absorption when the drug is at a high concentration and all the carrier is combined with it, S is the concentration of the drug, and K_m is the Michaelis constant that expresses the tendency of the carrier-drug to decompose.

The nasal absorption of the amino acid L-tyrosine was measured in a nasal in situ rat preparation at 37° C and a pH of 7.4; the data of Hussain et al.[170] as read from their graph is:

Data for *Problem 19–8*

$10^{-3} \times S^{-1}$ (concentration^{-1})(M^{-1})* of L-tyrosine	0.42	0.86	1.79	3.58
$10^{-3} \times V^{-1}$ (absorption rate^{-1})(M^{-1} hr)	3.19	4.62	5.72	8.00

*Note that the value 0.42, for example, expressed as 10^{-3} × (concentration) is actually $0.42 \times 10^{3} = 420$. And 3.580×10^{-3} × (concentration) means 3580. Likewise for the reciprocal concentration $S^{-1} = 3580$ in the table, V^{-1} is equal to 8.00×10^{3} or 8000. That is to say, when the exponent on a unit in a table heading is negative, as in (mole/liter) × 10^{-3}, the actual exponent is to be read 10^{+3}. When the exponent in the table heading is 10^{+3}, the actual exponent is read as 10^{-3}

(a) Using linear regression analysis, calculate V_m, the maximum rate of nasal absorption of L-tyrosine.

(b) Also from regression analysis, calculate the Michaelis constant K_m and give an interpretation of this constant in nasal absorption. (*Hint:* Return to the word-definition of K_m on page 294 and the formula $K_m = (k_2 + k_3)/k_1$.

(c) Plot the data on a rectangular coordinate graph and carry the straight line to a point where it intersects the *horizontal* axis, to the *left* of the vertical or y-axis. At this point, $-1/K_m$ may be read. Use the Lineweaver-Burk expression to show that this point on the horizontal axis provides the value, $-1/K_m$. (*Hint:* Set $1/V$, the value on the y-axis, equal to zero.) Finally, read the value $-1/K_m$ on the x-axis, invert it, and change the sign to obtain K_m. How does this value of K_m compare with K_m obtained from the slope of the line in (b) above?

(d) At a concentration $S = 4.26 \times 10^{-4}$ molar, such that $1/S = 2347$ M^{-1}, what is the absorption rate of L-tyrosine in molar concentration per hour?

Answers: (a) $V_m = 3.32 \times 10^{-4}$ M hr^{-1}; (b) $K_m = 4.75 \times 10^{-4}$ M; (c) $K_m = 4.74 \times 10^{-4}$ M; (d) $1/V = 6359.5$ M^{-1} hr; $V = 1.57 \times 10^{-4}$ molar concentration per hour (mole/liter hr)

19–9.* An aerosol was administered to an isolated perfused rat lung preparation. Using equation (19–22), compute the particle transfer B at $t = 20$ min. The transferable amount, $A = 30$ μg, the respiratory frequency $RF = 14$ min^{-1}, the dose number $n = 20$ min × 14 cycles/min, and the rate constant $k = 0.058$ min^{-1}. (See *Example 19–11.*)

Answer: $B = 12.3$ μg

19–10. An aerosol was administered to an isolated perfused rat lung preparation. Compute the particle transfer B at $t = 40$ min. The transferable amount $A = 7.8$ μg, the respiratory frequency $RF = 14$ min^{-1}, the dose number $n = 280$, and the rate constant $k = 0.07$ min^{-1}. *Hint:* You will need equation (19–22) to compute B_{20} for $t = 20$ min, and use this value in equation (19–23) to obtain the value of B_{40} at $t = 40$ min.

Answer: $B_{40} = 3.61$ μg

19–11. A penicillin derivative has a K_a of 3.5×10^{-3} mole/liter at 25° C and a solubility C_s in the stationary layer of solvent in contact with the drug particle of 2.6×10^{-3} g/cm³. In the bulk phase of the solution, the concentration of drug, c_g is 1.7×10^{-4} g/cm³. The diffusion coefficient D of the drug in the medium is 6.8×10^{-7} cm²/sec, the total surface area S of the particles is 1.5×10^{4} cm², and the thickness h of the stationary layer is 8.0×10^{-3} cm. Hoener and Benet[171] modified the Nernst–Brunner equation as follows:

$$\frac{dM}{dt} = \frac{DS}{h}\left\{ C_s\left(1 + \frac{K_a}{[H^+]}\right) - C_g \right.$$

to calculate the dissolution rate of weak acids such as penicillin in solutions of increasing pH. Calculate the dissolution rate dM/dt of the penicillin derivative in solution of increasing pH that would occur in the stomach and the small intestine, viz., pH = 0, 1.0, 2.0, 3.0, 4.0,

*Problem 19–9 was prepared by Dr. P. R. Byron, Medical College of Virginia, Virginia Commonwealth University.

5.0, 6.0, and 7.0, and plot dM/dt versus pH on rectangular coordinate paper. You may also care to plot log (dM/dt) versus pH to obtain a much-improved curve.

Answer:

pH	0	1	2	3	4	5	6	7
(dM/dt) g/sec	0.003	.00321	.0042	.0147	0.119	1.163	11.6	116

19–12. A new drug, gastrogen, was developed to inhibit gastric acid secretion and was formulated into an osmotic gastrointestinal therapeutic system. The area S of the semipermeable membrane of the new dosage form is 2.0 cm^2, the membrane thickness h is 0.019 cm, the permeability coefficient K of the drug in gastric fluid is 5.0×10^{-6} cm^2/(atm hr), and the osmotic pressure π, provided by KCl in this osmotic pump-like dosage form, is 120 atm. The solubility of the drug in the gastric fluid C_s at 37° C is 750 mg/cm^3. What is the zero-order delivery rate of the drug in mg/hr from this system? Disregard any drug diffusion through the membrane. Use equation (19–50).

Answer: $(dM/dt)_z = 47.4$ mg/hr

19–13.* (a) A formulation scientist prepares a batch of 400-mg tablets (surface area $S = 2$ cm^2) and coats them to a 10% w/w loading with an enteric coating acidic polymer, HA. The pK_a of the polymer is 4.5 and its intrinsic solubility $[HA]_s = 6$ mg/mL. If these tablets are tested under simulated gastric conditions (pH = 1.5) and intestinal conditions (pH = 6.8) in well-buffered media, will they meet the specification criteria of staying intact in gastric conditions for at least 2 hours but disintegrating within 30 minutes in the intestine? Use equation (19–41) to compute the rate of dissolution, ν of the polymer at sink conditions, where $C_{T,b} = 0$. The diffusion coefficient of the polymer is $D_p = 5 \times 10^{-8}$ cm^2/sec in aqueous media and the boundary layer thickness h is 50 μm. Assume that the coating remains intact until 90% has dissolved.

(b) If specification criteria are not accomplished with these tablets, what changes in the formulation can be used to meet specifications? *Hint:* The concentration of polymer at the surface–liquid interface, $C_{T,s}$, can be computed from equation (19–42) using the pH values given above.

Answers: (a) Polymer dissolution rate at gastric pH is 72×10^{-4} mg/min; at intestinal pH it is 1.44 mg/min. The time required for dissolution before the coating ruptures is 83 hr in the gastric medium and 25 minutes in the intestinal medium. The release meets specifications. (b) If release does not meet specifications, slightly less coating could be used. Or, a polymer that provides an enteric coating could be used with lower pK_a and/or higher solubility.

19–14. (a) Using equations (19–48) and (19–43), compute the surface pH value and the solubility, $C_{T,s}$, at the solid–liquid interface of papaverine, a weak base, in a matrix-type dosage form. The pH of the bulk is 3.0. The intrinsic solubility of the drug is $[B]_s = 3.08 \times 10^{-5}$ M, the dissociation constant of the conjugate acid is $K_a = 1.26 \times 10^{-6}$, and the diffusivities of the nonionized and ionized species are $D_B = D_{BH^+} = 6.8 \times 10^{-6}$ cm^2/sec, and $D_{H^+} = D_{OH^-} = 2.7 \times 10^{-5}$ cm^2/sec. Assume sink conditions, i.e., $[B] = [BH^+] = 0$. That is to say, in the sink the concentrations are reduced to zero. (Data from Ozturk et al.[101]). *Hint:* Use the values given in Table 19–1 for basic drugs to compute the terms a, b, and c in equation (19–48).

(b) Using equation (19–41), compute the in vitro rate of dissolution, ν. The surface area of the matrix is 1.8 cm^2. The thickness of the aqueous layer is 100 μm. *Hint:* Use the diffusivity $D_B = 6.8 \times 10^{-6}$ cm^2/sec and the value $C_{T,s}$ obtained in part (a) in equation (19–41). Under sink conditions, $C_{T,b}$ in equation (19–41) is equal to zero. *Example 19–14* shows the calculations for an acidic drug.

Answers: (a) The pH at the surface is 3.85: $C_{T,s} = 3.47 \times 10^{-3}$ M; (b) $\nu = 4.25 \times 10^{-6}$ mole cm^{-2} sec^{-1}

19–15. The rate of delivery into a biologic system of a weak electrolyte drug from an aqueous vehicle depends on the solubility and the ionization of the drug, which are functions of the pH. Roy and Flynn[178] studied the aqueous solubility of fentanyl, a synthetic analog of morphine, at 35° C and at various pH values. Fentanyl is a basic drug, and its equilibrium in water can be expressed as

$$BH^+ + H_2O \rightleftarrows B + H_3O^+$$

where B is the free base and BH^+ its conjugate acid. The pK_a of the conjugate acid is obtained from

$$pK_a = pH - \log \frac{[BH^+]}{[B]} \qquad (19-95)$$

Using the equation

$$pH = pK_a + \log \frac{S_o}{S - S_o} \qquad (19-96)$$

where S is the total solubility at a given pH value and S_o the solubility of the free base, B, independent of pH. Compute the solubility S of fentanyl at pH values 5.48 and 7.04. The pK_a value of the conjugate acid is 8.99 (obtained from solubility measurements), and the solubility S_o of the free base is 0.0099 mg/mL.

Answer: $S = 32$ mg/mL at pH 5.48, and $S = 0.89$ mg/mL at pH 7.04

19–16. From in situ perfusion experiments using the rat intestine, cephalexin, one of the cephalosporin antibiotics, is absorbed by a nonpassive mechanism involving a biochemical carrier that ferries the drug across the living membrane.[93] Michaelis–Menten kinetics, pages 293 to 294, was found useful in modeling the carrier-mediated absorption of the drug, as shown on pages 530 and 531.

(a) Compute the "intrinsic" (dimensionless) permeability P_c^* of the carrier, given that the maximum flux J_{max}^* is 9.1. The Michaelis constant, K_m is 7.2. Use equation (19–35).

(b) The following concentrations C_w of drug were found at the intestinal wall from a series of experiments: $C_w = 0.01$, 0.05, 0.1, 5.0, 10.0, 50.0, and 100.0 mM. Compute the intrinsic intestinal wall permeability, P_w^*, using equation (19–36) for a combination of carrier P_c^* and passive membrane P_m^* permeabilities, and the drug concentrations C_w given above. For cephalexin, P_m^* was found to be zero.

(c) Plot P_w^* (y-axis) against C_w. Is the relationship linear? Does a logarithmic relationship in C_w yield a straight line? How would you interpret the shape of this plot?

Partial Answer: (a) $P_c^* = 1.264$; (b) $P_w^* = 1.262$ for $C_w = 0.01$ mM; (c) Compare your graph with that given in Sinko and Amidon.[93]

19–17. (a) Calculate the intrinsic permeability P_c^* of the carrier-drug complex responsible for transporting the drug cephradine across the intestine. The values of J_{max}^* and K_m, obtained experimentally by Sinko and Amidon[93] for cephradine transport, are given as $J_{max}^* = 1.60$; $K_m = 1.50$.

(b) Calculate the total permeability P_w^* of cephradine at the wall of the rat intestine when the gut wall concentration, C_w, has the values 0.10 mM, 7.2 mM, and 50 mM. The passive permeability P_m^* was found to be 0.30 for cephradine.

Answers: (a) $P_c^* = 1.067$; (b) $P_w^* = 1.300$, 0.484, 0.331

19–18. (a) Compute the Graetz number, Gz, for the human intestine using an intestinal length L of 500 cm, a volume flow rate V_m of 0.5 mL/min, and a diffusivity D of 5.0×10^{-6} cm^2/sec. What are the dimensions on Gz? The Graetz number is defined as $G_z = \pi DL/2V_m$, where π is the ratio of the circumference of a circle to its diameter.

(b) Compute the fractional dose F absorbed at the human intestine for the following wall permeability values: $P_w^* = 0.5$, 1, 1.5, 2, 2.5, and 3 (dimensionless quantities). The fractional dose absorbed is $F = 1 - ex(-4G_zP_w^*)$.[95] Plot the results on a graph of F (y-axis) against P_w^*. (Data from Amidon et al.[95])

Partial Answer: (a) $Gz = 0.47$; (b) For $P_w^* = 0.50$, $F = 0.61$. See pages 530 to 531 to assist you in answering this problem.

19–19. Compute the pH at which the apparent absorption rate constant, K_{app}, of a cephalosporin is 0.173 min^{-1} as obtained by Prieto et al.[96] in the in situ rat intestinal technique. The weight of the rat is 248 g, the pK_a of the drug is 2.76, and the contributions of the nonionized and ionized forms of the drug to V_{app}, the apparent

*Problem 19–15 was prepared by Dr. J. B. Dressman, College of Pharmacy, University of Michigan.

absorption rate constant per metabolic weight unit, are $V_o = 57.312 \times 10^{-3}$ min^{-1} g^{-1} and $V_{-1} = 1.860 \times 10^{-3}$ min^{-1} g^{-1}, respectively. See *Example 19–13* and equations (19–38) and (19–39).

Answer: pH = 4.54

19–20. The approximate osmotic pressure π produced by a saturated phenobarbital sodium solution in an osmotic pump-like device is given by the equation

$$\pi = \nu \frac{C_s}{M} RT$$

in which ν is the number of particles into which a molecule of phenobarbital sodium ionizes, namely about 2. The saturation concentration (solubility) of phenobarbital at ordinary temperatures is $C_s = 100$ g/liter. The molecular weight of the drug M is 254.2 g/mole, R is 0.082 liter atm mole^{-1} deg^{-1}, and T is 310° K for body temperature on the Kelvin scale.

Calculate the osmotic pressure produced by the drug (exclusive of any added osmotic agent mixed with the drug) using the equation just given.

Answer: 20 atm

19–21. If the new drug, gastrogen, has a diffusion coefficient $D = 6.3 \times 10^{-6}$ cm^2/sec at 37° C, and the path length L of the orifice in the osmotic pump-type dosage form is 10×10^{-4} cm, what is the maximum size S_{max}, (diameter in μm) of the orifice for proper delivery of the drug from the device? $C_s = 750$ mg/cm^3 at 37° C in the gastric fluid. Assume the dimensionless sizing factor f has a value of 50, and the zero-order delivery rate (dM/dt), is 35 mg/hr at body temperature. *Note: D* must be in cm^2/hr. See the calculations of S_{max} on p. 536 where $(dM/dt)_o$ is given.

Answer: 72.5 μm diameter

19–22. Compute the radius of the pores in the colonic mucosa after treatment with the enhancer, sodium laurate, at 37° C. The ratio of the osmotic water permeability coefficient to the permeability coefficient of tritiated water through the membrane, P_f/P_d, is 17.48. The viscosity and diffusion coefficient of water at 37° C are 6.915×10^{-3} poise and 3.24×10^{-5} cm^2/sec, respectively. The molar volume of water is 18.14 cm^3/mole at 37° C and the radius a_w of the water molecule is 1.5 Å. The gas constant R is 8.3143×10^7 erg deg^{-1} mole^{-1} (Data from Tomita et al.[125]). See *Example 19–16*, page 538 and equations (19–58) and (19–59).

Answer: Pore radius $r = 13.1$ Å

19–23. The total flux, J, of an acidic drug through the skin at several pH values is given by the equation

$$J = P_{HA}[HA] + P_{A^-}[A^-]$$

where P_{HA} and P_{A^-} are the permeability coefficients of the nonionized HA and ionized A^- species, respectively. The concentration of the ionized species, $[A^-]$, can be computed from the equation

$$[A^-] = \frac{10^{(pH - pK_a)}}{1 + 10^{(pH - pK_a)}} [T]$$

where $[T] = [A^-] + [HA]$ is the total concentration of ionized A^- and nonionized HA species.

Fleeker et al.[135] studied the diffusion of an acidic drug, indomethacin (see Fig. 11–6) through hydrated snake skin as a biologic membrane at pH 7.0 and 32° C. The pK_a of indomethacin is 4.5.

(a) Calculate the total flux J of indomethacin at pH 7. The total concentration [T] of indomethacin at pH 7 is 916.6 μg/mL and the permeability coefficients are $P_{HA} = 3.62 \times 10^{-3}$ cm/hr and $P_{A^-} = 2.19 \times 10^{-5}$ cm/hr.

(b) In a second experiment the snake skin was pretreated with dodecyl N, N-dimethylamino acetate, a new enhancer. The permeability coefficients of indomethacin were found to be $P_{HA} = 3.90 \times 10^{-3}$ cm/hr and $P_{A^-} = 7.97 \times 10^{-4}$ cm/hr in the presence of the enhancer. The total concentration of indomethacin and the pH were kept unchanged, [T] = 916.6 μg/mL and pH = 7. $[A^-]$ is calculated using the equation above, together with the equation $[HA] = [T] - [A^-]$. Compute the total flux of indomethacin in the presence of the enhancer.

(c) Using the flux values obtained in (a) and (b) compute the amount of indomethacin penetrated per unit area, Q (μg/cm^2) = Jt, at $t = 5$ hr and $t = 20$ hr. Plot Q (y-axis) against time (x-axis).

Answers: (a) J (without enhancer) = 0.0305 μg/(cm^2 hr); (b) J (after treatment with enhancer) = 0.739 μg/(cm^{2}hr).

19–24. Compute the permeability coefficients P_{HA} and P_{A^-} for the nonionized and ionized forms of Chromocarb, a chromone-2-carboxylic acid; through excised human skin at 37° C. Chromocarb is under clinical trial as a capillary protectant is diabetes. The ratios of the flux to the concentration of ionized form, $J/[A^-]$ at three pH values, are:

Data for *Problem 19–24*

pH	5	6	7
$J/[A^-] \times 10^5$ (cm/hr)	158	48	7.3

The pK_a of the compound is 1.93. P_{HA} and P_{A^-} are computed using equation (19–75) together with linear regression of $J/[A^-]$ against $[H^+]$. Is the drug more liable to penetrate the skin in the ionized or nonionized form?

Answer: $P_{HA} = 1.639$ cm/hr; $P_{A^-} = 19.3 \times 10^{-5}$ cm/hr

19–25. Compute the solubility C of desoxycorticosterone in the stratum corneum using the following data obtained from in vitro experiments with intact and stripped mouse skin (data from Table II in reference 132). The lag times across the intact and stripped skin are $t_2 = 3.90$ hr and $t_1 = 1.20$ hr; the permeation rates are $(dQ/dt)_2 = 4.73$ μg/(cm^2 hr) and $(dQ/dt)_1 = 12.1$ μg/(cm^2 hr). The thickness, h_2, of the stratum corneum is 10 μm. See *Example 19–19*.

Answer: $C = 32.3$ mg/mL

19–26.* When a penetration enhancer was used, the lipid–protein partition coefficient of the new drug referred to in *Example 19–18* increased by 100-fold, the other properties remaining unchanged. Using the random brick model and the data given in *Example 19–18*, calculate the flux and the per cent increase in the flux due to the action of the enhancer.

Partial Answer: The flux J is 0.038 μg/(cm^2 sec)

19–27. The in vitro binding of vasopressin using rat skin at 30° C was analyzed according to the Langmuir approach (pp. 380–382). The following results were found (data calculated from the constants given in P. S. Banerjee and W. A. Ritschel[136]):

Data for *Problem 19–27*

$c/(x/m)$(mL^{-1} mg)	c (μg/mL)
21.32	10
21.46	20
21.60	30
21.87	50
22.15	70
22.57	100
23.27	150

(a) using equation (19–76) together with regression analysis, compute the *affinity constant* b (mL/μg) of vasopressin for adsorption on the skin, and the *maximum adsorption capacity* y_m (μg/mg).

(b) Do you believe that the authors were justified in using an

*Problem 19–25 was prepared by Dr. K. Toio, Kyushu Institute of Technology, Kyusnu, Japan.

adsorption model and the Langmuir equation to study the binding of vasopressin to the proteins in the skin?

Answers: (a) $b = 6.56 \times 10^{-4}$ mL/μg; $Y_m = 71.94$ μg/mg; (b) Review the section on protein binding, Chapter 11, to answer this question.

19–28. K. Hirano and H. Yamada[164] studied the subcutaneous absorption of *p*-hydroxyazobenzene from aqueous suspensions. The ratios of the cube root of drug amount W at the subcutaneous injection site to the applied dose, W_o, at several times are given in the table:

Data for ***Problem 19–28***

$(W/W_o)^{1/3}$	1	0.958	0.916	0.874	0.832
t (hr)	0	1.0	2.0	3.0	4.0

(a) Plot $(W/W_o)^{1/3}$ (*y*-axis) against t and compute the absorption rate constant, k, from the slope using equation (19–88). You can also use regression analysis to obtain k.

(b) Compute k from equation (19–89), (page 547) given the solubility of *p*-hydroxyazobenzene, $C_s = 0.034$ mg/mL, and substitute the k value into equation (19–88) to predict $(W/W_o)^{1/3}$. If the initial dose W_o is 2.5 mg, what is the remaining amount W after 5 hours?

(c) According to the authors, equation (19–89) allows one to compute the absorption rate constant for drugs in suspension having similar particle size and sedimentation volume. Using equation (19–89), calculate k for betamethasone ($C_s = 0.002$ mgmL), sulfamethoxazole ($C_s = 5.7$ mg/mL), and *p*-aminoazobenzene ($C_s = 0.049$ mg/mL). The experimental k values are 0.0096, 0.374, and 0.065 hr^{-1}, respectively. How well do your calculated k values agree with the experimental values?

Answers: (a) $k = 0.042$ hr^{-1}; (b) $k = 0.045$ hr^{-1}; after 5 hr, $W = 1.16$ mg; (c) betamethasone, $k = 0.010$; sulfamethoxazole, $k = 0.659$; *p*-aminoazobenzene, $k = 0.054$ hr^{-1}